

## ABSTRACT

Title of Thesis: DEVELOPMENT OF A COUPLED FDS MODELING  
AND VIDEO ANALYSIS APPROACH TO  
ESTIMATE THE BURNING CHARACTERISTICS OF  
A THIN-WALLED HUMANITARIAN SHELTER

Genevieve C. Tan  
Master of Science, 2022

Thesis Directed By: Dr. James A. Milke, Advisor  
Department of Fire Protection Engineering  
Dr. Arnaud Trouvé, Co-Advisor  
Department of Fire Protection Engineering

Large fires in humanitarian settlements lead to enormous losses in material, time, and resources that organizations allocate toward supporting refugee camps and displaced persons. In the absence of full-scale shelter fire experiments in humanitarian settlements, a combination of video analysis and fire modeling can be used to estimate burning characteristics of the shelter fire.

A MATLAB-based image binarization method is developed to measure the flame height and structure loss over the course of fire development in footage from a shelter burn test conducted in Cox's Bazar, Bangladesh. The conditions of the shelter fire are recreated in Fire Dynamics Simulator (FDS). Diagnostics in the FDS models provide estimates for the flame height, heat release rate, heat flux, and radiant integrated intensity in and around the shelter. The FDS models exhibit a 10-25 second delay in matching key events in the fire development timeline of the original shelter fire. Otherwise, measurements from the FDS simulations show good agreement to measurements from image processing.

Based on results from image processing and FDS models, the steady burning HRR is approximately 900 kW for a shelter fire with a flame height range of approximately 4.1-4.5 m.

DEVELOPMENT OF A COUPLED FDS MODELING  
AND VIDEO ANALYSIS APPROACH  
TO ESTIMATE THE BURNING CHARACTERISTICS  
OF A THIN-WALLED HUMANITARIAN SHELTER

by

Genevieve C. Tan

Thesis submitted to the Faculty of the Graduate School of the  
University of Maryland, College Park, in partial fulfillment  
of the requirements for the degree of  
Master of Science  
2022

Advisory Committee:

Dr. James A. Milke, Chair/Advisor

Dr. Arnaud Trouvé, Co-Advisor

Dr. Peter Sunderland

© Copyright by  
Genevieve C. Tan  
2022

## Acknowledgements

I would not have been able to complete this project without all the support I received these past few years. First, I must express my sincere thanks to the FPE department for awarding me the John L. Bryan Chair Endowed GRA, which gave me the opportunity to forge this unique research topic in the first place. I found a home in this department, and I hope that those who come after me will feel the same way.

Thank you to Dr. Milke and Dr. Trouvé for serving as co-advisors for this research. From the beginning when I first expressed an interest in creating a research topic relating to disaster and community resilience, Dr. Milke has worked with me, providing me with group research opportunities, connections with experts, and lots of great advice. In the half-year leading up to project completion, Dr. Trouvé has helped me refine my project scope, understand the capabilities of FDS, and find ways to approach the novel problems that arose over the course of my research. I would also like to thank Dr. Sunderland, for serving as the third member of my committee and checking through my image processing methods.

Thank you to the contacts who took the time to talk with me and guide the shape of this research, most notably Paul Chamberlain, Dan Graham, Danielle Antonellis, Dr. Richard Walls, Dr. Natalia Flores-Quiroz, Dr. Erica Kuligowski, and Dr. David Rush.

I would also like to acknowledge the supercomputing resources at the University of Maryland (<http://hpcc.umd.edu>) made available for conducting the research reported in this paper. I am also grateful that UMD provides licenses to students for Adobe Premiere Pro and MATLAB by MathWorks, which allowed me to conduct parts of my research.

Thank you to the developers of FDS and Smokeview at the National Institute of Standards and Technology, for making these programs freely available for research purposes. Thank you also to Thunderhead Engineering for providing me with a license to use Pyrosim to visualize my FDS output files.

Thank you to my parents, who brought me tea and snacks on my late nights, and special thanks to Christine, my sister and my best friend, who brought me distractions during the day.

To my friends inside and outside FPE, thank you for crossing my path and making life all the better for it. To Matthew, thank you for showing me the world. To Mairead, thanks for offering your couch to me when my lease ended. To Mahdi, Rob, EJ, Aviv, and all my friends a half step ahead—thank you for showing me the way. Finally, to Alexi, Jeff, Kelliann, and Sofia—the infamous residents of Cubicle Area 1—thank you for making this semester one to remember.

The biggest lesson I learned in school is that I will be thanking people all my life. As this adventure comes to a close, I am grateful that I can look back fondly on the memories I made, and I am excited for what the future holds.

# Table of Contents

Acknowledgements.....	ii
Table of Contents.....	iii
List of Figures.....	v
List of Tables.....	vii
Introduction.....	1
1.1 Motivation.....	2
1.2 Scope of Work.....	3
1.3 Image Processing Background.....	3
1.4 Computational Modeling Background.....	4
Fire Risk and Mitigation Work in Informal and Humanitarian Settlements.....	6
2.1 LMICs and Informal Settlements.....	6
2.1.1 What are informal settlements?.....	7
2.1.2 Fire risk factors.....	7
2.1.3 Experimental and Modeling Work for informal settlements.....	8
2.2 Humanitarian settlements.....	9
2.2.1 What is a refugee? What are humanitarian settlements?.....	9
2.2.2 Fire risk factors.....	10
2.2.3 Fire mitigation efforts.....	11
2.3 The Rohingya Refugee Camps in Bangladesh.....	12
2.3.1 Fire incidents and perception of fire risk.....	14
2.3.2 A “Standard” Shelter.....	16
2.2.3 Fire mitigation efforts.....	19
The Rohingya Shelter Burn Test.....	22
3.1 Determination of Interior Fuel Load.....	22
3.2 Shelter Burn Test Timeline.....	24
3.3 Unique Challenges.....	26
Image Processing Methods.....	28
4.1 Measured and Estimated Quantities.....	28
4.1.1 Tarp Consumption and Flame Height Measurements.....	28
4.1.2 Heat Release Rate Estimation.....	30
4.2 Binarization in MATLAB.....	31
4.2.1 Otsu Thresholding.....	31
4.2.2 Specified RGB Thresholding.....	32
4.3 Stabilization, Cropping, and Calibration.....	35
FDS Model Construction and Setup.....	37
5.1 Shelter and Fuel Pile Geometry.....	37
5.2 Instrumentation Devices and Spacing.....	39
5.3 Model and Preliminary Material Properties.....	42
5.3.1 Grid Resolution.....	42
5.3.2 Simple Chemistry Model and Reaction Properties.....	42
5.3.3 Material Properties from Literature.....	44
5.4 Hand Calculations and Preliminary FDS Simulations.....	45
5.4.1 NIST Tarp Experiment Replication in FDS.....	45

5.4.2 Tarp Burn Away Time Hand Calculations .....	50
5.4.2 Preliminary Shelter Fire Simulations .....	51
5.5 Full FDS Shelter Fire Simulations .....	56
Results .....	59
6.1 Shelter Burn Test Image Processing Results .....	59
6.2 Validation of the FDS Model Against Image Processing Data .....	62
6.3 FDS Results .....	67
Final Remarks .....	71
7.1 Conclusions .....	71
7.2 Limitations and Future Work .....	72
Appendix .....	75
A4.2 .....	75
A5.1 .....	81
A5.2 .....	84
A5.5 .....	85
A6.3 .....	86
References .....	96

## List of Figures

Figure 2-1. Urban population living in slum conditions in 2018 [16] .....	7
Figure 2-2. A UNHCR map with population distribution and camp numbering system [37] ....	13
Figure 2-3. A map of the Kutupalong area, showing the overlapping zoning and camp numbering systems [37] .....	14
Figure 2-4. A map of area affected by the March 2021 fire in Camps 8W, 8E, and 9 [37] . .....	15
Figure 2-5. Technical design drawings developed by the Shelter/NFI Partners.....	17
Figure 2-6. Photographs of Rohingya camp shelters (P. Chamberlain and D. Graham, personal communication, March 26, 2022). .....	18
Figure 2-7. Photographs of the interior of shelters (P. Chamberlain and D. Graham, personal communication, March 26, 2022). .....	18
Figure 2-8. Burn tests with shelters built with bamboo framing, woven-bamboo walls, and a tarp roof (photo ownership Mehedi Rahman). .....	19
Figure 3-1. NFI Shelter plans (left) were used to calibrate measurements of the Shelter 1 Re-burn in Kinovea (right). The unburned contents of the Shelter 1 Re-burn (bamboo walls and scraps) can be seen. ....	23
Figure 3-2. NFI Shelter plans (left) were used to calibrate measurements of Shelter 2 in Kinovea (right). .....	23
Figure 3-3. Timeline of benchmark shelter burning behaviors, where time = 0 seconds would be ignition.....	25
Figure 3-4. After volunteers extinguish the fire, the burn away that occurred on the back wall is visible. ....	26
Figure 4-1. The Shelter 2 tarp on the roof and walls has burnt away, and the flame tip extends past the height of the roof. Timestamp: 62.45 seconds. ....	29
Figure 4-2. Shelter 1 binarized with the <i>rgb2gray</i> , <i>graythresh</i> , and <i>imbinarize</i> functions in MATLAB. ....	31
Figure 4-3. RGB combinations associated with fire, tarp, and greenery.....	33
Figure 4-4. Tarp Area (left) and binarized with a blue criterion (right). Timestamp: 39.14 seconds. ....	33
Figure 4-5. RBG samples from regions in the shelter images and methods to increase contrast to fire. ....	34
Figure 4-6. Colored photo of shelter fire (left), binarized photo with red criterion (middle), and binarized photo with red and intensity criteria (right).....	35
Figure 4-7. Flame height measurement. Timestamp: 55.55 seconds.....	35
Figure 4-8. Tracking markers in Kinovea.....	36
Figure 4-9. A stabilized and unstabilized cropped frame from the same time. ....	36
Figure 5-1. Exterior view of the shelter. ....	38
Figure 5-2. Front and back views of the shelter. ....	38
Figure 5-3. Side view of the shelter. ....	38
Figure 5-4. Fuel pile with a base of 1 m x 2 m and sloped rise to a height of 1.6 m.....	39
Figure 5-5. The column of HRRPUV devices is shown in green. The center of the roof is zoomed-in on the right. ....	40
Figure 5-6. Layout of heat flux and integrated intensity devices inside the shelter. ....	41
Figure 5-7. Layout of heat flux and integrated intensity devices inside and around the shelter. ....	41

Figure 5-8. Tarp experiment by NIST [60] .....	46
Figure 5-9. HRR profile of tarp, experiment by NIST [60] .....	47
Figure 5-10. NIST experiment imitation simulation in FDS. ....	48
Figure 5-11. A t = 100 s, the FDS tarp simulation with the ignitor particles turned off at t = 30 s (left) and the FDS tarp simulation with the ignition particles remaining on for the whole simulation (right). ....	49
Figure 5-12. Burning rate over time for a single cell.....	49
Figure 5-13. Series_BH shelter visualization at t = 20, 30, and 60 seconds. ....	52
Figure 5-14. Wide ignition portion of the fuel pile, indicated in red.....	54
Figure 5-15. Series_WideCorner FDS visualizations of the back wall at 35, 45, and 100 seconds. ....	55
Figure 5-16. Wide Corner Configuration (left) and Stout Corner Configuration (right).....	57
Figure 5-17. Flame height results from image processing, for comparison to FDS results. ....	58
Figure 5-18. FDS flame height results for the Wide Corner and Stout Corner configurations. ...	58
Figure 6-1. Tarp area loss over time found through IP.....	60
Figure 6-2. ROC of the tarp area loss over time found through IP.....	60
Figure 6-3. Flame height over time found through IP. ....	61
Figure 6-4. HRR estimated over time using the Heskestad correlation and flame heights found through IP. ....	61
Figure 6-5. Tarp consumption over time from IP compared to the Wide Corner and Stout Corner models. ....	63
Figure 6-6. Tarp consumption ROC over time from IP compared to the "Wide Corner" and "Stout Corner" models.....	63
Figure 6-7. Flame height over time from IP compared to the measurements from the FDS models. ....	65
Figure 6-8. HRR over time from the IP estimate compared to the total simulation HRR from the FDS models. ....	65
Figure 6-9. A side view of the Wide Corner (left) and Stout Corner (right) simulations, at 120 seconds. ....	66
Figure 6-10. A back view of the fluid velocity slice file for the Wide Corner (left) and Stout Corner (right) simulations, at 120 seconds.....	66
Figure 6-11. A side view of the fluid velocity slice file for the Wide Corner (left) and Stout Corner (right) simulations, at 120 seconds.....	66
Figure 6-12. Heat flux and integrated intensity over time from the left, center, and right temperature devices in FDS. ....	68
Figure 6-13. Integrated intensity at varying distances from the shelter, averaged over 100-150 s. ....	69

## List of Tables

Table 2-1. Burn tests of shelters built to the NFI design specifications. ....	21
Table 5-1. Reaction Properties used in FDS. ....	44
Table 5-2. Material Properties from Literature. ....	45
Table 5-3. Summary of test results for the NIST tarp experiment [60] .....	47
Table 5-4. Hand calculations for $t_{\text{burnout}}$ , modifying HRRPUA and $k_{\text{pc}}$ . ....	51
Table 5-5. Material Properties used in FDS. ....	56



# Chapter 1

## Introduction

Fire safety in informal and humanitarian settlements is an under-researched issue. In March 2021, a large conflagration in Bangladesh destroyed more than 9,500 homes in the Cox's Bazar settlement for Rohingya refugees, and there have been over 200 reported fire incidents since [[1] , [2] ]. Each fire results in homes and livelihoods lost. Humanitarian organizations such as UNHCR (United Nations High Commissioner for Refugees) and MOAS (The Migrant Offshore Aid Station) fund the maintenance and improvement of these camps; large fires present enormous losses in material, time, and resources that these organizations allocate toward the camps.

To gain a better understanding of the fire risk in the Cox's Bazar settlements, live burn tests were conducted with sample shelters. These sample shelters were built to the general specifications provided in the camps, using materials such as tarp and bamboo. Video recordings from test to test are not standardized and measurements were not captured for many of the quantities often collected in full scale experiments (ceiling temperature, mass loss rate, heat flux, etc.).

The following report will demonstrate that, in the absence of full-scale experiments for a burning shelter, a combination of video analysis and fire simulations can supply estimates of the flame height and heat release rate, along with other quantities.

## 1.1 Motivation

Maintaining fire safety in informal settlements and humanitarian settlements is a challenge, exacerbated by factors such as a high density of dwellings, low access to fire fighting resources, and informal or worn-down infrastructure leading to unsafe conditions (such as exposed wiring or broken gaskets in propane stoves) [3] . Unfortunately, 95% of fire deaths occur in low-to-middle-income countries, where informal settlements are common due to growing or displaced populations [3] . A framework developed by Arup identifies research gaps in informal settlement fire safety and posits that risk can be addressed by supporting four areas in vulnerable communities: mitigation<sup>1</sup>, preparation<sup>2</sup>, response<sup>3</sup>, and recovery<sup>4</sup>.

In humanitarian settlements (i.e., settlements for refugees or displaced populations), where organizations such as UNHCR or Shelter Projects provide funding and oversight for the development, layout, and maintenance of settlements, there is greater potential to implement improvements in fire safety before and after large fire incidents. There is more uniformity between dwellings in humanitarian settlements than in other “informal settlements” because residents are provided with a more consistent set of materials by humanitarian organizations, and ideally, camp managers direct communities to build according to guidelines set by documents such as Shelter/NFI Sector Technical Designs [5] . An analysis of the burning behavior of dwellings and the associated risks may inform future settlement guidelines for dwelling spacings, building materials, or camp layouts that could mitigate the effects of fire.

<sup>1</sup> Mitigation – reduction of fire causes and risk factors in the natural and built environment [4] .

<sup>2</sup> Preparation – formulation of strategies and allocation of resources to reduce the impact of fire [4] .

<sup>3</sup> Response – actions during a fire incident to protect life, property, and critical infrastructure [4] .

<sup>4</sup> Recovery – actions in the aftermath of a fire to return communities to normal life and potentially make improvements in fire safety [4]

## 1.2 Scope of Work

The focus of this research is to combine video analysis with FDS simulations to characterize the fire risk of a burning thin-walled shelter and provide estimates for the flame height, heat release rate, and other quantities that would otherwise be collected through experiments.

Frame-by-frame image processing of the burn test footage will generate flame height estimates that are then used to validate that the FDS simulations adequately reproduce the burn test conditions. Then, the FDS simulations can provide estimates of the temperature, heat release, and heat flux profiles at varying distances from the shelter.

## 1.3 Image Processing Background

In this project, frame-by-frame video processing was used to analyze footage of a full-scale shelter burn test in Cox's Bazar, Bangladesh. In previous work by Carmignani [6], where a Python-based video processing tool was created to track flame frame-by-frame in video footage, the following tracking methods were available as separate modes:

- Manual tracking – the user may point-and-click on the flame front or flame tip as desired;
- Luma tracking – luminous objects are isolated (binarized) from the background using the luma intensity of each pixel;
- RGB tracking – fire is isolated (binarized) from the background using intensity thresholds for each of the RGB (red, green, blue) channels in each pixel.
- HSV tracking – conceptually similar to the RGB method, but criteria are based on hue, saturation, and value.

Examples of the tool's usage in [6] show lab experiments where a flame or flame front was documented against a high-contrast background. Videos should be pre-edited (rotated, scaled, and cropped) to isolate a constant region of interest.

Alternatively, MATLAB-based scripts have robust image processing capabilities, with the added benefit of being entirely customizable to case-by-case processing needs. Several preset functions for converting video or image file types, grayscaling, and binarization are provided in the MATLAB Image Processing Toolbox (IPT). MATLAB has been used in several studies for image processing-based measurement of flame height [7] as well as for image processing-based pyrometry [8] .

While the tool developed by Carmignani [6] could be used on footage from a full-scale burn test, especially with the intuitive point-and-click manual tracking features, a MATLAB-based tool was most appropriate for the particular case of video-processing the Rohingya shelter tests. It was found that a combination of techniques similar to the Luma tracking and RGB tracking from [6] would produce the clearest binarization of the flame footage from the Rohingya shelter tests. The MATLAB-based tool, to be described in Chapter 2, was developed in order to automate the cropping, binarization, and flame height measurements from shelter burn test footage.

## 1.4 Computational Modeling Background

In this project, the burning behavior of a full-scale shelter burn test in Cox's Bazar, Bangladesh was simulated using computational modeling. Fire Dynamics Simulator (FDS) is a software developed by the National Institute of Standards and Technology (NIST) to model fire-driven fluid flow. The software Smokeview, also developed by NIST, is used to visualize the results of FDS. An additional software, Pyrosim, was developed by Thunderhead Engineering as a graphic user interface to streamline the process of creating FDS files, viewing results, and saving results as movie files. In this report, the newest versions of FDS (6.7.9), Smokeview (6.7.21), and Pyrosim (2022.2.0803) are used to develop computational models that recreate the conditions of a burning test shelter from the Rohingya camp at Cox's Bazar, Bangladesh.

FDS is a computational fluid dynamics (CFD) model developed to simulate thermally driven flows (such as smoke or heat transport in fires) by numerically solving a form of the Navier-Stokes equations appropriate for low-speed ( $Ma < 0.3$ ) flow [9] . By default, FDS uses a single-step chemical reaction to represent combustion, where species are lumped into air, fuel, and products [9] . The radiative heat transport

solver uses a technique similar to finite volume methods (FVM) for convective heat transport; by default, calculations are completed using 100 discrete angles [9] . The governing equations and numerical methods used in FDS are fully described in the FDS Technical Reference Guide [10] .

Parallel Processing of FDS models with multiple meshes defined can be performed by assigning each mesh to a different single core processor. The number of computational cells per mesh should be distributed equally if possible, to minimize stalling (since calculations in one mesh rely on the completion of calculations in all other meshes to proceed). The high-performance computing (HPC) clusters at UMD, Deepthought2 (DT2) and Zaratan (ZT) (accessible at <https://hpcc.umd.edu/>), are utilized for parallel processing in this project. Within computing clusters like DT2 and ZT, FDS employs Message Passing Interface (MPI) to compute the flow field in each mesh as an MPI process [9] .

Validation cases comparing FDS simulation results with measurements from a collection of experiments can be found in the FDS Validation Reference Guide [11] . This research aims to represent an outdoor shelter fire where the shelter itself burns away as part of the fuel load; these conditions are most similar to that of outdoor fire or wildfire FDS models as well as other informal dwelling models. Previous studies have used FDS and WFDS (Wildland-urban-interface Fire Dynamics Simulator) to recreate the outdoor fire conditions of the Meteotron fire experiment [12] and to model wildfire spread through vegetation [13] . FDS has also been used in [14] to model a set of full-scale fire experiments with informal dwellings in Cape Town, South Africa in order to estimate a critical separation distance between dwellings.

FDS has not been previously used for a case with an outdoor dwelling or facade fire with thin walls that burn away. One goal of this report is to begin addressing this research gap.

## Chapter 2

# Fire Risk and Mitigation Work in Informal and Humanitarian Settlements

In this section, the state of fire risk will be discussed in increasingly narrowed contexts: from low- and middle-income countries (LMICs) and informal settlements to specifically humanitarian settlements, and finally to the humanitarian settlements near Cox’s Bazar, Bangladesh. Experimental work and/or efforts to mitigate fire risk will also be described for each section.

### 2.1 LMICs and Informal Settlements

There is a clear link between socioeconomic factors and fire risk: low- and middle-income countries (LMICs) have a lower capacity for enforcing fire safety, fire response, and fire recovery and thus bear a higher risk of experiencing unwanted fire and its consequences.

Of the estimated 300,000 fire-related fatalities that occur annually around the world, more than 95% occur in LMICs [15] . As the global population rises, the lack of affordable housing in LMICs especially has pushed an estimated 1.6 billion people into “slum conditions” or “inadequate housing,” a number that is anticipated to reach 3 billion by 2030 [16] . In Figure 1-1, a map of data from UN-Habitat and the World Bank show that as of 2018, large portions of Africa and Asia have countries with more than 20% of their urban population living in “slums” [16] . In 2018, the countries mentioned in this report, Bangladesh (47.2%) and Myanmar (56.1%), both fell within the range of 40-60% of the urban population living in slums [16] .

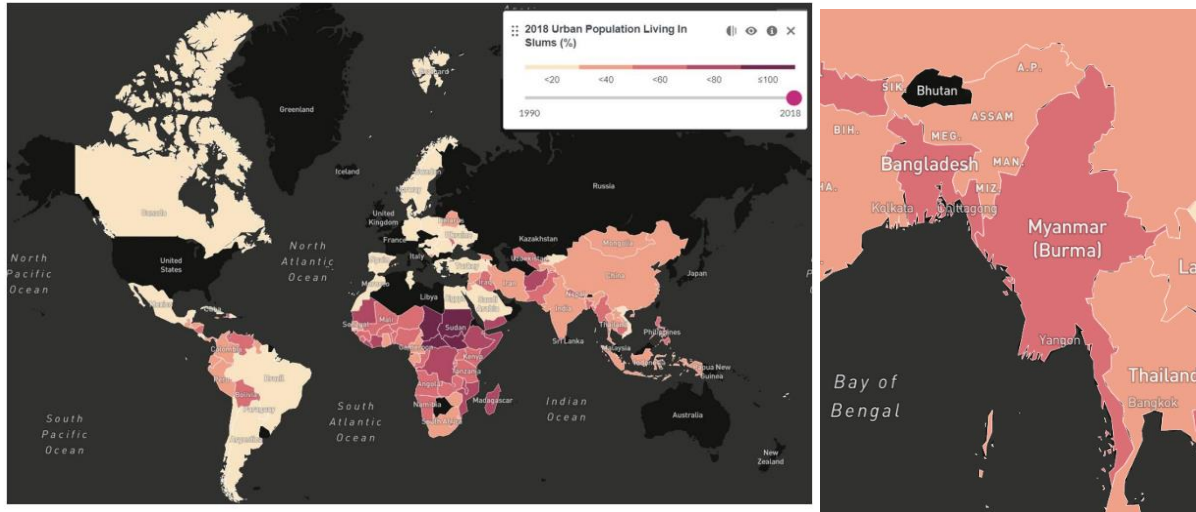


Figure 1-1. Urban population living in slum conditions in 2018 [16] .

### 2.1.1 What are informal settlements?

In this report, the term “informal settlements” will be used to refer to communities with “slums,” “slum conditions,” or “inadequate housing.” UN-Habitat describes informal settlements as “residential areas where inhabitants have no security of tenure, neighborhoods usually lack or are cut off from basic services and city infrastructure, or housing may not comply with current planning and building regulations, and is often situated in geographically and environmentally hazardous areas” [17] .

### 2.1.2 Fire risk factors

In informal settlements, fire risk is dependent on the built environment, the natural environment, and the behavior and culture of the community. Tools, materials, climate, and practices vary greatly from settlement to settlement, but the following general fire risk factors were described in ARUP’s framework for fire safety in informal settlements [4] :

- Built: A high density of unstable dwellings made of highly combustible materials such as timber, plastic, cardboard, or bamboo can increase the likelihood as well as the severity of fires. Limited separation distance between dwellings may result in fire spread through a settlement.

- Natural: Arid and hot climates produce the most dry vegetation, which is readily combustible. Weather and land topography can influence fire behavior, as fire spread can be exacerbated by high wind speeds and sloped building sites.
- Behavioral: Open flames sources that are commonly used for warmth or cooking may cause unwanted fire if left unattended or devices are poorly maintained. Other behaviors that increase the risk of accidental fire include children playing with fire, alcohol intoxication, and poor disposal of cigarettes. Arson is also a cause of deliberate fire incidents.

Climate change presents an additional threat in the natural environment. Rising global temperatures may lead to drier conditions, longer fire seasons, and more severe fires [18] . Changing climate conditions demand constant adaptation in fire responses.

### 2.1.3 Experimental and Modeling Work for informal settlements

The largest body of work relating to burning behavior in informal settlements has analyzed full-scale experiments that approximate the conditions of a South African informal settlement dwelling (ISD) fire.

Cicione et al. [14] investigated the effect of cladding material on burning behavior based on experiments with a single mock ISD built with steel cladding and a single mock ISD built with timber cladding. Another set of experiments by Cicione et al. [19] compared fire spread between a group of three steel-clad ISDs and a group of three timber-clad ISDs. It was found that timber-clad dwellings are more prone to fire spread.

FDS (Fire Dynamics Simulator) simulations were also developed based on the single-dwelling experiments by Cicione et al [14] . The simulation results were used to determine a critical separation distance between dwellings based on the critical heat flux of cardboard, the most flammable dwelling material. In other studies, Beshir et al. used modified FDS simulations to investigate whether different ventilation conditions created by different roof and window openings would have an effect on fire spread.

The studies found that roof openings reduced the heat fluxes emitted to surroundings [20] and that the position of windows in relation to fires significantly affected heat fluxes emitted to surroundings [21] .

GIS (Geographic Information System) techniques have also been employed to quantify fire risk. Wang et al. [22] compared two methods of estimating critical separation distance, using single-dwelling experiment data and using aerial photography for four fire events paired with GIS analyses. It was found that the GIS analysis provided a more conservative prediction of critical separation distance. Stevens et al. [23] also presented preliminary methods and results for a model that uses GIS techniques to map fire risk in settlements with respect to previous fire incident data and three metrics: dwelling spacing, edge density, and critical patch size. The results suggest that settlement layout is a critical factor in the development of large conflagrations.

## 2.2 Humanitarian settlements

Refugee camps, or “humanitarian settlements,” are often discussed together with informal settlements at large and have similar fire risk factors. Aspects of “humanitarian settlements” fall under the UN-Habitat definition of “informal settlements,” but the main distinction is that humanitarian settlements receive assistance from agencies in order to shelter and support displaced persons.

### 2.2.1 What is a refugee? What are humanitarian settlements?

According to the UNHCR, “A refugee is someone who has been forced to flee his or her country because of persecution, war or violence” [24] . As of May 2022, 100 million individuals worldwide were forcibly displaced as they faced conflicts or persecution in Europe, Asia, Africa, and Latin America [25] . In addition to conflicts, the worsening severity of natural disasters as a result of climate change is also expected to displace populations [26] .

“Humanitarian settlement” will be used to refer to a camp or community built, supported, and managed with the assistance of a humanitarian agency. Like other informal settlements, humanitarian

settlements may be “cut off from basic services and city infrastructure” and may be “situated in geographically and environmentally hazardous areas” [17] . Some settlement planning services are provided by agencies, but large populations and a lack of space may still lead to unplanned and poorly spaced construction.

Refugees may spend years or even decades living in camps; for ongoing crises, agencies may set up semi-permanent shelters and provide more services, such as education facilities for new generations [24] . The average time a displaced person spends in a camp is now estimated to be 17 years [27]

The largest refugee camps are the Kutupalong-Balukhali camp for Rohingya (Bangladesh), Bidi Bidi refugee camp (Uganda), Dadaab and Kakuma refugee camps (Kenya), Azraq and Zaatari refugee camps (Jordan), Nyarugusu, Nduta, and Mtendeli refugee camps (Tanzania), and Aw-barre and Sheder refugee camps (Ethiopia) [24]. There are also humanitarian settlements for Syrian refugees in Lebanon [28] , for Afghan refugees and victims of natural disasters in Pakistan [29] , for persons displaced by natural disasters in the Philippines [30] , for Venezuelan refugees in Colombia and Brazil [31] , [32] , for asylum seekers at the US-Mexico border [33] , and US asylum seekers in Costa Rica [34] .

### 2.2.2 Fire risk factors

Unintended fires and large conflagrations occur in refugee camps for similar reasons that they occur in other informal settlements. The built-environmental, natural-environmental, and behavioral risk factors described previously in 2.1.1 all apply in humanitarian settlements too. In 2020 and 2021, large refugee camp fires occurred successively in Greece (Lesbos), Bosnia (Lipa Camp), England (Napier barracks), Spain (Nijar), Bangladesh (Cox’s Bazar), Iraq (Sharya camp), Italy (Castelvetrano), and Lebanon (Miniyeh), to name a few that reached international news [35] . The fire severity and fatalities varied across incidents, with the largest being in Lipa Camp (1,400 people left without shelter in winter), Lesbos (12,000 people without shelter), and Cox’s Bazar (45,000 people without shelter and 15 dead) [35] .

When fire incidents destroy facilities or shelters, humanitarian agencies incur financial losses and have the additional burden of quickly providing more shelter and supplies. This interferes with the agencies' ability to assist already-struggling communities, as resources must be redirected from planned improvements into fire recovery efforts.

UN agencies and NGOs (non-governmental organizations) oversee camp layout and construction during initial settlement and recovery from disasters. More uniformity between dwellings in humanitarian settlements is expected compared to other informal settlements because residents are provided with a more consistent set of materials by humanitarian organizations, and ideally, camp managers direct communities to build according to guidelines set by documents such as Shelter/NFI Sector Technical Designs [5] or The Sphere Handbook [26] .

### 2.2.3 Fire mitigation efforts

Even with guidelines and standards, large gaps exist in humanitarian settlements regarding fire safety, as the issue involves cooperation between managing organizations, suppliers, the host community, and the displaced community. As an example, it is difficult to enforce fire safety-related guidelines like shelter separation distances if the residents do not understand that gaps between shelters cannot be used for storage, rubbish, or shelter expansion. Mitigation measures must be multi-pronged, involving fire departments, camp managers, and an educated community.

To address these gaps, organizations like Save the Children International and Operation Florian have provided fire safety consulting, health services, and education in refugee camps and informal settlements. In a recent joint effort in 2017, Save the Children and Operation Florian collaborated with the Lebanese Civil Defense fire fighting service to train, educate, and distribute fire extinguishers to the Syrian displaced peoples and host community living in Lebanon [36] .

## 2.3 The Rohingya Refugee Camps in Bangladesh

### Backdrop of the crisis

The Rohingya people were previously a Muslim ethnic minority living in the Rakhine State of Myanmar. In 1982, a new law denied them from claiming Myanmar citizenship, leaving the entire Rohingya population stateless <sup>5</sup> [37]. In the 1990s, increased military operations in the Rakhine State forced 250,000 Rohingya to find refuge in the neighboring Cox's Bazar region of Bangladesh [37].

Violence in 2017 led to a mass exodus of 1.1 million Rohingya refugees [37]. Of those displaced persons, 90% found refuge in Bangladesh and Malaysia [25]. In March 2018, 127 agencies partnered to provide shelter and resources to the sudden influx of 671,000 refugees to the existent camps at Cox's Bazar. As of January 2022, the total Rohingya refugees encamped in the Cox's Bazar district and southeastern districts of Bangladesh numbered 920,994 individuals [38].

<sup>5</sup> "A stateless person is someone who is not a citizen of any country. Citizenship is the legal bond between a government and an individual, and allows for certain political, economic, social and other rights of the individual, as well as the responsibilities of both government and citizen." [24]

### Challenges

Complications in tracking resources and assessing issues arose in 2018 due to a lack of consensus between the humanitarian actors on how to zone the camps in the Cox's Bazar district. Camps were divided into zones of 45-150 acres each, but the notation of the zones that was used by much of the humanitarian community (AA, BB, CC, etc.) was not adopted by other parties, such as the Government's Office of the Refugee Relief and Repatriation Commission (RRRC), the Bangladesh Army, and refugees themselves (who use a camp numbering system) [37]. This led to difficulties in communication and incorrect allocation of resources. Issues in coordination and ownership of plans led to the failure of the MSDP (Macro Settlement Development Plan) tool, a live document that would have compiled and analyzed all

topographical and planning data between humanitarian groups. Figure 1-2 displays a map compiled by the UNHCR showing the population distribution across camps (using the camp numbering system). Zooming into the Kutupalong area and surrounding camps, Figure 1-3 maps both the humanitarian community’s zoning system and the camp numbering system to show the overlap of the systems.

An additional challenge of housing so many Rohingya refugees in the southeastern districts of Bangladesh is friction with host communities. Both refugees that are living in camps and those that have settled in the urban areas of Bangladesh compete with the host population for space, resources, and labor opportunities [39]. Early construction of the camps led to severe deforestation in the Cox’s Bazar area as well [39]. Some local impoverished communities feel neglected by humanitarian agencies who from their view selectively aid the Rohingya people, leading to tension between Rohingya and Bangladeshi communities [39].

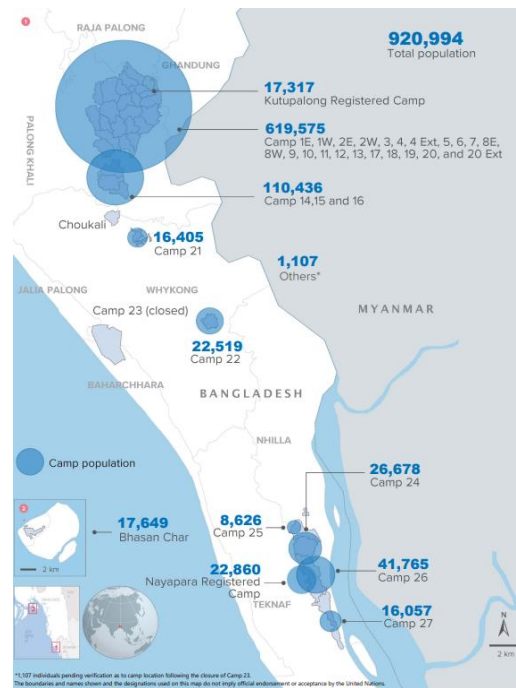


Figure 1-2. A UNHCR map showing the population distribution and the camp numbering system [37].



*The government, humanitarians and refugees were all using different zoning systems, which created confusion and caused coordination challenges. To address this, the Site Management Sector conducted a lengthy exercise to adopt a joint approach between the government's "camp" system and the international community's zones (Source: ISCG, 12 Feb 2018).*

Figure 1-3. A map of the Kutupalong area, showing the overlapping zoning and camp numbering systems [37] .

### 2.3.1 Fire incidents and perception of fire risk

As described in previous sections, the risk of fire increases in refugee camps like those in Bangladesh because of factors like a high density of dwellings, low access to fire fighting personnel/equipment, and informal or worn down infrastructure. In the Rohingya humanitarian settlements, depending on the camp in which a fire incident may take place, it can take 30 minutes to over an hour for the nearest personnel from Bangladesh fire stations to arrive on scene to control a fire due to limited road access [40] . Coordination of large fire fighting and fire recovery efforts are also challenging due to the lack of consensus between all parties on how to refer to locations, as some bodies use the zoning system and others use the camp numbering system.

In March 2021, a fire spread through Camps 8W, 8E, and 9, destroying more than 9,500 homes, displacing over 45,000 people and resulting in 15 fatalities [1] . Figure 1-4 shows the affected area, with red depicting burnt shelters and orange depicting the border of the affected camps [41] . Over 200 more fires were reported over the course of 2021 alone [2] . These incidents lead to enormous losses for the families with nowhere else to go as well as the humanitarian agencies who must provide for them and bear growing financial burdens.

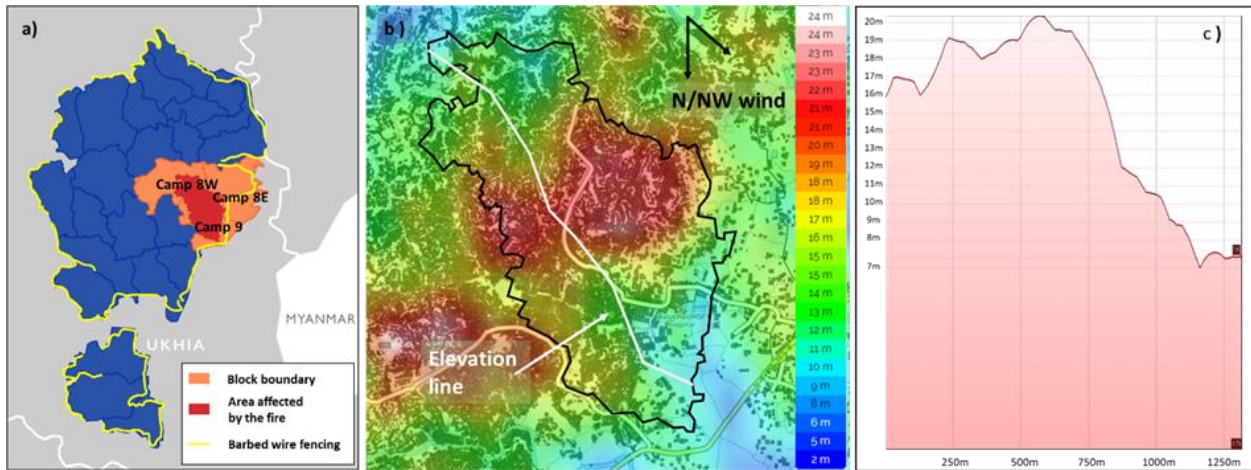


Figure 1-4. A map of the area affected by the March 2021 fire in Camps 8W, 8E, and 9 [37] .

A survey conducted by IOM included a question on how households in the Rohingya camps perceive fire risk. Only 11% of respondents reported feeling fully protected from fire in their home, with 42% of the remaining respondents feeling some protection and the last 47% feeling unprotected or unsure how to respond [42] . Clearly, a fire issue exists in the Rohingya settlements, and a majority of households feel insecure about their safety.

## 2.3.2 A “Standard” Shelter

What does a typical shelter look like?

Some level of uniformity is expected from dwelling to dwelling in the refugee camps at Cox’s Bazar, since organizations allocate “shelter kits” with similar materials and procedures for construction. However, there is no strict control over modification to or expansion of shelters, and some camps may undergo upgrade phases in order to increase the resilience of shelters against weathering or to provide more space or dignity to families. Also, different camps fall under the jurisdiction of different agencies. Although all organizations will typically refer to international guidelines for shelters and settlements, there is no requirement for shelter designs to be identical or consistent from jurisdiction to jurisdiction. In spite of differences in design and management, shelters will still use similar materials because there is an incentive to use local materials and bulk-order supplies to decrease transportation and material costs.

For these reasons, though there is no single “standard” shelter and though the camp will continue to grow and change with time, there will be many similarities between the size and construction of shelters within the Cox’s Bazar camps. In this report, the shelters built to the NFI design specifications [5] are regarded as an approximation of a typical shelter.

### The NFI Design

Technical design drawings were developed by the Shelter/NFI Partners [5] to rebuild or upgrade shelters affected by the March 2021 camp fire in Cox’s Bazar. Based on these drawings (shown in Figure 1-5), the dimensions of a typical shelter and its components can be approximated as:

- Overall living space (10’ x 15’ x 8’ or 3.06m x 4.6m x 2.5m)
- One door (30” x 72” or 0.8m x 1.8m)

The materials list in the NFI technical drawings provides a list of materials provided to build the shelters in Cox’s Bazar. The largest components are the bamboo structural framing, tarpaulin sheets and

polythene rolls for the walls and roof, and a concrete floor. Another execution of the design involves bamboo structural framing and woven-bamboo walls, tarpaulin sheets and polythene rolls for the roof, and a concrete floor.

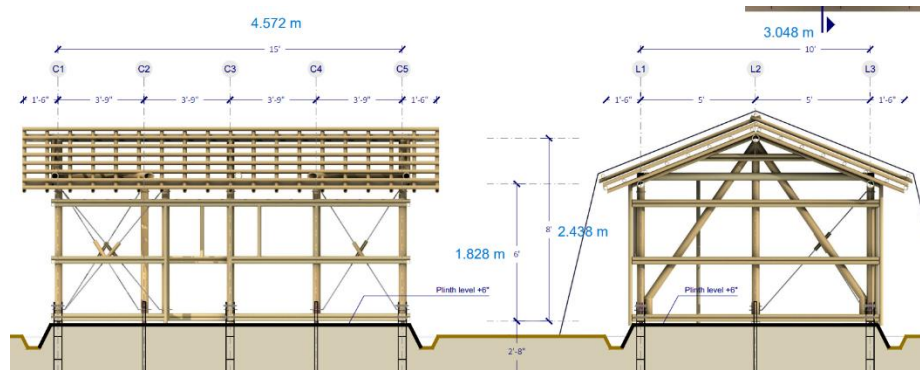


Figure 1-5. Technical design drawings developed by the Shelter/NFI Partners.

### Justifying the NFI design as a typical shelter

The NFI design drawings were created in the effort to rebuild shelters damaged in Camps 8E, 8W, and 9 during the March 2021 fire. However, several camps underwent drastic rebuilding and upgrading throughout 2017 and 2018 to provide more stable shelter for camp inhabitants in preparation for the monsoon season [37]. According to the Shelter Projects 2017-2018 overview, the “Upgrade Shelter Kit” provided to 180,000 households is similar to the construction materials provided in the NFI design drawings, so even if the scale of the upgraded and rebuilt “standard” shelters are not identical, the construction is similar.

The 2019-2020 edition of the Shelter Projects overview provides more detail into recent developments in shelter size, construction, and fire resistance. To address some fire safety concerns of residents, a fire-resistant material has been provided for wall protection in cooking areas [43]. Some shelters started to implement the “Mid-Term Shelter” design, which increases the height from that of the NFI standard shelter design (approximately 8 feet = 2.5 m) to approximately 14 feet (4.3 m) so that a mezzanine level could be built to provide more living space.

The 10' x 15' NFI design information would provide a rough estimate of shelter size and material, but it is clear from the two photographs in Figure 1-6 that there is a wide variation in shelter sizing, covering, configuration, and spacing.

The interior surfaces and property of camp inhabitants may also include plastic furniture, mosquito nets, hanging clothes, woven baskets, and some electric appliances (see Figure 1-7).



Figure 1-6. Photographs of Rohingya camp shelters (P. Chamberlain and D. Graham, personal communication, March 26, 2022).



Figure 1-7. Photographs of the interior of shelters (P. Chamberlain and D. Graham, personal communication, March 26, 2022).

### 2.2.3 Fire mitigation efforts

To address the fire issue in the Rohingya settlements, groups within IOM (International Organization for Migration), WFP (World Food Programme), UNHCR, and MOAS coordinated to form SMEP, the Site Management Engineering Project. The SMEP group develops engineered solutions for fire suppression and runs field tests, such as shelter burn tests in 2021 and material flammability tests with jute fiber and bamboo in 2022.

In 2021, SMEP developed portable pump-driven suppression systems and provided training for volunteers within the camp community so that residents could serve as first responders. Toward the end of observing shelter burning behavior and providing training to firefighting volunteers, teams in SMEP have run and recorded a series of full-scale burn tests.

In October to December 2021, different teams involved with SMEP conducted full-scale burn tests with shelters built to different specifications. One group burned shelters built with bamboo framing, woven-bamboo walls, and a tarp roof (as depicted in Figure 1-8).



Figure 1-8. Burn tests with shelters built with bamboo framing, woven-bamboo walls, and a tarp roof (photo ownership Mehedi Rahman).

Another group including staff from MOAS burned three shelters with NFI design dimensions, with two shelters using regular tarpaulin for the walls and roof (Shelters 1 and 2) and the third using a fire-retardant tarpaulin (Shelter 3). Table 2-1 provides overviews and links to the burn tests of Shelters 1, 2, and 3. Each fire was allowed to fully develop, then a team of suppression volunteers used water jets to extinguish the flames. For Shelters 1 and 3, another round of burning was recorded in corners of the shelters that were unaffected by the first burn test.

This project will analyze the burn tests of the non-fire-retardant NFI shelters, with a particular focus on Shelter 2. Shelter 2 was selected because the stationary, front-facing footage would be the most straightforward to calibrate and process.

Table 2-1. Burn tests of shelters built to the NFI design specifications

	<p>Shelter 1</p> <ul style="list-style-type: none"> <li>• Non Fire-Retardant Tarpaulin</li> <li>• <a href="https://youtu.be/q37mMzN5NqE">https://youtu.be/q37mMzN5NqE</a></li> <li>• Exterior, angled view</li> <li>• Stationary</li> </ul>
	<p>Shelter 1 Re-burn</p> <ul style="list-style-type: none"> <li>• Non Fire-Retardant Tarpaulin</li> <li>• <a href="https://youtu.be/KGd6ZYCngAI">https://youtu.be/KGd6ZYCngAI</a></li> <li>• View moves from interior to exterior</li> </ul>
	<p>Shelter 2</p> <ul style="list-style-type: none"> <li>• Non Fire-Retardant Tarpaulin</li> <li>• <a href="https://youtu.be/Xeho7THOWM0">https://youtu.be/Xeho7THOWM0</a></li> <li>• Exterior, front view</li> <li>• Stationary</li> </ul>
	<p>Shelter 3</p> <ul style="list-style-type: none"> <li>• Fire-Retardant Tarpaulin</li> <li>• <a href="https://youtu.be/WyjK4jHpQmo">https://youtu.be/WyjK4jHpQmo</a></li> <li>• Exterior, angled view</li> <li>• Stationary</li> </ul>
	<p>Shelter 3 Re-burn</p> <ul style="list-style-type: none"> <li>• Fire-Retardant Tarpaulin</li> <li>• <a href="https://youtu.be/0qN_7ge548M">https://youtu.be/0qN_7ge548M</a></li> <li>• View moves from interior to exterior</li> </ul>

## Chapter 3

# The Rohingya Shelter Burn Test

In this chapter, an initial analysis was performed for the Shelter 2 footage from the Rohingya shelter burn tests conducted by SMEP. The fuel load dimensions and the fire behavior timeline were determined.

The footage of the shelter burn tests were captured with a smartphone camera and uploaded to YouTube.com as videos with a frame size of 1280x720 pixels and a speed of 29.97 fps. For manipulation and analysis, the files were downloaded from YouTube.com as MP4 files with a resolution of 1920x1080 pixels and a speed of 29.97 fps.

The software used for initial video analysis is briefly described below:

- Kinovea: a free 2D motion analysis software with object-tracking and calibrated line measurement capabilities [44] .

### 3.1 Determination of Interior Fuel Load

The dimensions and composition of the interior fuel load used in Shelter 2 were estimated from video footage and correspondence with the SMEP members who ran the test. For a summary of each of the tests see Chapter 2, Section 2.2.3 “Fire mitigation efforts.”

The SMEP members who conducted the test have confirmed that similar fuels were used for each test, and that ignition was accelerated using diesel poured over the fuel pile (P. Chamberlain and D. Graham, personal communication, May 9, 2022).

Because there was no interior documentation of the fuel load in the Shelter 2 footage, a combination of images from the Shelter 1 Re-burn and the Shelter 2 test was used to determine the approximate geometry of the fuel pile inside of Shelter 2. An image of fuel load of Shelter 1 Re-burn was used to approximate the

fuel types and approximate geometry. In addition, the tarp wall in Shelter 2 burns away to reveal the interior fuel pile, providing more information on the geometry of the fuel load.

Length measurements were made using the Kinovea software, which performs automatic pixel-to-length conversions once provided with a reference length. Reference lengths for the pixel-to-length conversion were based on plans from the NFI Shelter Design (see Chapter 2).

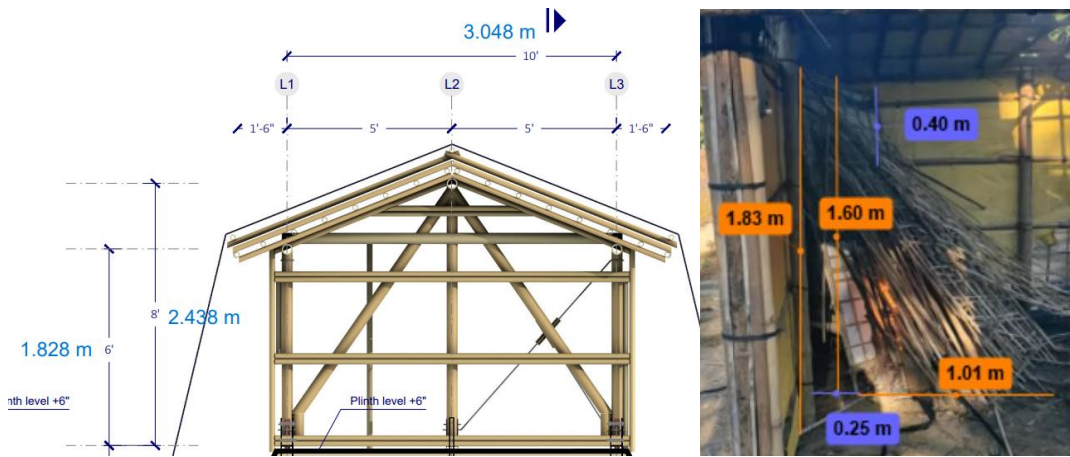


Figure 3-1. NFI Shelter plans (left) were used to calibrate measurements of the Shelter 1 Re-burn in Kinovea (right). The unburned contents of the Shelter 1 Re-burn (bamboo walls and scraps) can be seen.



Figure 3-2. NFI Shelter plans (left) were used to calibrate measurements of Shelter 2 in Kinovea (right).

In Figure 3-1, the unburned fuel used in the Shelter 1 Re-burn can be seen. The bulk of fuel appears to be a loose pile of the same bamboo used to provide structural framing in the shelter, with some tarpaulin stretched across the wall piece at the back of the pile. In Figure 3-1 and 3-2, Kinovea measurements provide estimates for the height of the pile in the Shelter 1 Re-burn and the length of the pile used in the Shelter 2 burn test.

Based on the Kinovea measurements and imagery from the tests, the Shelter 2 internal fuel load consisted mainly of bamboo arranged in a sloped pile. Going forward, the assumed dimensions of the fuel pile are: a height of 1.6 m, a base width of 1.0 m, and a base length of 2.0 m.

## 3.2 Shelter Burn Test Timeline

In order to provide benchmarks to compare results in FDS models to the experiments, a timeline of the shelter burning behavior was established from the video Shelter 2 footage.

The timeline is summarized in Figure 3-3. Benchmark behaviors include the first sign of smoke outflow, the beginning of rapid burn away for the tarp roof, the beginning of rapid burn away for the tarp wall, the first peak in flame height, the dip in flame height, and finally, growth into a fully developed flame.

Coordinators of the burn test provided estimates in the range of 10 to 60 seconds for the time between ignition of the internal fuel load and the beginning of recording. This creates a range of possible timelines (shown in Figure 3-3). An estimation of the pre-footage time,  $x$ , as 10 seconds would point to aggressive fire development. An estimation of  $x = 60$  seconds would point to relatively slow fire development, and an estimation of  $x = 30$  seconds would provide a timeline in between. Given that a diesel accelerant was placed on the fuel pile, the results of the FDS model would be reasonable if the benchmark behaviors fall between the possible timelines where  $x = 10$  seconds and  $x = 30$  seconds.

Time in video + x: (s)	22 + x	30 + x	40 + x
Video			
Observation:	Smoke outflow visible.	Rapid roof tarp burn away.	Rapid wall tarp burn away.
Possible timelines: (s) x = 10 x = 30 x = 60	30 50 80	40 60 90	50 70 100

Time in video + x: (s)	45 + x	52 + x	98 + x
Video			
Observation:	First peak in flame height.	Flame decreases in size.	Fire grows until fully developed. Volunteers extinguish fire.
Possible timelines: (s) x = 10 x = 30 x = 60	55 75 105	62 82 112	108 128 158

Figure 3-3. Timeline of benchmark shelter burning behaviors, where time = 0 seconds would be ignition.

Though the timeline does not extend to the natural extinction of the flame, after the volunteers douse the flame, the front wall (i.e. the wall with the door, furthest from the camera) can be seen through the hole that the fire burns through in the back wall. The post-extinguishment state of the shelter is shown in Figure 3-4.



Figure 3-4. After volunteers extinguish the fire, the burn away that occurred on the back wall is visible.

### 3.3 Unique Challenges

Some unique challenges presented by this case are that the thin tarp walls burn away as the fire develops and that the fuel pile must be involved in burning gradually through flame spread.

In a typical enclosure fire, the flame is allowed to develop within a space where the volume and ventilation openings are assumed constant. A correlation based on a series of enclosure fire experiments was created by Kawagoe et al. for fully developed, ventilation-controlled wood fires [45] :

$$\dot{Q} = 0.09 A_o \sqrt{H_o} \Delta H_{eff} , \quad (1)$$

where  $\dot{Q}$  is the heat release rate (or fire size) in kW,  $A_o$  is the area of the ventilation opening ( $m^2$ ),  $H_o$  is the height of the ventilation opening (m), and  $\Delta H_{eff}$  is the effective heat of combustion of wood. The correlation shows that in a fully-developed room fire, the fire size is largely dependent on the dimensions of the ventilation opening.

However, ventilation openings do not remain constant in informal shelter fires, where roofs and walls are consumed during fire development. A modeling approach is necessary to estimate the conditions

within the shelter because previously developed correlations of estimating fire size and temperature changes within enclosures cannot account for changes in ventilation dimensions, nor do they consider the contribution of convective cooling on fire development.

The additional challenge is that the model developed for this scenario must include a mechanism for gradual fire spread through the fuel pile, due to the observation that the roof burns away approximately 10 seconds before the wall burns away (see Figure 3-3). The fuel pile is essentially flush against the tarp walls; if the whole pile were to uniformly radiate heat and burn, the walls would heat up before the roof. The only way to recreate the condition where the roof has time to burn away first is to introduce a mechanism for the fire to spread from a distant side of the pile toward the tarp wall. Moreover, to approximate the speed at which fire spreads through the pile in the burn test, the properties of the modeled bamboo fuel pile must be adjusted in order to reflect the fact that the pile is covered in an accelerant with a lower ignition temperature than bamboo.

# Chapter 4

## Image Processing Methods

Through image processing, the consumption rate of the burning tarp wall and flame height of the Shelter 2 fire were measured, and the heat release rate of the fire was estimated. The results of image processing and the validation of FDS results against the image processing data can be found in Chapter 6.

The software packages used for video analysis and editing were Premiere Pro, Kinovea, and MATLAB. A brief description of each software's relevant capabilities is provided below:

- Adobe Premiere Pro: a video editing software with video stabilization capabilities.
- Kinovea: a free 2D motion analysis software with object-tracking and calibrated line measurement capabilities.
- MathWorks MATLAB (abbreviation of "MATrix LABoratory"): a programming language and computing environment with several preset functions for image grayscaling and binarization provided in the Image Processing Toolbox (IPT).

### 4.1 Measured and Estimated Quantities

#### 4.1.1 Tarp Consumption and Flame Height Measurements

Two metrics that could be measured from the Shelter 2 footage were the tarp burn away over time and the flame height over time. The tarp area consumption and the flame height will be compared to FDS results in Chapter 6 in order to validate the models developed for this scenario (see Chapter 5 for FDS model development). A description of the assumptions used to measure these quantities is provided in this section, and the methods and implementation are provided in 4.2 and 4.3.

The main assumption about the loss of tarp area on the wall of the shelter is that the loss is due to ignition and burn away. Other factors may play a role in the loss of the tarp, such as pure melting of the plastic coating of the tarp (that is not followed by gasification and combustion) or tearing due to shrinkage from exposure to heat. In an image (such as Figure 4-1), there is no discernable difference between tarp area that has been lost due to burning away, melting, or tearing, so it will be assumed that all tarp area lost has been involved in burning.

The area of the blue wall, visible in Figure 4-1, was processed between 23.32 - 66.66 seconds (frames 700 to 1700 from the Shelter 2 footage). Every pixel containing a blue hue associated with the tarp was counted and converted to an area value, which could be tracked over time. The range of time for tarp area consumption analysis was selected because rapid burn away was observed in this time frame. Before this range of time, no change in the tarp was observed, and after this range of time, the tarp burn away was gradual. The blue side wall was selected for analysis because the pixel-to-area calculations are simple (compared to calculations for an angled plane like the roof).



Figure 4-1. The Shelter 2 tarp on the roof and walls has burnt away, and the flame tip extends past the height of the roof. Timestamp: 62.45 seconds.

For flame height, it was assumed that the location of the topmost image pixel with a red hue associated with flames could be converted into a length, which could be tracked over time. Several

definitions exist for flame height, such as the chemical flame height, which can be defined as the axial location of 99% complete combustion or the location where the ratio of CO to CO<sub>2</sub> is 0.15 [46]. In a study measuring the height of small jet flames through image processing, Zheng defined flame height as the height of the blue reaction zone caused by CO<sub>2</sub> and CH\* chemiluminescence [46].

In an image of the large shelter fire (such as Figure 4-1), the blue reaction zone of the flames would not be visible. Fortunately, the green background of the forest provides contrast to the red, luminous flames rising from the shelter, so a red hue was the main criterion for measuring flame height. Because some of the luminous gases rising from the shelter may be smoke rather than gases participating in combustion, an additional luminous intensity criterion was also used to filter out pixels with a low brightness.

The flame heights were tracked between 43.34 - 96.70 seconds (frames 1300 to 2900 from the Shelter 2 footage). This is the range of time where the flame is visible through the burnt away tarp wall and roof, before the flame is extinguished by volunteers.

#### 4.1.2 Heat Release Rate Estimation

An approximation of the heat release rate (HRR) of the shelter fire was made using the Heskestad correlation relating pool fire flame height and diameter to fire size [47]:

$$z_f = 0.23 \dot{Q}^{2/5} - 1.02 D, \quad (2)$$

where  $z_f$  is the flame height (m),  $\dot{Q}$  is the HRR or fire size (kW), and  $D$  is the pool diameter (m).

Though the Heskestad correlation is intended for pool fire applications, it provides an order of magnitude estimate for the shelter fire. Some sources of uncertainties are as follows. The fuel package in the shelter is not a pool of liquid fuel but a mixed fuel pile with diesel, plastics, and bamboo. The exact dimensions of the fuel pile are also unknown. In addition,  $z_f$  is considered the flame height above the virtual origin of the flame, but with a sloped fuel pile, the virtual origin may be higher up than the ground and may even rise with time as the flame spreads up through the pile and to shelter walls. The calculations will merely provide an order-of-magnitude estimate of HRR.

The estimation of the HRR provided by the Heskestad correlation will be compared to the HRR data generated by FDS models.

## 4.2 Binarization in MATLAB

### 4.2.1 Otsu Thresholding

The pre-existing binarization functions in MATLAB are not able to narrowly select regions of interest such as tarp area or flame, as seen in Figure 4-2. However, it is important to understand how they work.



Figure 4-2. Shelter 1 binarized with the *rgb2gray*, *graythresh*, and *imbinarize* functions in MATLAB.

The established method for binarizing images that MATLAB uses in its functions was developed by Nobuyuki Otsu for already grayscale images.

The MATLAB *imread* function reads images into the MATLAB workspace as an  $m \times n \times 3$  matrix, with  $m \times n$  elements representing the total pixels in the image. Each pixel is assigned three values representing the intensities of Red, Green, and Blue in that pixel (this is RGB, or “truecolor” imaging). Hence, each pixel will have an R, G, and B value associated with it that falls between 0 and 255.

Grayscale is automatic in MATLAB using the *rgb2gray* function, where images in the RGB format are reassigned a grayscale value between 0 and 1. The *graythresh* and *imbinarize* functions then apply the Otsu method to the grayscale image.

In the Otsu threshold method, a threshold value is determined below which pixels are black (re-assigned the value of 0) and above which pixels are white (re-assigned the value of 1). The threshold is arrived at through an iterative algorithm that minimizes the variance between foreground pixels (those that will be assigned to white) as well as the variance between all background pixels (those that will be assigned to black). The formula for the within-class variance at threshold  $t$  is [48]:

$$\sigma^2(t) = \omega_{bg}(t)\sigma_{bg}^2(t) + \omega_{fg}(t)\sigma_{fg}^2(t), \quad (3)$$

where  $\sigma^2(t)$  is the variance of color values,  $\omega_{bg}(t)$  and  $\omega_{fg}(t)$  represent the probability of the number of pixels for each class at the threshold  $t$ , and  $\sigma_{bg}^2(t)$  and  $\sigma_{fg}^2(t)$  are the variance for each class.

The result is color-blind, one might say. In Figure 4-2, regions like the sky or bright pieces of the tarp or ground are as likely to be re-assigned a white value as regions with fire.

## 4.2.2 Specified RGB Thresholding

A modified method of binarizing in MATLAB was made in order to select for particular colors in an image, such dark blue for tarp area consumption or red/orange for flame height measurements.

To do this, RGB value thresholds were determined that maximized the contrast between the target region of interest and all other colors that should be relegated to the background. Figure 4-3 very broadly describes patterns in RGB values that produce certain target colors for fire, tarp, or greenery.

				<b>Colors Associated with Fire</b>
R 255	R 255	R 255	R 233	Red is characterized by high values of R, and yellow by high values of R and G.
G 0	G 255	G 150	G 99	Orange hues are similarly characterized by high values of R, but the values of G are lower than R, and the values of B are even lower.
B 0	B 0	B 0	B 32	
				<b>Others (tarp, greenery)</b>
R 12	R 140	R 73	R 10	Dark blues: very low R, very low G, high B.
G 30	G 200	G 253	G 102	Light blues: low R, high G, high B.
B 186	B 240	B 85	B 16	Light greens: low R, high G, low B.
				Dark greens: very low R, low G, very low B.

Figure 4-3. RGB combinations associated with fire, tarp, and greenery.

For the tarp consumption analysis, the target region is the blue tarp. The left image of Figure 4-4 shows narrow cropping of the tarp wall. The close cropping eliminates the need to maximize contrast against colors such as green (forest), light blue (sky), or brown (ground). When pixels with a B value greater than 30 are reassigned to a black color, the binarized image displays both consumed tarp and bamboo supports as white (see Figure 4-4, right). An averaged value for the non-tarp area over 5 seconds before the tarp begins to burn away gives an estimate of the area of bamboo present in the frame. The averaged bamboo area may be subtracted from the non-tarp area measurements in order to isolate only the area that is being consumed as the tarp burns away.

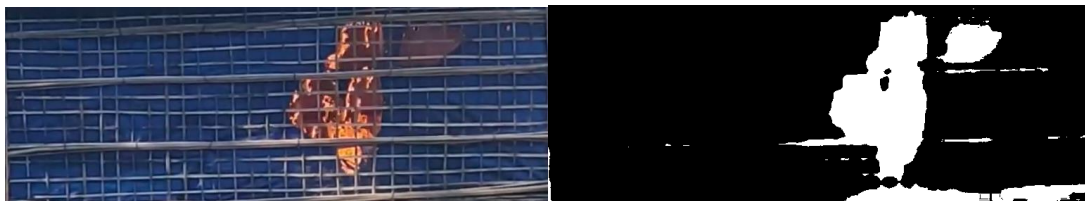


Figure 4-4. Tarp Area (left) and binarized with a blue criterion (right). Timestamp: 39.14 seconds.

For the flame height analysis, the target region is the luminous parts of the flame, excluding soot and smoke. The flame extends from the shelter (with bamboo and tarp) up to a region with trees and sky. To binarize an image with several regions of color, the color thresholds must maximize the contrast of the

fire region to everything else. Figure 4-5 shows colors sampled from each region and describes methods to increase the contrast of each region to the fire colors. In addition, applying the Otsu intensity threshold described in the previous section further eliminates smoky areas.

In summary, the fire region can be successfully contrasted from all background colors if pixels are selected with the Otsu intensity criterion as well as with R values that are greater than 130 *and* that are greater than G values by 50. An example of a processed flame height frame is provided in Figure 4-6.

From there, the location of the topmost white pixel can be used to calculate the flame height, and the lengths can be tracked over time. Figure 4-7 shows how the location is calculated.

All MATLAB scripts are commented and included in Appendix section A4.2.

Region:	Sample Colors:	Methods to Increase Contrast to Fire:
Bamboo	[215 181 148], [254 207 187], [80 47 40] 	<ul style="list-style-type: none"> <li>• <math>R &gt; 130</math></li> <li>• <math>G &lt; R - 50</math>, G values are always higher so no dependence on B</li> </ul>
Fire	[243 169 127], [251 188 89], [191 106 98] 	
Sky	[147 187 240], [126 171 230], [182 205 243] 	<ul style="list-style-type: none"> <li>• <math>G &lt; R</math></li> <li>• <math>B &lt; R</math></li> </ul>
Smoke	[185 112 82], [118 37 29], [67 75 79] 	<ul style="list-style-type: none"> <li>• Red/Orange tones might be included in "Fire" so a criterion for pixel intensity is needed.</li> <li>• <math>G &lt; R</math></li> <li>• <math>B &lt; R</math></li> </ul>
Tarp	[255 253 254], [25 30 56], [78 84 138] 	<ul style="list-style-type: none"> <li>• <math>G &lt; R - 50</math></li> <li>• <math>B &lt; R</math></li> </ul>
Trees	[155 155 0], [47 51 38], [72 86 43] 	<ul style="list-style-type: none"> <li>• <math>G &lt; R - 50</math></li> <li>• G values are always higher so no dependence on B</li> </ul>

Figure 4-5. RGB samples from regions in the shelter images and methods to increase contrast to fire.

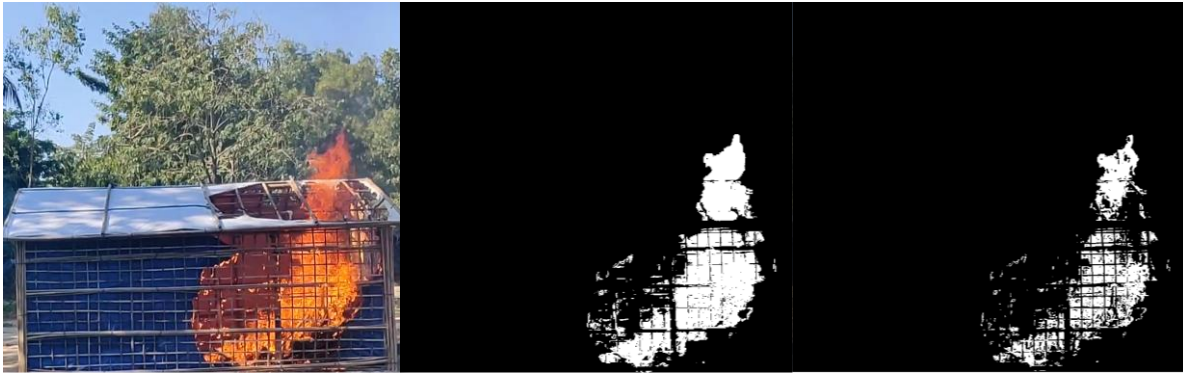


Figure 4-6. Colored photo of shelter fire (left), binarized photo with red criterion (middle), and binarized photo with red and intensity criteria (right).

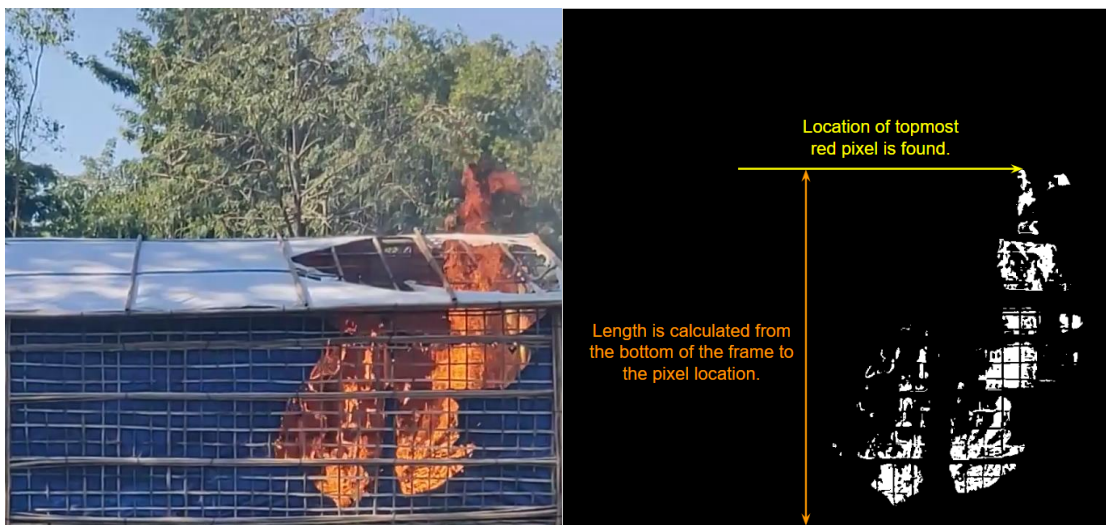


Figure 4-7. Flame height measurement. Timestamp: 55.55 seconds.

### 4.3 Stabilization, Cropping, and Calibration

Because the burn test footage was taken with a handheld smartphone camera, the position of the shelter drifts within frame. Thus, the crop window must be changed frame-by-frame so that the bottom of the shelter aligns to the bottom of the cropped frame and the sides of the shelter wall align with the sides of the cropped frame.

To eliminate some drifting, the Shelter 2 footage was edited using the Adobe Premiere Pro “Warp Stabilizer” effect with the “No Motion” setting, which uses position, scale, and rotation adjustments to let

large objects appear as if they are not moving in the frame. Because the video was scaled and rotated, near the end of the fire development, the flame is cut off at the top of the frame.



Figure 4-8. Tracking markers in Kinovea.

All cropping was completed in MATLAB using the *imcrop* function, which requires the coordinates of the crop window. The coordinates were found using the Kinovea software, which tracks markers that are placed on objects in a video and provides the pixel coordinates. Figure 4-8 shows markers dropped at the bottom corners of the shelter. The coordinates were manually collected into an Excel spreadsheet at an interval of every 10 frames, and the spreadsheet was referenced by the MATLAB for the cropping coordinates.

The stabilization step is crucial before cropping, because even with approximate coordinates tracked by Kinovea, the shelter may be crooked inside the crop window, which drastically changes the flame height measurement, as shown in Figure 4-9.

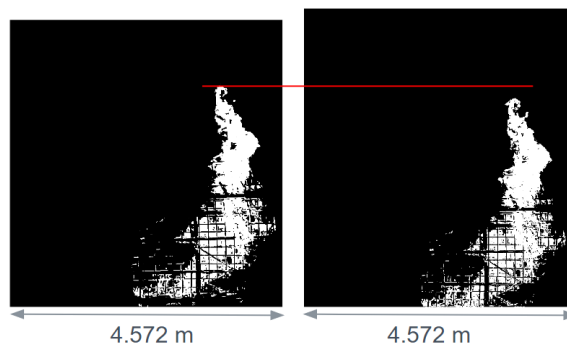


Figure 4-9. A stabilized and unstabilized cropped frame from the same time.

## Chapter 5

# FDS Model Construction and Setup

The following section will summarize the FDS model set-up, including the model geometry, FDS devices used, fuel properties, fuel validation, and variations of fuel configuration used for the shelter burn simulations. All simulations were run using parallel processing on the UMD High Performance Clusters, Deepthought2 and Zaratan. FDS was designed such that each mesh in a model should be assigned to a single MPI processor; shelter simulations used one node and up to 8 processors. Run times varied between 6 and 15 hours, depending on simulation duration and diagnostics included.

### 5.1 Shelter and Fuel Pile Geometry

The shelter was situated in the center of the simulation domain, which was split into 8 meshes. Each mesh was 4.0 m x 3.5 m x 3.0 m, for a total domain of 8.0 m x 7.0 m x 6.0 m. The extension of the mesh by at least 1 m beyond the walls of the shelter allowed for the placement of instrumentation and a more accurate representation of air entrainment into the shelter. All boundaries, except for the ZMIN boundary (the ground) were assigned the OPEN condition. Ambient conditions remained set to the FDS defaults, as the weather conditions during the burn test were unknown.

The shelter geometry was based on the NFI Design described in 2.3.2. The dimensions of the shelter were 4.6 m x 3.0 m x 1.8 m with a 0.8 m x 1.5 m door opening in the front. The roof was sloped at an angle of approximately 18 degrees. The walls and roof were assigned the material properties of tarp. To approximate the bamboo mesh from the shelter design, thin strips with the properties of bamboo were placed between the walls and the roof. The ground was assigned the properties of concrete.

Visualizations of the shelter from the exterior, front, back, and side are provided in Figures 5-1 to 5-3.

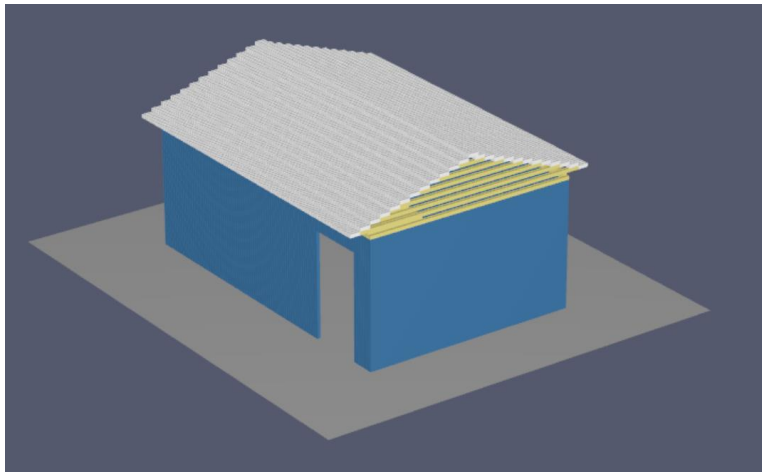


Figure 5-1. Exterior view of the shelter.

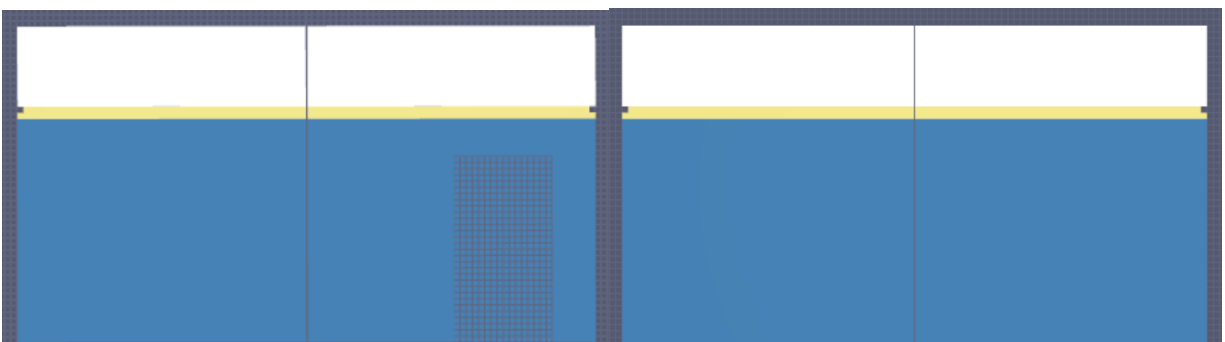


Figure 5-2. Front and back views of the shelter. (The grid is shown to provide contrast between the door and the blue tarp walls.)



Figure 5-3. Side view of the shelter.

The fuel pile geometry was approximated from the images and measurements summarized in 3.1. Two channels were cut into the fuel pile using the HOLE feature in FDS, in order to better represent the porous nature of the fuel pile. Figure 5-4 provides a visualization of the fuel pile.

Baseline material properties for the shelter and fuel pile can be found in 5.3.3. The full FDS scripts including the model geometry are in Appendix section A5.1.

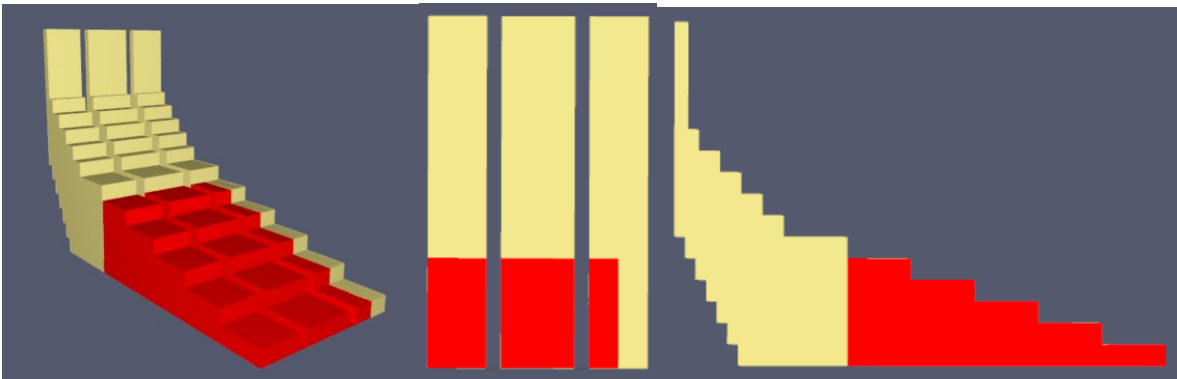


Figure 5-4. Approximate fuel pile with a base of 1 m x 2 m and sloped rise to a height of 1.6 m.

## 5.2 Instrumentation Devices and Spacing

Devices were placed in and around the shelter to collect flame height, temperature, and heat flux data as the simulated fire spread through the fuel pile and consumed the shelter.

Flame height measurements are recorded using a modified version of the flame height diagnostic described in the FDS User Guide in Chapter 21.10.6. The modification reduces the recorded quantities from flame tilt and flame height to only flame height. The criterion that FDS User Guide suggests for finding flame height is the elevation below which lies 95 percent of the HRRPUV (Heat Release Rate Per Unit Volume). A column of DEVC instruments with QUANTITY = 'HRRPUV' is needed to find that 95 percent location. With the modification, the devices do not need to be placed at the center of the fire, and so the column is placed at the center of the shelter. The placement of the column of HRRPUV devices is shown in Figure 5-5.

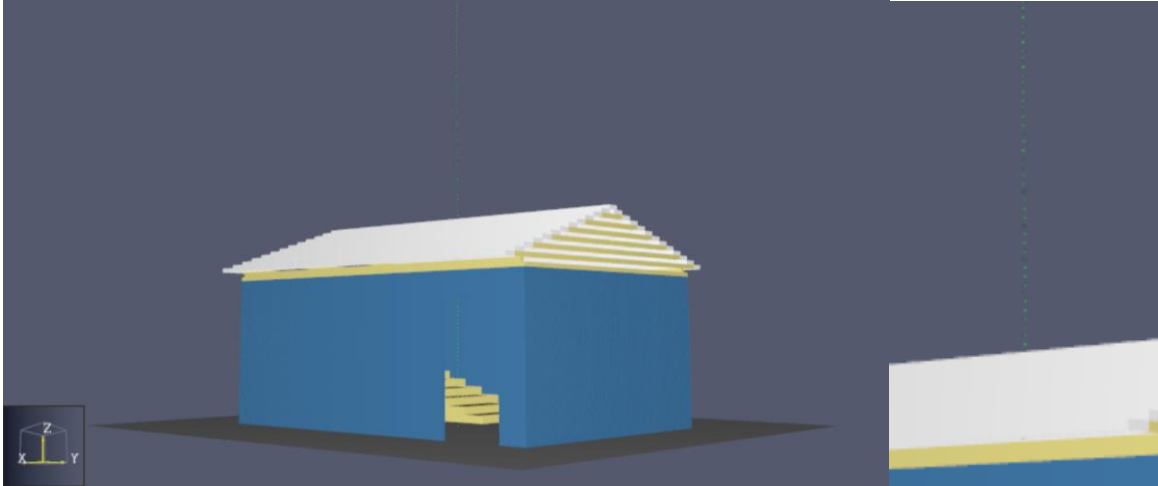


Figure 5-5. The column of HRRPUV devices is shown in green. The center of the roof is zoomed-in on the right.

Heat flux (HF) information is collected using DEVC instruments with QUANTITY = 'RADIATIVE HEAT FLUX GAS'. The orientation of these devices is such that they are pointed toward the center of the shelter at an angle perpendicular to the nearest wall. The resulting data approximates processed data from a heat flux gauge.

Because the 'RADIATIVE HEAT FLUX GAS' device collects heat flux information dependent on orientation to the source of radiation and the orientations of devices are not optimized to capture the maximum possible radiative heat flux, another metric called 'INTEGRATED INTENSITY' is used to track the total incoming radiative energy at a point from all angles. The 'INTEGRATED INTENSITY' devices produce an output in  $\text{kW}/\text{m}^2$ , like the 'RADIATIVE HEAT FLUX GAS' devices. Integrated intensity and radiative heat flux measurements in FDS are related in that 'INTEGRATED INTENSITY' measures intensity over a  $4\pi$  solid angle while 'RADIATIVE HEAT FLUX GAS' measures intensity over a  $2\pi$  solid angle. Equations describing this relationship are in Appendix section A5.2.

Three heat flux and integrated intensity devices are placed inside the shelter, 0.05 m from the floor. The layout for the devices inside the shelter is shown in Figure 5-6.

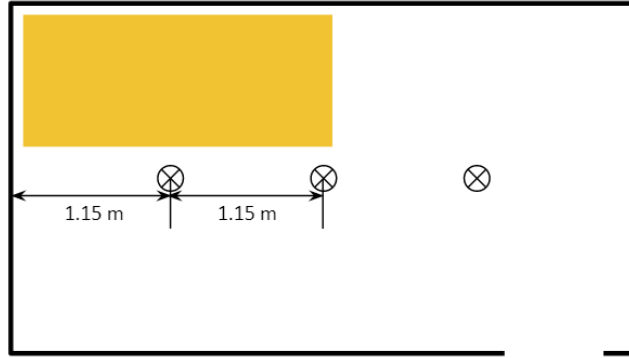


Figure 5-6. Layout of heat flux and integrated intensity devices inside the shelter.

All heat flux devices outside the shelter are placed at the elevation of 1.5 m, which is slightly above the height where burn away begins on the tarp wall, as well as at 2.0 m, which would be at roof level for another shelter. The layout for the heat flux and integrated intensity devices outside the shelter is shown in Figure 5-7.

Refer to Appendix A5.1 for the full annotated FDS code for the placement of devices.

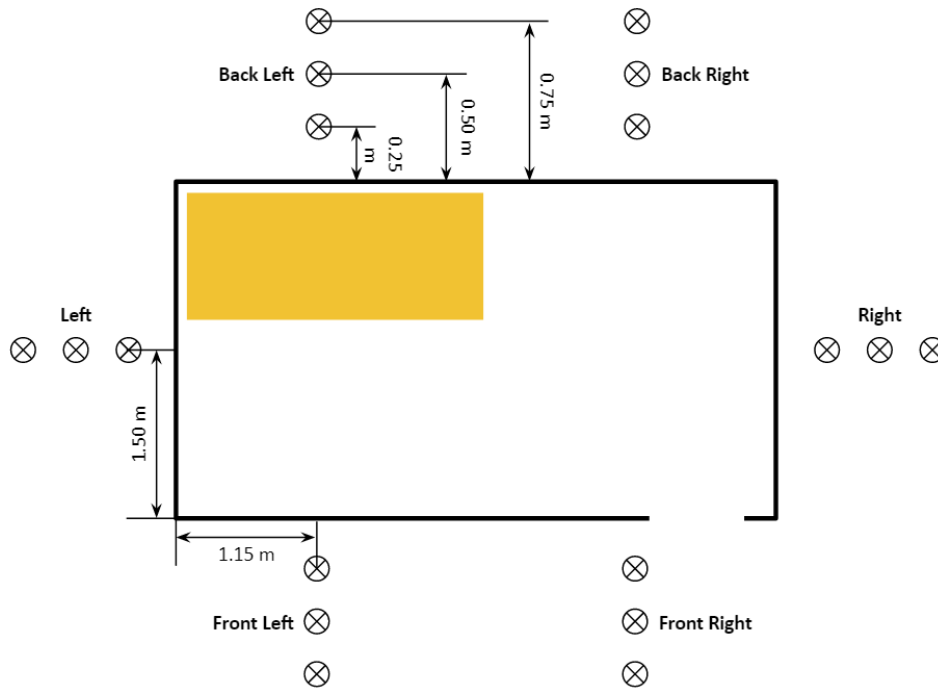


Figure 5-7. Layout of heat flux and integrated intensity devices inside and around the shelter.

## 5.3 Model and Preliminary Material Properties

### 5.3.1 Grid Resolution

The grid size used for all shelter simulations was 5 cm or 0.05 m. Grid size should be carefully considered when modeling in FDS, since a large grid size will not resolve the physics of the problem correctly, but a grid size that is too small will drastically increase the run time as the computational cost scales with grid size to the fourth power.

For this scenario, the relevant length scale,  $L$ , could be identified as the door opening, the gap length between the strips of bamboo, the width of the fuel pile, or the tarp thickness. Entrainment of air and smoke transport takes place through the door opening and the gaps between the strips of bamboo, and fire spreads through the fuel pile and to the tarp.

The general rule of thumb to size the computational grid is  $L/\Delta x \geq 10$ , where  $\Delta x$  is the grid size.  $L = 0.8$  m for the door opening,  $L = 0.05$  m for the gaps between bamboo strips,  $L = 1.0$  m for the fuel pile width, and  $L = 0.00036$  m for the tarp thickness. The resulting  $\Delta x$  are 0.08 m, 0.005 m, 0.1 m, and 0.000036 m, respectively. To prevent unreasonably long run times, the grid resolutions of 0.005 m and 0.000036 m for the gaps between bamboo and the tarp thickness were eliminated. A grid size of 0.05 m, or 5 cm, was selected to resolve the length scales of the door and fuel pile.

All thin materials (bamboo strips and tarp) were assigned a length of one-cell for their thickness dimension as an obstruction. However, in the SURF lines, bamboo and tarp were defined as having a THICKNESS = 0.018 and 0.00036 m to be used for all heat transfer calculations.

### 5.3.2 Simple Chemistry Model and Reaction Properties

By default, FDS uses a simple chemistry mixing-controlled model to define pyrolysis and combustion as a single step. Pyrolysis is the solid phase heating process that generates flammable vapor at the fuel surface, whereas combustion is the gas phase reaction between the fuel vapors and oxygen. When using the simple

chemistry model in FDS, only one fuel reaction per simulation can be prescribed. The reaction is assumed to be infinitely fast and governed by the mixing of fuel and oxygen [9] .

The lumped species simplification for the combustion reactions combines all species into groups, with fuel, air, and products being the lumped species. FDS uses the prescribed information from the reaction (REAC) line (chemical formula, soot yield, CO yield, and heat of combustion) to calculate the stoichiometric coefficients of the combustion reaction equation. More details can be found in the FDS User Guide [9] and the Technical Reference Guide [10] .

The approximate reaction properties for bamboo and the heat of combustion of tarp, which are the two components involved in burning, are summarized in Table 5-1. Though only one main reaction can be defined in FDS, every other fuel should have its own heat of combustion prescribed. In the case of the shelter, bamboo is the main fuel so the reaction line in FDS uses the burning properties of bamboo or wood. The tarp walls and roof are also involved in combustion, so the heat of combustion for tarp is included on the tarp material line so that the heat release rate of burning tarp cells can be more accurately calculated using the heat of combustion of tarp rather than that of bamboo.

The soot yield fraction is based on the findings of a study by [49] , where enclosure fires were modeled in FDS with different soot yield fractions. It was found that using a range of 0.05 to 0.20 for the soot yield of upholstered furniture fires, the models over-predicted the smoke density. Even a fraction of 0.05 still provided the closest by still conservative agreement with smoke density compared to experiments. Therefore, a soot yield of 0.04 is used for the mixed fuel package of bamboo, tarp, and diesel. The CO yield is approximated as 0.0075 kg CO/kg fuel, which is based on the CO yields of 0.007 and 0.008 kg/kg measured by [50] for laminated bamboo exposed to calorimeter heat fluxes of 50 and 75 kW/m<sup>2</sup>. Likewise, the heat of combustion is approximated as 11,750 kJ/kg, the average of the measured heats of combustion for laminated bamboo exposed to calorimeter heat fluxes of 50 and 75 kW/m<sup>2</sup>.

Though the bamboo pile is the main fuel source for the shelter fire, the tarp shelter material will also burn, so “HEAT\_OF\_COMBUSTION= 43300” [51] is prescribed on the MATL line for tarp.

See the REAC line used in the full FDS code provided in Appendix section A5.1.

Table 5-1. Reaction Properties used in FDS.

Reaction (REAC) Line Quantities	Value
FUEL (name string)	'REAC_FUEL'
C	3.4
H	6.2
O	2.5
SOOT_YIELD (kg/kg)	0.04
CO_YIELD (kg/kg)	0.0075
HEAT_OF_COMBUSTION (kJ/kg)	11750

### 5.3.3 Material Properties from Literature

The materials used in a typical Rohingya camp shelter are described in 2.3.2. To simplify the model, only a few components are included in the simulations– bamboo for the fuel load and some shelter structure components, tarpaulin (tarp) for the walls and roof, and concrete for the floor and surrounding ground.

Properties found in literature are compiled in Table 5-2. Many of the properties for tarp could not be found, so approximations for specific heat, conductivity, and emissivity are drawn from the properties of polyethylene, which forms the coating for most tarps [52] . For some properties with a range of values (such as the specific heat and conductivity of polyethylene), approximately average values were used in FDS. Hand calculations or preliminary FDS models were done for other properties with a large margin of uncertainty, such as the tarp and bamboo densities, ignition temperatures, and HRRPUA values. A summary of the hand calculations and series of preliminary simulations is provided in 5.3.4.

Table 5-2. Material Properties from Literature.

Material	Density [kg/m <sup>3</sup> ]	Thickness [m]	Specific heat [kJ/kg-K]	Conductivity [W/m-K]	Ignition Temp. [C]	HRRPUA [kW/m <sup>2</sup> ]
Bamboo (Structure and fuel load)	687 <sup>[50]</sup>	0.018 <sup>[5]</sup>	2.26 <sup>[53]</sup>	0.25 <sup>[53]</sup>	297 - 320 <sup>[50]</sup>	100 - 200 <sup>[50]</sup>
Tarpaulin (Walls and roof)	519.4 - 636.6 <sup>[54]</sup>	0.00036 <sup>[54]</sup>			150 - 980 <sup>[55]</sup>	~ 16 <sup>[60]</sup>
Polyethylene (Tarpaulin coating)	HD: 965 <sup>[56]</sup> LD: 926 <sup>[56]</sup>		1.83 (linear) <sup>[57]</sup>	HD: 0.44-0.52 <sup>[58]</sup> LD: 0.33 <sup>[58]</sup>	349 <sup>[51]</sup>	
PCC concrete (Floor)	2400 <sup>[59]</sup>	0.3 <sup>[5]</sup>	0.6918 <sup>[59]</sup>	1.625 <sup>[59]</sup>		

## 5.4 Hand Calculations and Preliminary FDS Simulations

Preliminary simulations and hand calculations were done with different material properties to ascertain the potential impacts of densities, ignition temperatures, and HRRPUA values upon flame height or burn away behavior. Modifications were made to achieve closer results to the results from image processing, and burning behaviors observed in the Shelter 2 Burn Test. Chiefly, the simulations should recreate conditions where the tarp roof begins to burn away before the tarp wall, and both should begin to burn away in under 60 seconds.

The image processing results are summarized later in Chapter 6, and the timeline of the Shelter 2 fire can be found in Section 3.2.

### 5.4.1 NIST Tarp Experiment Replication in FDS

The first set of preliminary simulations focused on recreating an experiment done by NIST [60], where a tarp sheet was ignited, and flames were allowed to spread until natural extinction. Photographs and the HRR profile from the experiment are provided in Figures 5-8 and 5-9.

This study also provided an estimate for the HRRPUA for the tarp, as the tarp in the experiment burned with a peak HRR of 16 kW (listed in Table 5-3), and the tarp dimensions were reported as 3.0 m x

2.4 m. The time to peak is listed as approximately 1 minute in Table 5-3. However, from the images in Figure 5-8, it is clear that the full surface area of the tarp could not have fully contributed to combustion, nor was all of the tarp burning at the same time. Roughly estimating that 1 m<sup>2</sup> of the tarp was involved at the time of the peak HRR, the HRRPUA would be approximately 16 kW/m<sup>2</sup>.



Figure 5-8. Tarp experiment by NIST [60] .

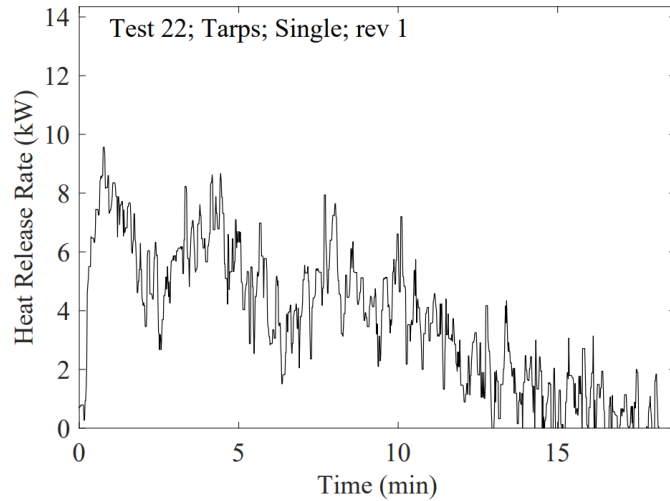


Figure 5-9. HRR profile of tarp, experiment by NIST [60] .

Table 5-3. Summary of test results for the NIST tarp experiment [60] .

Test No.	Item	No. Items	Initial Mass (kg)	Final Mass (kg)	$\Delta H_{O_2}$ (MJ/kg)	Peak HRR (kW)	Total Energy (MJ)	Time to Peak (min)	$\Delta H$ (MJ/kg)	CO Yield	CO <sub>2</sub> Yield	Soot Yield
24	Tarp	2	1.56 ± 0.02	—	13.1 ± 0.7	16 ± 5	8.3 ± 4.5	1.2 ± 0.2	—	—	—	—

Using tarp material properties from Table 5-3 and known dimensions from the NIST experiment, a small-scale simulation was run in FDS to recreate the experiment. The grid resolution of these simulations was 0.05 m. Since the sheet of tarp was folded over in half, two 2.4 m x 1.5 m x 0.05 m slabs were created in FDS with a separation thickness of one cell. The bottom edges of the slabs were ignited with hot particles at 1000°C, to imitate ignition with a lighter flame. The tarp surfaces were set with the condition “BURN\_AWAY=.TRUE.” so that the material could be consumed at the rate prescribed by the HRRPUA. The visualization of the FDS simulation is shown in Figure 5-10.

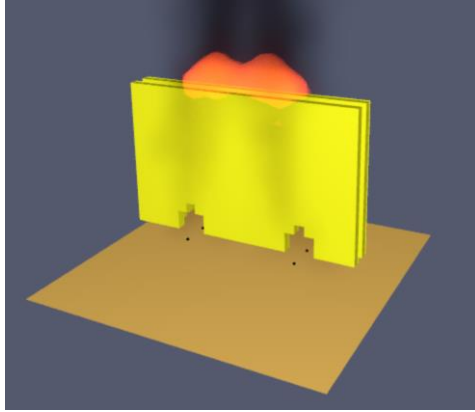


Figure 5-10. NIST experiment imitation simulation in FDS.

The burning of the tarp in the NIST test took over 20 minutes, so to save computational time, the FDS model was modified to have an accelerated fire development. Instead of prescribed HRRPUA values on the same order of magnitude as shown in Figure 5-9, a value of  $50 \text{ kW/m}^2$  was chosen in order to observe how FDS executes burn away behavior on a shorter timeline. Simulations showed that when the tarp material reached the prescribed ignition temperature, it would lose mass at a rate determined by the HRRPUA and the heat of combustion for the tarp.

It was also found that exposure to the hot particles was the dominant mode of ignition. In some versions of the simulations, the hot particles were “turned off” after 30 seconds, and the ignited area of the tarp would no longer spread. In versions of the simulations where the hot particles remained on, the areas of the tarp exposed to the plume of warmed air created by the hot particles were involved in burning. This reveals that the combustion of the tarp, as simulated in FDS, is not energetic enough to sustain ignition and spread without external heating. Because the grid resolution is 0.05 m, the small scale reactions cannot be properly resolved. However, in the shelter fire scenario, the tarp walls will be exposed to a large source of heat, and so it is acceptable for the combustion of the tarp alone to be unable to sustain flame spread. Figure 5-11 shows the difference between a simulation where the ignitor particles turn off and a simulation where the ignitor particles remain on.

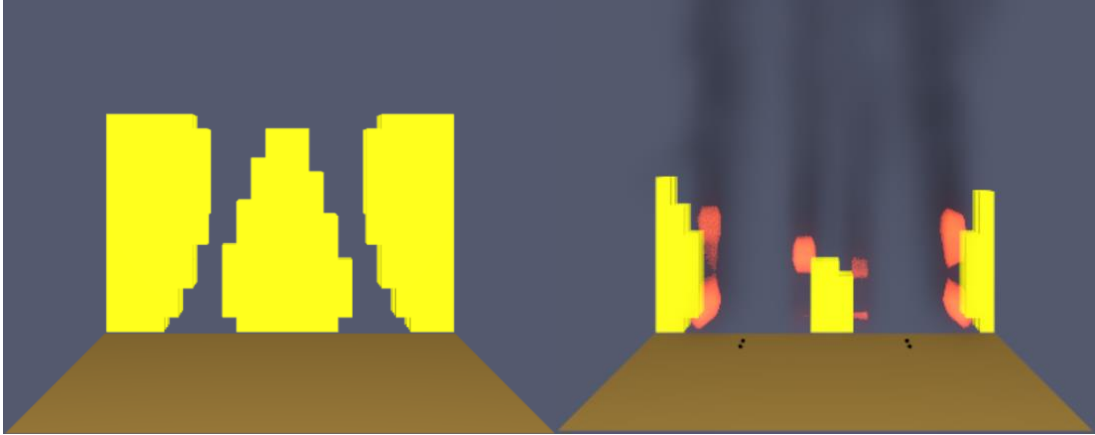


Figure 5-11. At  $t = 100$  s, the FDS tarp simulation with the ignitor particles turned off at  $t = 30$  s (left) and the FDS tarp simulation with the ignition particles remaining on for the whole simulation (right).

After the accelerated simulations, 20-minute simulations were run with a HRRPUA value of  $10 \text{ kW/m}^2$ . In these simulations, it was observed that one cell of tarp would burn away 232 seconds after reaching ignition temperature. This is based on metrics from BURNING RATE devices that were placed on the tarp near the ignition particles. The burning rate over time for a single cell is shown in Figure 5-12. The burn away time of 232 seconds, nearly four minutes, is too high to represent the Shelter 2 fire, where significant portions of the tarp must burn away by 60 seconds of simulation time.

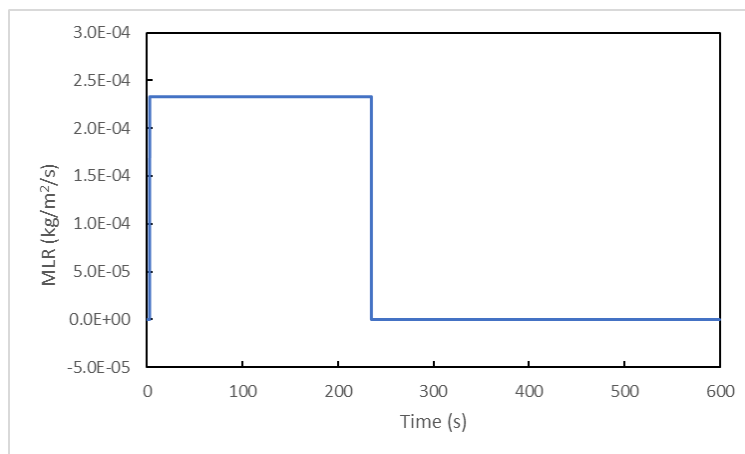


Figure 5-12. Burning rate over time for a single cell.

## 5.4.2 Tarp Burn Away Time Hand Calculations

In order to bring burn away behaviors simulated in FDS closer to those observed in the Shelter 2 footage, it was necessary for  $t_{burnout}$ , the time for a cell of tarp to burn away, to be less than 60 seconds.

To do this, modifications were made to the HRRPUA and  $k\rho c$  for the tarp material, as both material properties are estimated with large uncertainty. The uncertainty stems from the properties being derived from specification sheets for tarp used in humanitarian settlements as well as from HRR data from a NIST experiment completed with different tarp.

Hand calculations for  $t_{burnout}$  were done by manipulating the HRRPUA and  $k\rho c$  (through the mass density,  $\rho$ ), using the following series of equations:

$$ML = \rho \times d , \quad (4)$$

$$MLRPUA = HRRPUA \div HOC , \quad (5)$$

$$t_{burnout} = ML \div (2 \times MLRPUA) , \quad (6)$$

where ML is the mass load, MLRPUA is the mass loss rate per unit area, and HRRPUA is the heat release rate per unit area. The thickness,  $d$ , is 0.00036 m, and the heat of combustion, HOC, is 43300 kJ/kg. The  $t_{burnout}$  is divided by a factor of two because when tarp reaches ignition temperature in FDS, the front and back surfaces of the tarp cell are engaged in burning, so the MLRPUA is doubled. The calculations are summarized under Table 5-4, where  $t_{burnout}$  values under 60 seconds were bolded.

Another motive to reduce the  $k\rho c$  was to decrease the time to ignition for the tarp material. The relationship between  $k\rho c$  and the time to ignition for thermally thin and thermally thick surfaces can be expressed as [47] :

$$\text{Thin: } t_{ig} = \frac{\rho c d (T_{ig} - T_o)}{\dot{q}''} \quad (7)$$

$$\text{Thick: } t_{ig} = \frac{\pi}{4} k \rho c \frac{(T_{ig} - T_o)^2}{\dot{q}''^2} \quad (8)$$

where  $t_{ig}$  is the ignition time (s),  $k$  is the thermal conductivity of the solid (kW/mK),  $\rho$  is the density of the solid (kg/m<sup>3</sup>),  $c$  is the specific heat of the solid (kJ/kgK),  $T_{ig}$  is the ignition temperature (°C),  $T_o$  is the initial

temperature of the solid ( $^{\circ}\text{C}$ ),  $\dot{q}''$  is the net heat flux on the surface ( $\text{kW}/\text{m}^2$ ), and  $d$  is the thickness or diameter of the fuel ( $\text{m}$ ).

It was determined that a  $kpc$  fraction of  $1/8$  and HRRPUA of  $30 \text{ kW}/\text{m}^2$  produced a  $t_{\text{burnout}}$  low enough to allow time for heating and to observe significant burn away of the tarp walls and roof within 60 seconds of simulation time.

Table 5-4. Hand calculations for  $t_{\text{burnout}}$ , modifying HRRPUA and  $kpc$ .

HRRPUA $\text{kW}/\text{m}^2$	$kpc$ Fraction	$\rho$ $\text{kg}/\text{m}^3$	Mass Load $\text{kg}/\text{m}^2$	MLRPUA $\text{kg}/\text{s}/\text{m}^2$	$t_{\text{burnout}}$ s
15	1	580	0.209	3.49E-04	299.3
15	1/2	290	0.104	3.49E-04	149.6
15	1/4	145	0.052	3.49E-04	74.8
15	1/8	72.5	0.026	3.49E-04	<b>37.4</b>
15	1/16	36.25	0.013	3.49E-04	<b>18.7</b>
20	1	580	0.209	4.65E-04	224.5
20	1/2	290	0.104	4.65E-04	112.2
20	1/4	145	0.052	4.65E-04	<b>56.1</b>
20	1/8	72.5	0.026	4.65E-04	<b>28.1</b>
20	1/16	36.25	0.013	4.65E-04	<b>14.0</b>
25	1	580	0.209	5.81E-04	179.6
25	1/2	290	0.104	5.81E-04	89.8
25	1/4	145	0.052	5.81E-04	<b>44.9</b>
25	1/8	72.5	0.026	5.81E-04	<b>22.4</b>
25	1/16	36.25	0.013	5.81E-04	<b>11.2</b>
30	1	580	0.209	6.98E-04	149.6
30	1/2	290	0.104	6.98E-04	74.8
30	1/4	145	0.052	6.98E-04	<b>37.4</b>
<b>30</b>	<b>1/8</b>	<b>72.5</b>	<b>0.026</b>	<b>6.98E-04</b>	<b>18.7</b>
30	1/16	36.25	0.013	6.98E-04	<b>9.4</b>

#### 5.4.2 Preliminary Shelter Fire Simulations

With the density and HRRPUA of tarp determined through calculation, the remaining variables were determined through short shelter fire simulations that focused on capturing key ignition behaviors. The

target of the preliminary simulations was to observe the tarp roof begin to burn away before the tarp wall, as well as observe significant burn away in both in under 60 seconds. The remaining variable material properties were the ignition temperature of the tarp, the HRRPUA of the bamboo fuel pile, and the configuration of the ignition region for the fuel pile.

First, a series of simulations were run with a tarp ignition temperature based on that of polyethylene, which is approximately 350°C. This temperature was on the lower end of the tarp ignition temperature range of 150-980°C. In these simulations, the full fuel pile was involved in burning from the beginning, so that variations due to spread across the fuel pile could be considered in later simulations. The bamboo HRRPUA (BH) was varied between 100, 150, and 200 kW/m<sup>2</sup>.

For all simulations in Series\_BH, the tarp wall was involved in burning before the roof, which does not align with observations from the Shelter 2 footage. The progression of the shelter fires for the varied bamboo HRRPUA is shown in Figure 5-13.

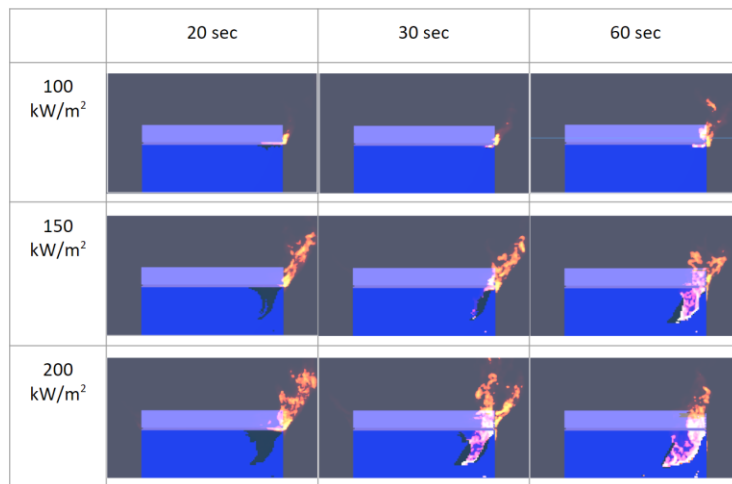


Figure 5-13. Series\_BH shelter visualization at t = 20, 30, and 60 seconds.

Dozens of 60-second simulations were run with variations in ignition area configurations along with tarp ignition temperature and bamboo HRRPUA values. Many failed to show tarp burn away comparable to that observed in the Shelter 2 footage. Observations from these failed simulations revealed trends, such as:

- Small ignition regions lead to burn away after the target of 60 seconds. The slow spread rate from the ignition region to the rest of the pile led to smaller fire sizes for longer periods of time, and thus a slower rise in temperature for the tarp walls and roof. An ideal model should have a larger ignition area, to accelerate fire spread and line up with the aggressive timeline of the footage.
- Ignition regions that extended fully to the side with the tarp wall led to the wall burning away before the roof, which is the opposite of the behavior from the footage. Ignition regions that are initially too close to the tarp wall provide heating too early in the shelter's fire development. An ideal model should have an ignition region that involves a corner of the fuel pile furthest from the tarp walls.
- All bamboo HRRPUA values and ignition configurations led to visible "flames" (HRRPUV, heat release rate per unit volume, visualizations in FDS) extending out of the shelter through the ventilation gaps at the side, while in the video only smoke was visible through the ventilation gaps, not flame. An ideal model would have a much milder initial fire development until the burn away of the tarp roof and walls. Unfortunately, to heat the tarp to potential ignition temperatures, the prescribed HRRPUA values for the bamboo pile needed to be at least 100 kW/m<sup>2</sup>, which led to the flames jetting out through the ventilation. Matching the burn away behavior of the FDS model to the video was prioritized over matching the flame heights during initial fire development.

The next series of shelter simulations, called "Series\_WideCorner," had a run time of 120 seconds. To save on computational time, devices were not run with this series. The tarp ignition temperature (TT) was reduced by more than half to 150°C, which is the lower bound of the tarp temperature range from literature. The bamboo HRRPUA was varied from 100 to 200 kW/m<sup>2</sup> by increments of 25 kW/m<sup>2</sup>. The ignition portion of the pile (shown in Figure 5-14) was a wide portion of the bottom corner, which allows for aggressive fire spread toward the wall and up the fuel pile toward the roof. FDS visualizations at 35, 45, and 100 seconds in the run time were collected for each simulation and summarized in Figure 5-15.

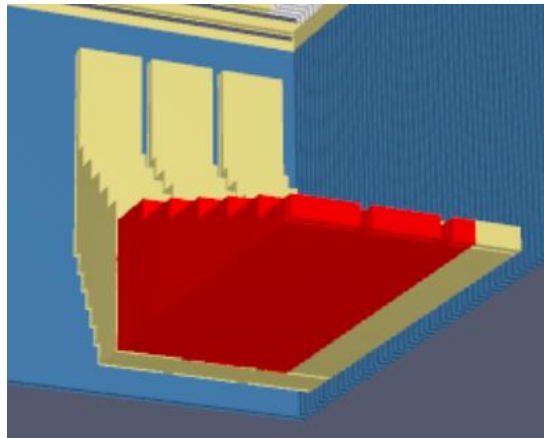


Figure 5-14. Wide ignition portion of the fuel pile, indicated in red.

In Series\_WideCorner, it was observed that in the 125 - 200 kW/m<sup>2</sup> simulations, there was almost complete burn away of the front wall (i.e. the wall with the door, which is opposite the fire) at 100 seconds. Also, visually gauging the flame heights around 100 seconds, it appeared that the flames were too high for the 200 and 175 kW/m<sup>2</sup> fuel pile HRRPUA, and too low for 100 kW/m<sup>2</sup>.

For the next series of simulations (which will be discussed in Section 5.5), the tarp ignition temperature was increased to 175°C to reduce the burn away at the front wall. In addition, to keep flame heights in an acceptable range to compare to the results of image processing, the range of the bamboo fuel pile HRRPUA was narrowed down to 125 and 150 kW/m<sup>2</sup>.

After the preliminary models, the range of properties was narrowed down to values that produced desired flame height behavior and burn away behavior in the tarp. Ultimately, only the HRRPUA of the bamboo fuel pile varies in the final series of simulations.

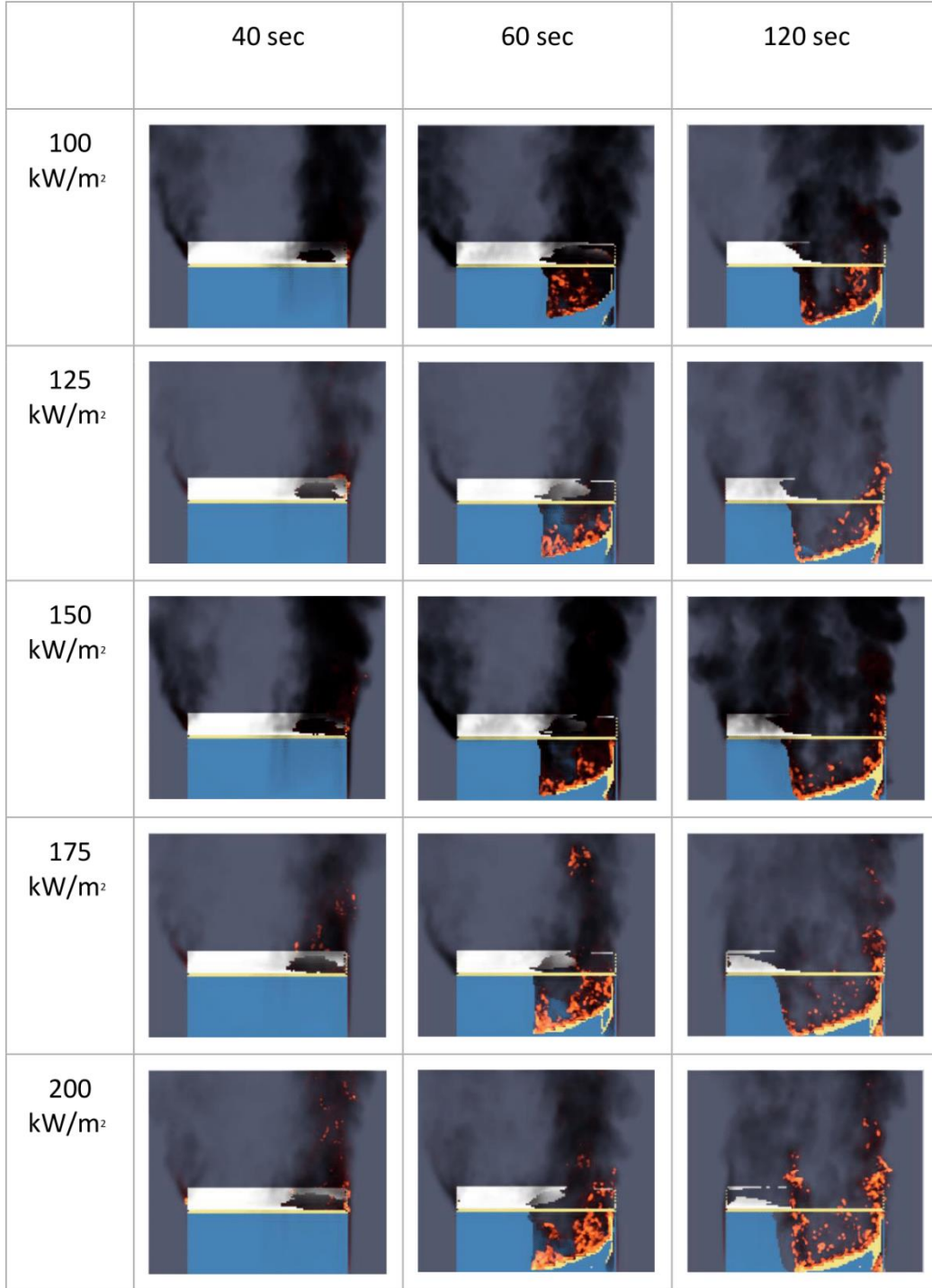


Figure 5-15. Series\_WideCorner FDS visualizations of the back wall at 35, 45, and 100 seconds.

## 5.5 Full FDS Shelter Fire Simulations

The final series of shelter simulations were run for 150 seconds to capture fully developed burning behavior. This section describes the set of material properties used for this series and the three configurations used for the fuel pile ignition zone.

The material properties used in FDS are summarized in Table 5-5. The bamboo HRRPUA, which varies between two values in the final series of simulations, is expressed as a range. See the SURF and MATL lines used to define all properties in the full FDS code provided in Appendix section A5.1.

Table 5-5. Material Properties used in FDS.

Material	Density [kg/m <sup>3</sup> ]	Thickness [m]	Specific heat [kJ/kg-K]	Conductivity [W/m-K]	Ignition Temp. [C]	HRRPUA [kW/m <sup>2</sup> ]
Bamboo	687	0.018	2.26	0.25	100	125-150
Tarpaulin	72.5	0.00036	1.80	0.44	175	30
Concrete	2400	0.3	0.69	1.62		

The ignition zone of the fuel pile was modified to create varying ignition conditions that could promote aggressive fire spread and heating of the tarp structure. It was found in the preliminary models that ignition zones that were too small would not promote fire spread or would lead to tarp burn away that was inconsistent with what was seen in the Shelter 2 footage. The Wide Corner and Stout Corner configurations were found to produce tarp burn away behavior consistent with the Shelter 2 burning timeline.

FDS visualizations for each configuration are presented in Figure 5-16. Please see Appendix section A5.5. for the OBST lines used to create the geometry for the fuel pile configurations in FDS.

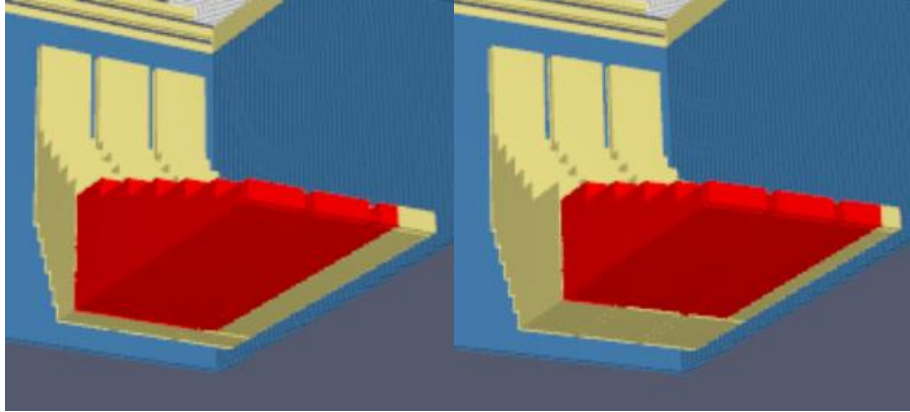


Figure 5-16. Wide Corner Configuration (left) and Stout Corner Configuration (right).

All FDS visualizations for the Wide Corner and Stout Corner configuration simulations at 125 and 150 kW/m<sup>2</sup> displayed the ideal burn away behavior, where the roof disappeared before the wall nearest to the fuel pile. Visually, the flame heights appeared to match the video.

These simulations were run with only flame height devices in order to single out the simulations that best match the results of image processing (shown in Figure 5-17 and reported fully in Chapter 6). The FDS flame height measurements are shown in Figure 5-18. The flame height of the Wide Corner simulation at 150 kW/m<sup>2</sup> exhibited too high of a second peak, and the Stout Corner simulation at 125 kW/m<sup>2</sup> failed to reach a second peak at all.

The flame height results of the Wide Corner simulation at 125 kW/m<sup>2</sup> and the Stout Corner simulation at 150 kW/m<sup>2</sup> were closest to the measured flame height from image processing.

The Wide Corner simulation at 125 kW/m<sup>2</sup> and the Stout Corner simulation at 150 kW/m<sup>2</sup> were run with devices to collect the flame height, shelter ceiling temperatures, heat flux, and integrated intensity profiles around the shelter. The same image processing techniques described in Chapter 4 were applied to the FDS movies to collect the tarp loss over time. The results from these simulations are summarized in Chapter 6.

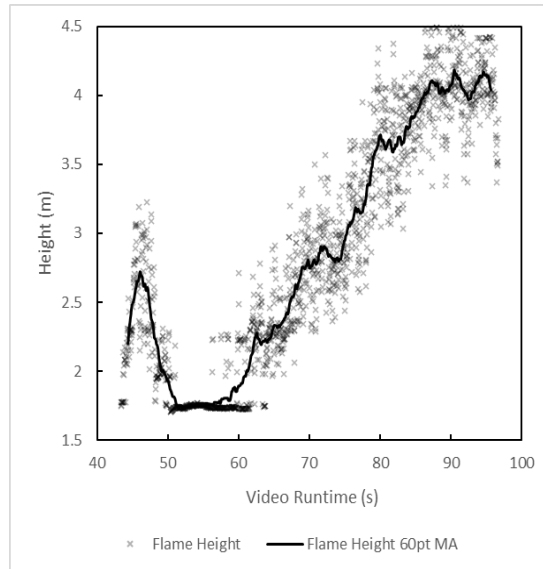


Figure 5-17. Flame height results from image processing, for comparison to FDS results.

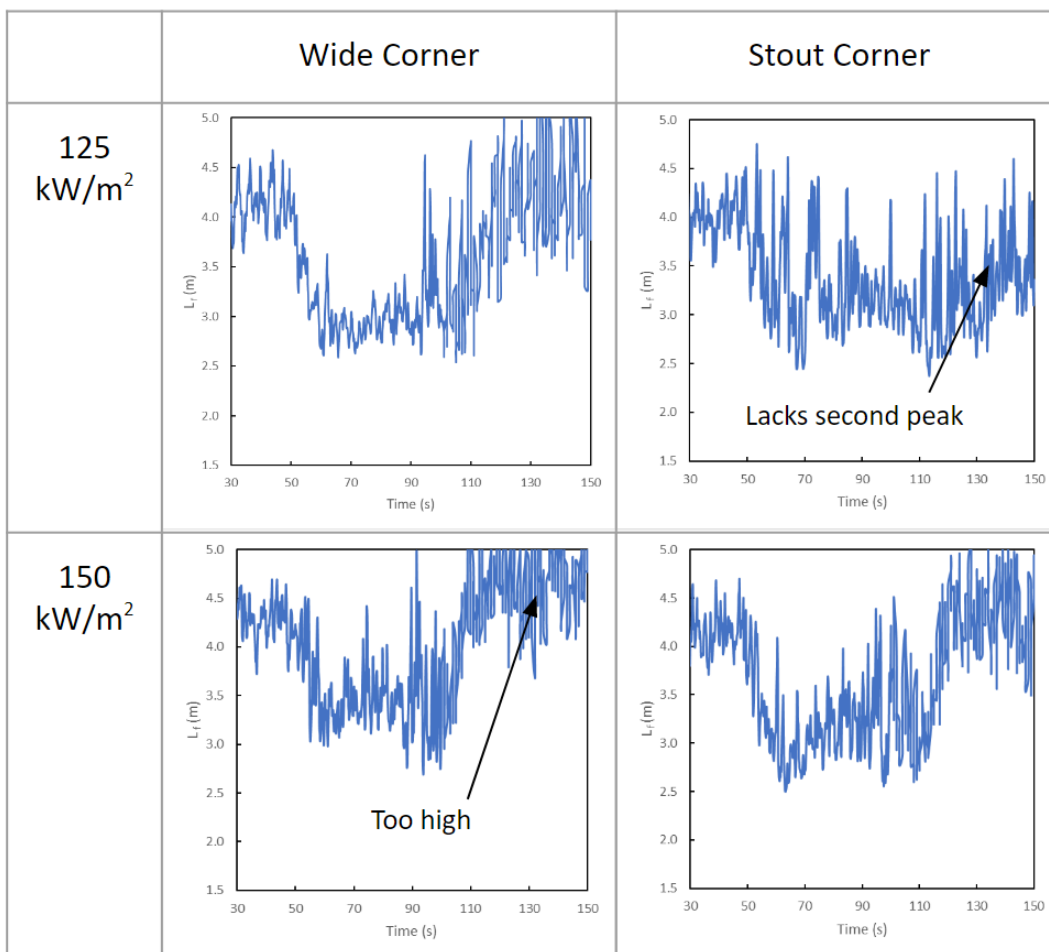


Figure 5-18. FDS flame height results for the Wide Corner and Stout Corner configurations.

# Chapter 6

## Results

This section will summarize the results of the image processing, the validation of FDS results against the image processed (IP) results, as well as the FDS temperature and heat flux instruments.

### 6.1 Shelter Burn Test Image Processing Results

The consumed area of the back tarp wall, consumption rate of change (ROC) of the back tarp wall, the flame height, and the Heskestad HRR estimate over time are reported in Figures 6-1, 6-2, 6-3, and 6-4. A 60-point moving average was used for each set of results, as x points is roughly equivalent to 2 seconds, which effectively smooths the data.

The IP results line up very well with the timeline of Shelter 2 burning behaviors previously compiled in Chapter 3. For instance, the timeline in Chapter 3 notes that rapid burn away of the wall begins around 40 seconds; this lines up with the rise in tarp loss between 30 and 50 seconds (visible in Figure 6-1) as well as the rise and plateau of the rate of consumption between 30 and 50 seconds (visible in Figure 6-2). Also, two flame height peaks were visually observed in the footage and noted in the timeline at 45 seconds and around 90 seconds. In Figure 6-3, the IP flame height measurements indicate two peaks, a short peak at 45 seconds and a higher peak at 90 seconds.

It is notable that the tarp consumption ROC begins to decrease at approximately 45 seconds, and at the same time, the flame height begins to decrease as well. The decrease in flame height is possibly due to the flame tilting; as the flame tilts away from the open wall, it would lead to a decrease in tarp consumption.

From IP flame height results, the steady burning flame height for a shelter is approximately 4.1 m.

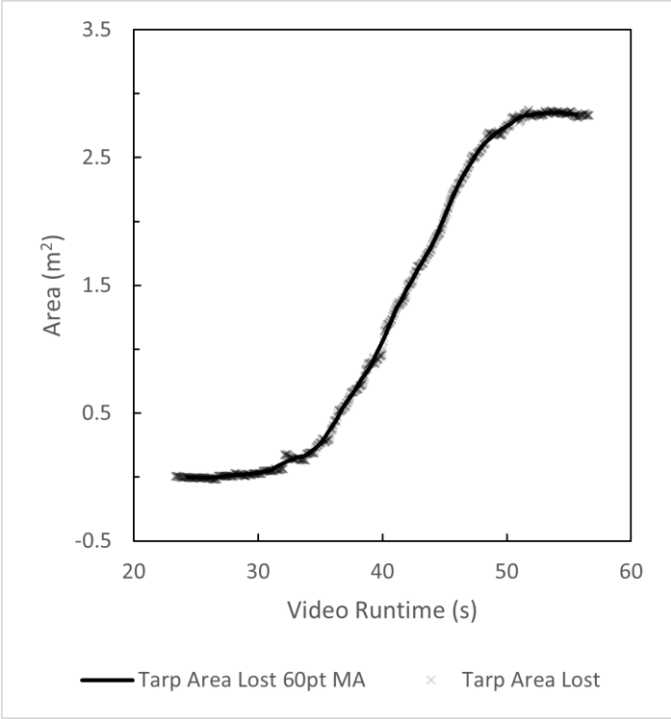


Figure 6-1. Tarp area loss over time found through IP.

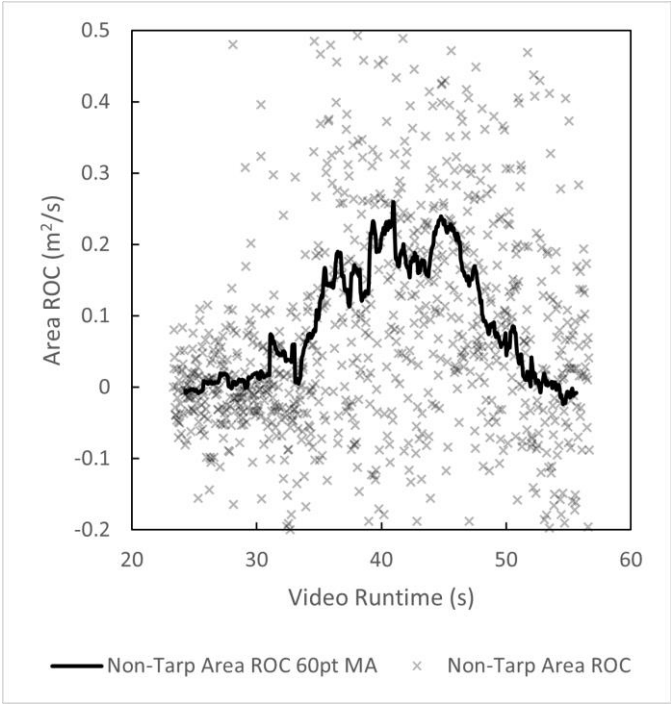


Figure 6-2. ROC of the tarp area loss over time found through IP.

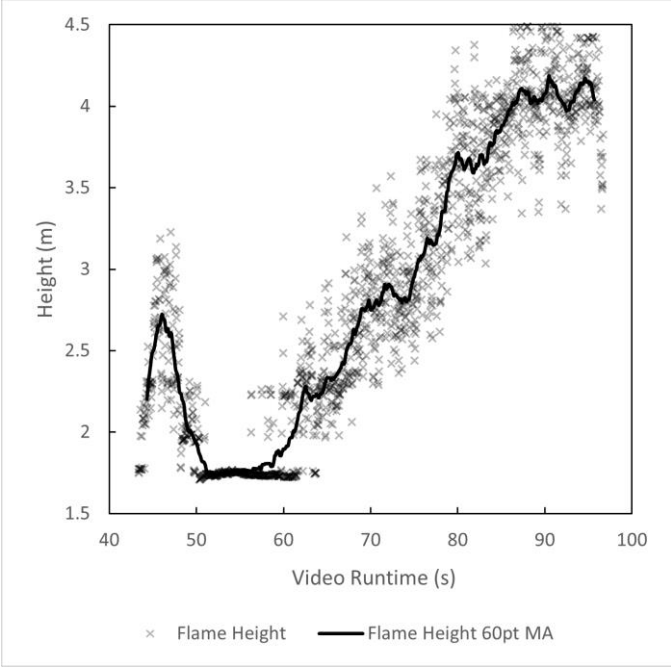


Figure 6-3. Flame height over time found through IP.

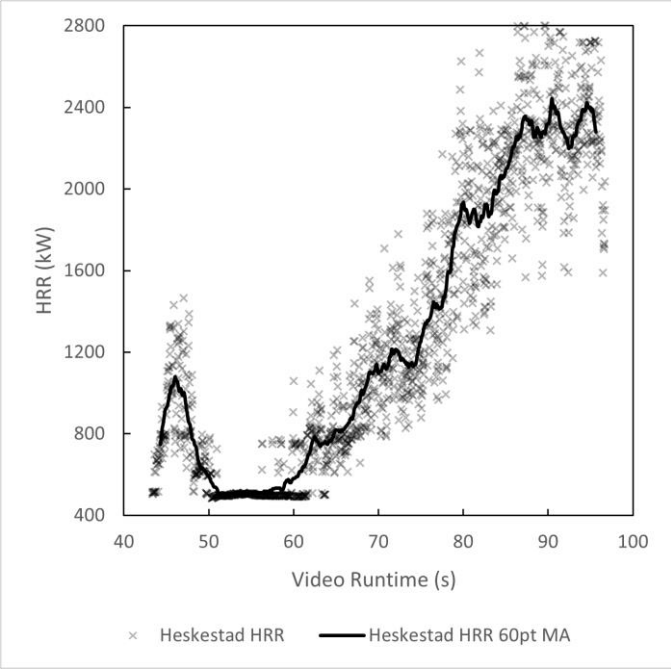


Figure 6-4. HRR estimated over time using the Heskestad correlation and flame heights found through IP.

## 6.2 Validation of the FDS Model Against Image Processing Data

To provide a validation of the FDS model, FDS measurements of the consumption and ROC of tarp, the flame height, and HRR are compared to the IP results reported in Section 6.1. All FDS results are reported using a 16-point (2.5 second) moving average to smooth the data.

As shown in Figure 6-5, the initial loss of tarp in the FDS simulations does not reach the amount lost in the IP results, but gradually between 60 and 100 seconds, the tarp loss catches up. The IP results roughly line up to the FDS results when offset by 10 seconds, suggesting the FDS simulation has a 10 second delay compared to the video. One difference between the results for each configuration is that more tarp area is lost in the Stout Corner simulation than in the Wide Corner simulation.

In Figure 6-6, an interesting result is that the peak ROC for the Wide Corner model (at  $t = 48$  seconds) occurs after the peak ROC for the Stout Corner model (at  $t = 45$  seconds); more rapid heating of the tarp wall is expected in the Stout Corner model because the Wide Corner model uses a prescribed HRRPUA of  $125 \text{ kW/m}^2$  while the Stout Corner model uses  $150 \text{ kW/m}^2$  and has an ignition region closer to the tarp wall. The steep peaks in tarp ROC from the FDS models do not match the gradual rise and plateau from the IP results; this may be due to the grid resolution of  $0.05 \text{ m}$ , which is too large to accurately capture the heating and combustion reactions for the tarp, which has a thickness of  $0.00036 \text{ m}$ .

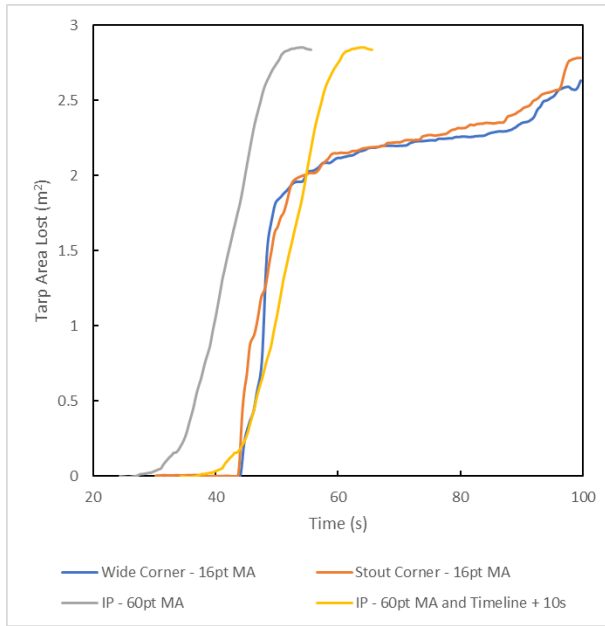


Figure 6-5. Tarp consumption over time from IP compared to the Wide Corner and Stout Corner models. An additional line indicates the tarp consumption from IP offset from its original timeline by 10 seconds.

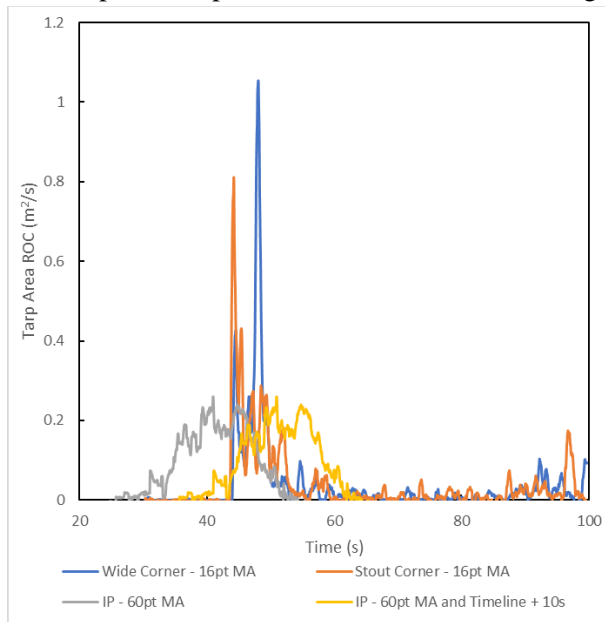


Figure 6-6. Tarp consumption ROC over time from IP compared to the "Wide Corner" and "Stout Corner" models. An additional line indicates the tarp consumption ROC from IP offset from its original timeline by 10 seconds.

In Figure 6-7, the flame height results from the FDS simulations show good agreement with the IP measurements at the second peak in flame height. However, the FDS flame heights for the initial peak (until

50 seconds) as well as dip (between approximately 60 and 100 seconds) do not match the initial peak and dip that were measured through IP. The way that the fuel pile is modeled in the Wide Corner and Stout corner simulations is to have a large portion already ignited with a prescribed heat release rate of 125 and 150 kW/m<sup>2</sup>, respectively. This is meant to shorten the delay between the burning behaviors in the video compared to events in the simulations, as well as approximate the aggressive growth of fire due to the presence of an accelerant. However, the initial aggressive growth in the FDS models leads to an artificially high flame height in the initial flame development and in the dip.

The IP measurements roughly line up to the FDS models when offset by 25 seconds, suggesting the FDS simulation has a 25 second delay to reach the second peak flame height. The FDS model shows only a 10 second delay when comparing tarp loss results, so the additional 15 seconds of delay comes from the elongated “dip” in the flame height, which lasts approximately 10 seconds in the video but lasts approximately 40 seconds in both the Wide Corner and Stout Corner models.

In Figure 6-8, the total HRR from the FDS simulations (including the fuel pile *and* the shelter itself) is reported along with the IP HRR estimation (based on the Heskestad correlation). A discrepancy of almost 250% exists between the steady state HRR for the FDS models (approximately 900 kW) and the peak HRR for the Heskestad estimate (approximately 2400 kW). The Heskestad estimate scales directly with the measured IF flame heights; however, the FDS model reveals that the HRR of a shelter fire (with complex geometry and changing ventilation conditions) does not necessarily scale with flame height. In fact, the total HRR peaks when the flame height is lowest, between approximately 60 and 100 seconds.

The increase in total HRR during the dip in flame height indicates that the flame does not “shrink” but instead tilts away from the back wall, where the growing opening in the wall causes an inflow of air beginning at approximately 50 seconds. The tilt of the flame toward the front wall heats the tarp there and on the left wall, causing the shelter to rapidly contribute to the total HRR.

Visualizations from the FDS model (see Figure 6-9) confirm that for both the Wide Corner and Stout Corner simulations, between 100 and 150 seconds, the flame does tilt toward the front wall. Slice files for the air velocity at the boundaries of the shelter (in Figures 6-10 and 6-11) indicate that when the

flame tilts, there is an inflow of air through the burnt away portions of the back and side walls. The inward flow of air pushes the flame from an upright position into a tilted position.

An additional finding is that the inward air velocities in the Stout Corner model are higher than the inward air velocities of the Wide Corner model, generating a more drastic flame tilt in the Stout Corner model that pushes the flame toward the center of the shelter.

From FDS and IP results, the steady burning HRR can be approximated as 900 kW for a shelter fire with a range of approximately 4.1-4.5 m for steady burning flame height.

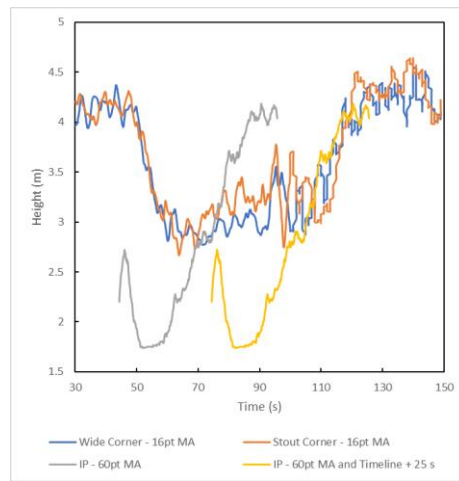


Figure 6-7. Flame height over time from IP compared to the measurements from the FDS models. An additional line indicates the flame height from IP offset from its original timeline by 25 seconds.

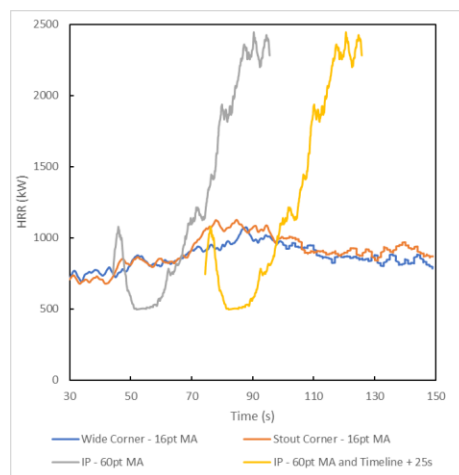


Figure 6-8. HRR over time from the IP estimate compared to the total simulation HRR from the FDS models. An additional line shows the IP estimate offset from its original timeline by 25 seconds.

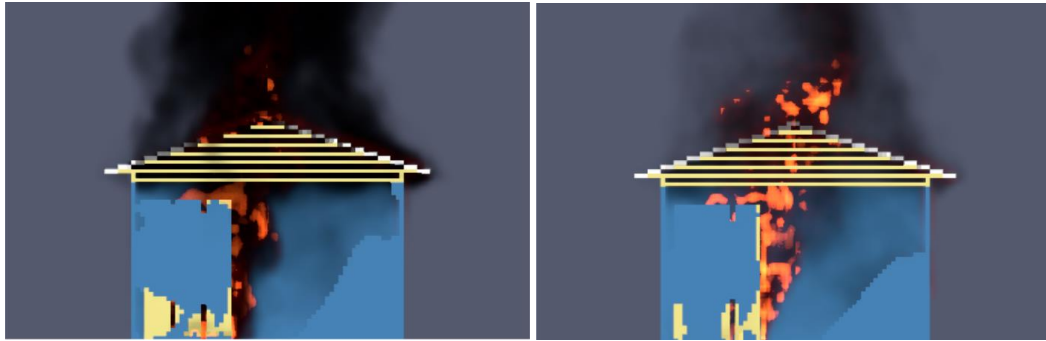


Figure 6-9. A side view of the Wide Corner (left) and Stout Corner (right) simulations, at 120 seconds.

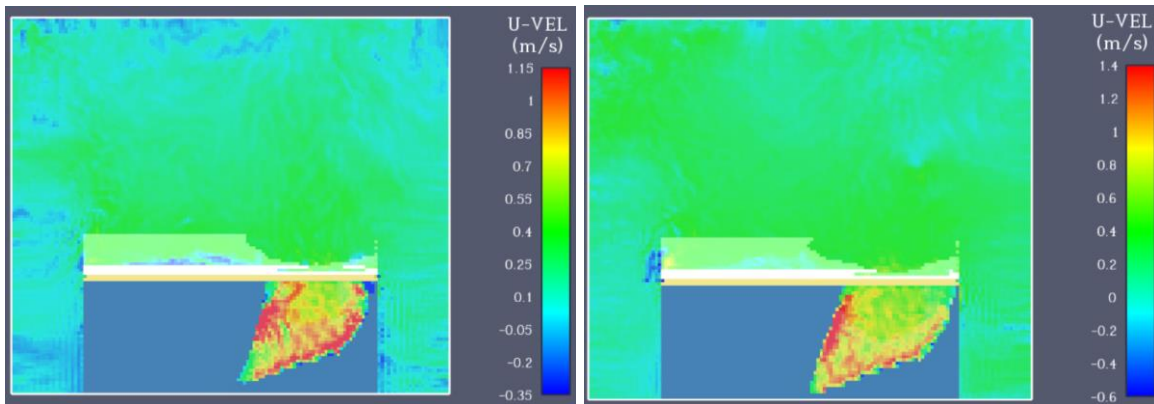


Figure 6-10. A back view of the fluid velocity slice file for the Wide Corner (left) and Stout Corner (right) simulations, at 120 seconds. Positive, or inward, flow is indicated in orange, yellow, and red.

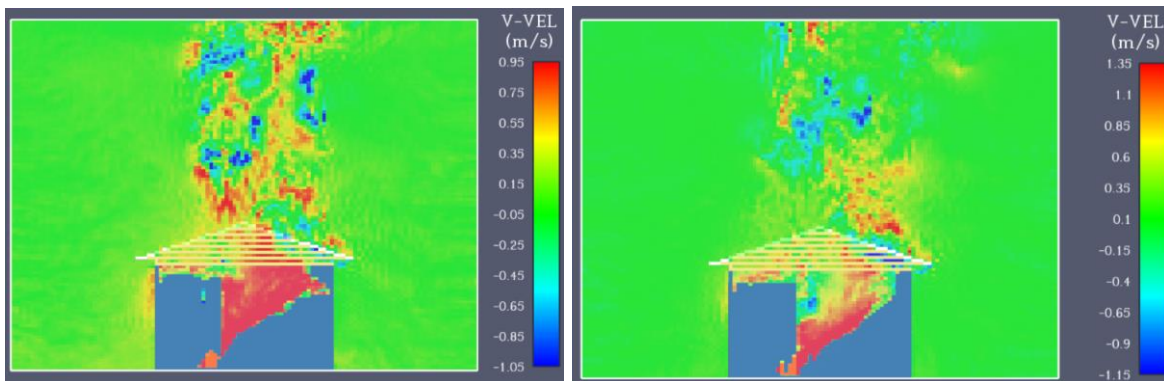


Figure 6-11. A side view of the fluid velocity slice file for the Wide Corner (left) and Stout Corner (right) simulations, at 120 seconds. Positive, or inward, flow is indicated in orange, yellow, and red.

## 6.3 FDS Results

In this section, the Wide Corner and Stout Corner configuration results are summarized for the heat flux and integrated intensity devices inside and outside the shelter. The devices inside the shelter are placed at the Left (L), Center (C), and Right (R) at 50 mm from the ground. The heat flux and integrated intensity devices are placed around the shelter at the Front Left, Front Right, Back Left, Back Right, Left, and Right at an elevation of 1.5 m or 2 m, and at distances varying between 0.25, 0.5, and 0.75 m away from the nearest wall.

The purpose of the devices inside and outside the shelter is to check if objects beyond the fuel pile or another shelter would be in danger of secondary ignition through radiation. According to [61],  $5 \text{ kW/m}^2$  would be the minimum heat flux to cause severe pain to human skin within 13 seconds or second-degree burns within 40 seconds. In Figures 6-11, 6-12, 6-13, and 6-14, the regions above  $5 \text{ kW/m}^2$  are shaded in light blue. For most common materials, the critical heat flux for ignition would be 10 to  $20 \text{ kW/m}^2$  [62].

The results from the devices inside the shelter are shown in Figure 6-12. Heat flux plots for each configuration are on the left, while integrated intensity plots are on the right. For each device location, the integrated intensity measurements are higher, given the larger solid angle of intensity integration ( $4\pi$ , as opposed to  $2\pi$  for radiative heat flux). Based on integrated intensity measurements, the shelter conditions may support secondary ignition of common materials within the shelter.

For the Wide Corner configuration, the floor device on the Left has the highest integrated intensity during the steady burning period, reaching values higher than the minimum critical heat flux for common material ignition,  $10 \text{ kW/m}^2$ .

On the other hand, in the Stout Corner configuration, both the Left and Center devices reach values higher than  $10 \text{ kW/m}^2$ . Measurements at the Center begin to exceed measurements at the Left in bursts starting around 100 seconds; this is likely linked to the flame behavior previously examined for the Stout Corner configuration, where higher velocities of air flowing in through breaches in the shelter walls leads to a more drastic flame tilt toward the center.

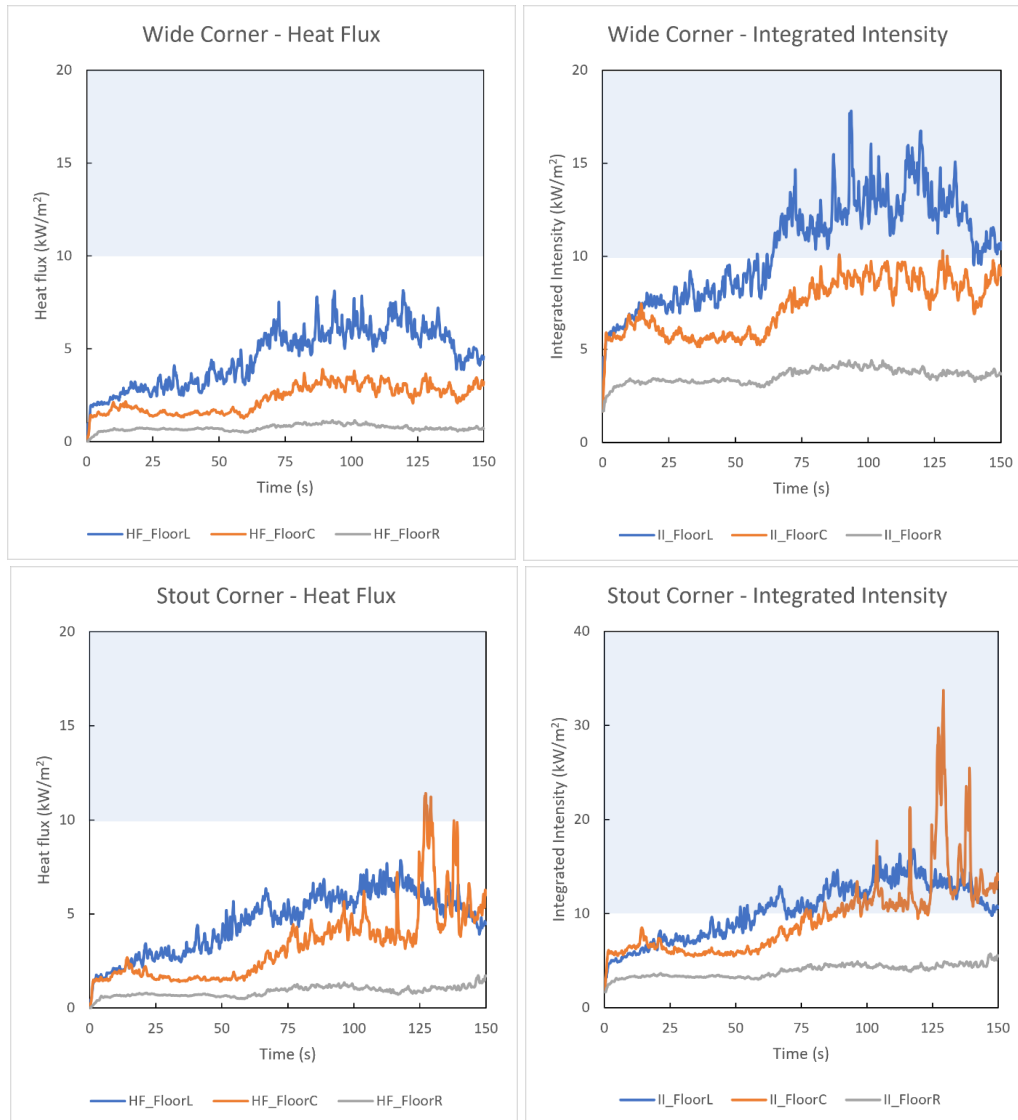


Figure 6-12. Heat flux and integrated intensity over time from the left, center, and right temperature devices in FDS. Blue shaded area indicates critical heat flux for common material ignition.

For the devices outside of the shelter, the heat flux results and integrated intensity results for each configuration are reported fully in Appendix section A6.3. This summary will include only the integrated intensity measurements for the Front Left, Back Left, and Left positions, which showed the highest values of all positions. Averages are taken the interval of 100 to 150 seconds to capture the steady burning period (after the dip in flame height). The averaged integrated intensity values are reported at the distances of 0.25, 0.5, and 0.75 m away from the nearest shelter wall. The blue shaded area indicates critical heat flux for pain to human skin.

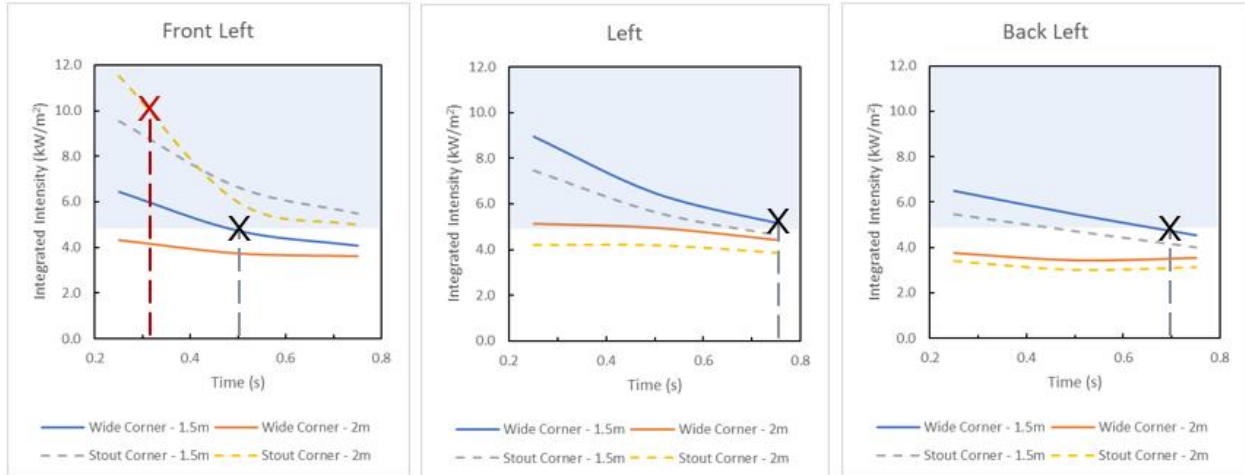


Figure 6-13. Integrated intensity at varying distances from the shelter, averaged over 100-150 s. Red and black 'x' marks indicate critical heat fluxes for common material ignition and pain to human skin.

The integrated integrity measurements, reported in Figure 6-13, reflect the incoming radiative energy to each device disregarding orientation. Though the measurements are an over-prediction compared to heat flux devices, they better reflect the radiant exposure at each device location since the heat flux devices could not be placed at an orientation optimized for the highest heat flux.

For the integrated intensities averaged over 100 to 150 seconds, both the 1.5 m and 2 m measurements taken at the Front Left for the Stout Corner simulation are higher than those for the Wide Corner simulation. At the location 0.25 m from the Left wall, the Stout Corner measurements are 9.5 and 11.5 kW/m<sup>2</sup>, approximately double the measurements from the Wide Corner simulation. The Stout Corner simulation uses a HRRPUA of 150 kW/m<sup>2</sup> for the fuel pile, which could lead to more radiant heating than in the Wide Corner simulation (where 125 kW/m<sup>2</sup> is used for the fuel pile). Flame tilt may also contribute to this disparity, as the flame tilts toward the front wall more drastically in the Stout Corner simulation than in the Wide Corner simulation, likely due to a larger ventilation area caused by the higher loss of tarp on the back wall, which is actually closer to the tarp loss measured through IP (evident in Figure 6-5). The impact of the flame tilt can be seen in the other Stout Corner integrated intensity averages from 100-150 seconds, which lag below the Wide Corner measurements at the other device locations.

When comparing the FDS integrated intensity measurements to critical heat fluxes for pain to skin and ignition of common materials, critical separation distances can be roughly approximated as 0.5 m and 0.3 respectively.

The 10-60 second average measurements were omitted from this section because heat flux and integrated intensity measurements were artificially high due to the aggressive initial fire development in the simulations that led to flames jetting through the ventilation gaps. The 10-60 second average measurements are included in Appendix section A6.3.

# Chapter 7

## Final Remarks

In the absence of full-scale experiments in humanitarian settlements, it was found that a combination of video analysis and FDS modeling may supply estimates of the flame height, heat release rate, ceiling temperatures, heat fluxes, and radiant integrated intensities in and around a burning shelter.

### 7.1 Conclusions

For this project, MATLAB-based image binarization method was developed to measure the flame height and structure loss over the course of fire development in footage from a shelter burn test conducted in Cox's Bazar, Bangladesh. The automated image processing method developed here is widely applicable to structure fire or burn test footage where the fire does not naturally have high contrast with the background (i.e., flame tests that are not filmed against a dark background or in the dark).

The humanitarian shelter fire posed a unique challenge, as the shelter structure itself is involved in burning and gradually disappears over the course of fire development. It was found that the "BURN\_AWAY" functionality in FDS could be used to replicate structure loss observed in burn test footage.

FDS models were developed through a trial and error process using known material properties and shelter dimensions to recreate observed flame behavior and structure loss. Diagnostics in the FDS models provide estimates for the flame height, heat release rate, heat flux, and radiant integrated intensity in and around the shelter.

Though the FDS models exhibited a 10-25 second delay in matching key events in the fire development timeline for the original shelter fire, there was otherwise good agreement in the comparison

of flame height measurements and tarp loss from both FDS simulations to those found by image processing the shelter fire footage. Based on results from image processing and FDS models, the steady burning HRR is approximately 900 kW for a shelter fire with a flame height range of approximately 4.1-4.5 m.

The 360° visualizations and air velocity slice files for the FDS models provided insight into the fact that the flame tilts toward the front wall of the shelter, causing tarp burn away in areas remote from the fuel pile, which is flush against the back wall. The change of ventilation conditions next to the fuel pile led to the fire tilting away from the back wall (the perspective from which the original burn test was filmed), which would lead to a decrease in flame height even though the flame length would be maintained. The tilting of the flame explains why the HRR appears to be independent of flame height.

## 7.2 Limitations and Future Work

The largest limitation of this project was that the burn test that is the base reference for all image processing and FDS modeling uses a fuel package that the coordinators chose to approximate the magnitude of a true shelter fire. While the flame height and HRR results collected from image processing and FDS methods may adequately characterize the burn test, these results cannot be extended to characterize shelter fires in general.

Another limitation was that models were based on approximated material properties and arrived at through trial and error by manipulating unknown properties to match observations from burn test footage. Future modeling efforts would benefit from experimental work to find flammability properties (ignition temperature, thermal inertia, etc.) for the construction materials in the humanitarian space, such as tarpaulin and dry raw bamboo.

Additional validation could also be provided for this modeling approach if a full scale experiment were conducted for the shelter fire. Ceiling temperature and heat flux measurements could then be directly compared. Also, because the main purpose of the burn tests was to test suppression equipment, the footage begins shortly before the appearance of smoke and ends shortly after the fire is fully developed and

volunteers extinguish the shelter fire with hoses. The amount of time between ignition and the beginning of filming was unknown. The amount of fuel placed in the shelter may not reflect the fire load of a real, lived-in shelter. Model development would greatly benefit a burn test of a fully-furnished shelter, filmed from the moment of ignition to the fire's natural extinction.

Future work in this area could use the image processing and modeling techniques developed in this report to find the critical separation distance between humanitarian shelters based on footage of real fires. The critical separation distance found in this report were only ballpark estimations, as the critical heat fluxes of the shelter materials (mainly tarpaulin and bamboo) were unknown. In addition, this critical separation distance reflects secondary ignition only through radiation and does not account for ignition through convection or direct flame impingement.

A future series of models could also investigate the impact of different weather conditions. The default ambient conditions of FDS were used for the simulations of this report, but the local temperature and wind conditions would certainly affect fire development and the ventilation conditions around the fire.

A final suggestion for future work would be to use the information collected for single-shelter simulations to develop several-shelter or even settlement-scale simulations, to estimate the linear spread rate of fire from shelter to shelter. The simulation configurations in FDS could be extremely flexible—following a uniform grid of shelters or even using aerial photographs of settlements to recreate real-life layouts in FDS—with the largest limitation being the available computing power. The linear spread rates found through modeling could be compared to fire spread rates from real fire events, extrapolated from GIS (geographic information system) mapping.

Estimates for critical separation distances and linear fire spread rates would be vital information for predicting the fire risks associated with different camp layouts. Displaced communities, settlement managers, and humanitarian organizations would all benefit from continued research in this space.



# Appendix

## A4.2

### Shelter Video Processing Code in MATLAB for Flame Height

```
%Binarization and Collecting Flame Height and HRR estimate Video Processing
clear; clc; close all;
%time that processing starts
t_start = 1300/29.97-1/29.97;
%conversion, length of bottom of shelter (m)
length = 4.572;
%estimated diameter of internal fuel load (m)
D = 1;
%calibration data
CropCal = readmatrix("C:\Users\drago\Documents\UMD\1 - Modeling\2. Image Processing\Bangladesh Burn Tests\Image Processing Finals\Fire Development - 1300 to 2900\Stabilized\Flame Height - frames 1300 to 2900_stabilized.xlsx");
%file format and name for photos
PNG = '.png';
name = 'S2P_';

%import video file and get number of frames, change directory
v = VideoReader("C:\Users\drago\Documents\UMD\1 - Modeling\2. Image Processing\Bangladesh Burn Tests\Image Processing Finals\Fire Development - 1300 to 2900\Stabilized\Shelter 2_stabilized.mp4");
frames = read(v,[1 1600]);
[sz_1,sz_2,sz_3,numframes]= size(frames);
cd 'C:\Users\drago\Documents\UMD\1 - Modeling\2. Image Processing\Bangladesh Burn Tests\Image Processing Finals\Fire Development - 1300 to 2900\Stabilized\Color'

%cropping, binarizing, writing frames into file
for num = 1:numframes
    %for every tenth frame, recalibrate the crop selection
    if mod(num-1,10)==0
        %https://www.kinovea.org/help/en/measurement/tracking.html
        row = (num-1)/10+1;           %location in Calibration data
        x = CropCal(row,6);           %top left x-coordinate
        y = CropCal(row,7);           %top left y-coordinate
        w = CropCal(row,8);           %width of crop rectangle
        h = ceil(CropCal(row,9));     %hieght of crop rectangle
    end
    %cropping and finding size: rectangle coord (x,y,w,h)
    %https://www.mathworks.com/help/images/ref/imcrop.html
    rgb = imcrop(frames(:,:,num),[x y w h]);
    [sz_row,sz_col,sz_rgb]= size(rgb);

    %greyscale with Image Processing Toolbox, values are between 0 and 255
    k=rgb2gray(rgb);
```

```

%calculate threshold using Otsu's method, compare to values in k/255
level=graythresh(k);

%display white when R is greater than both R and B plus a threshold
%and intensity of the greyscaled image would have been above OTSU threshold
r_threshold = 130;
g_threshold = 50;
b_threshold = 0;
off = 1;
for i = 1:1:sz_row
    for j = 1:1:sz_col
        if rgb(i,j,1) > r_threshold && rgb(i,j,1) > (rgb(i,j,2)+g_threshold) && rgb(i,j,1) >
(rgb(i,j,3)+b_threshold) && k(i,j)/255>=level
            bnw(i,j) = 1;    %display white
        else
            bnw(i,j) = 0;    %display black
        end
        if bnw(i,j) == 1 && off == 1    %if it's the first white pixel
            L_f_x = j;
            L_f_y = i;
            off = 0;
            height(num) = (sz_row - L_f_y)*(length/sz_col);
        end
    end
end

%convert integer to string
Sx = num2str(num);
%concatenating strings
fullname = strcat(name, Sx, PNG);
%export frames in bnw or rgb using either of the following lines:
%imwrite(bnw, fullname);
%imwrite(rgb, fullname);

clearvars bnw
end

%storing in an Excel file
Q = ((height + 1.02*D)/0.23).^(5/2);
time = t_start:(1/29.97):(t_start + num/29.97-1/29.97);
Time = time';
Height = height';
HRR = Q';
THQ = table(Time, Height, HRR);
filename = 'Height and HRR.xlsx';
writetable(THQ,filename,'Sheet',1)

%plotting
figure(1)
subplot(2,1,1)
plot(time,height)
title("Instantaneous flame height")
xlabel("Time, sec")
ylabel("Flame height, m")

```

```

subplot(2,1,2)
plot(time,Q)
title("Instantaneous HRR")
xlabel("Time, sec")
ylabel("Q, kw")

```

*[Published with MATLAB® R2020a](#)*

## Shelter Video Processing Code in MATLAB for Tarp Area

```

%Binarization for tarp
%Video Processing
clear; clc; close all;

%conversion, length of bottom of shelter (m)
t_start = 700/29.97-1/29.97;
length = 4.572;
%calibration data
CropCal = readmatrix("C:\Users\drago\Documents\UMD\1 - Modeling\2. Image Processing\Bangladesh
Burn Tests\Image Processing Finals\Tarp Burnaway - 700 to 1700\Stabilized\Tarp Area_coord.xlsx");
%file format and name for photos
PNG = '.png';
name = 'S2TP_';

%import video file and get number of frames, change directory
v = VideoReader("C:\Users\drago\Documents\UMD\1 - Modeling\2. Image Processing\Bangladesh Burn
Tests\Image Processing Finals\Tarp Burnaway - 700 to 1700\Stabilized\Shelter 2_TarpBurn.mp4");
frames = read(v,[1 1000]);
[sz_1,sz_2,sz_3,numframes]= size(frames);
cd 'C:\Users\drago\Documents\UMD\1 - Modeling\2. Image Processing\Bangladesh Burn Tests\Image
Processing Finals\Tarp Burnaway - 700 to 1700\Stabilized\Color'

%cropping, binarizing, writing frames into file
area = zeros([numframes 1]);
area_ROC = zeros([numframes 1]);
for num = 1:numframes
    %for every tenth frame, recalibrate the crop selection
    if mod(num-1,10)==0
        %https://www.kinovea.org/help/en/measurement/tracking.html
        row = (num-1)/10+1;          %location in Calibration data
        x = CropCal(row,8);          %top left x-coordinate
        y = CropCal(row,9);          %top left y-coordinate
        w = ceil(CropCal(row,10));   %width of crop rectangle
        h = ceil(CropCal(row,11));   %hieght of crop rectangle
    end
    %cropping and finding size: rectangle coord (x,y,w,h)
    %https://www.mathworks.com/help/images/ref/imcrop.html
    rgb = imcrop(frames(:,:,num),[x y w h]);

```

```

[sz_row,sz_col,sz_rgb]= size(rgb);

%display white when the red value is greater than both
%green and blue values plus a threshold
r_threshold = 5;
g_threshold = 5;
b_threshold = 30;
pixel_total = 0;
for i = 1:1:sz_row
    for j = 1:1:sz_col
        if rgb(i,j,3) > b_threshold && rgb(i,j,3) > (rgb(i,j,2)+g_threshold) && rgb(i,j,3) >
(rgb(i,j,1)+r_threshold)
            bnw(i,j) = 0; %display black if tarp/thin bamboo
        else
            bnw(i,j) = 1; %display white otherwise
        end
        if bnw(i,j) == 1 %if a white pixel, add
            pixel_total = pixel_total+1;
            area(num) = area(num)+(1*length/sz_col)^2;
        end
    end
end
if num ~= 1
%area rate of change
area_ROC(num) = (area(num)-area(num-1))/(1/29.97);
end
%convert integer to string
Sx = num2str(num);
%concatenating strings
fullname = strcat(name, Sx, PNG);
%export frames in bnw or rgb using either of the following lines:
%imwrite(bnw, fullname);
%imwrite(rgb, fullname);

clearvars bnw
end

%plotting
time = t_start:(1/29.97):(t_start + num/29.97-1/29.97);
figure(1)
subplot(2,1,1)
plot(time,area)
title("Non-tarp area")
xlabel("Time, sec")
ylabel("Area, m^2")
subplot(2,1,2)
plot(time,area_ROC)
title("Non-tarp area ROC over 1")
xlabel("Time, sec")
ylabel("Area ROC, m^2/s")

%storing in an excel file
Time = time';
Non_Tarp_Area = area;

```

```

Area_ROC = area_ROC;
TTR = table(Time, Non_Tarp_Area, Area_ROC);
filename = 'Area and ROC.xlsx';
writetable(TTR,filename,'sheet',1)

```

*[Published with MATLAB® R2020a](#)*

## FDS movie Processing Code in MATLAB for Tarp Area

```

%Binarization for tarp in FDS
%Video Processing a pre-cropped FDS movie
clear; clc; close all;

%conversion, length of bottom of shelter (m)
t_start = 30;
length = 4.572;
%file format and name for photos
PNG = '.png';
name = 'S2TP_';

%import video file and get number of frames, change directory
v = VideoReader("C:\Users\drago\Documents\UMD\1 - Modeling\2. Image Processing\Bangladesh Burn Tests\Image Processing Finals\Tarp Burnaway - 700 to 1700\FDS - 30 to 100\Config3_tarp.mp4");
frames = read(v);
[sz_1,sz_2,sz_3,numframes]= size(frames);
cd 'C:\Users\drago\Documents\UMD\1 - Modeling\2. Image Processing\Bangladesh Burn Tests\Image Processing Finals\Tarp Burnaway - 700 to 1700\FDS - 30 to 100\Config3'

%cropping, binarizing, writing frames into file
area = zeros([numframes 1]);
area_ROC = zeros([numframes 1]);
for num = 1:numframes

    rgb = frames(:,:, :,num);
    [sz_row,sz_col,sz_rgb]= size(rgb);

    %greyscale with Image Processing Toolbox, values are between 0 and 255
    k=rgb2gray(rgb);
    %calculate threshold using Otsu's method, compare to values in k/255
    level=graythresh(k);

    %display white when the red value is greater than both
    %green and blue values plus a threshold
    r_threshold = 5;
    g_threshold = 5;
    b_threshold = 150;
    pixel_total = 0;
    for i = 1:1:sz_row
        for j = 1:1:sz_col

```

```

        if rgb(i,j,3) > b_threshold && rgb(i,j,3) > (rgb(i,j,2)+g_threshold) && rgb(i,j,3) >
(rgb(i,j,1)+r_threshold)
            bnw(i,j) = 0;    %display black if tarp/thin bamboo
        else
            bnw(i,j) = 1;    %display white otherwise
        end
        if bnw(i,j) == 1    %if a white pixel, add
            pixel_total = pixel_total+1;
            area(num) = area(num)+(1*length/sz_col)^2;
        end
    end
end
if num ~= 1
%area rate of change
area_ROC(num) = (area(num)-area(num-1))/(1/29.97);
end
%convert integer to string
Sx = num2str(num);
%concatenating strings
fullname = strcat(name, Sx, PNG);
%export frames in bnw or rgb using either of the following lines:
%imwrite(bnw, fullname);
%imwrite(rgb, fullname);

clearvars bnw
end

%plotting
time = t_start:(1/30):(t_start + num/30-1/30);
figure(1)
subplot(2,1,1)
plot(time,area)
title("Non-tarp area")
xlabel("Time, sec")
ylabel("Area, m^2")
subplot(2,1,2)
plot(time,area_ROC)
title("Non-tarp area ROC over 1")
xlabel("Time, sec")
ylabel("Area ROC, m^2/s")

%storing in an Excel file
Time = time';
Non_Tarp_Area = area;
Area_ROC = area_ROC;
TTR = table(Time, Non_Tarp_Area, Area_ROC);
filename = 'Area and ROC.xlsx';
writetable(TTR,filename,'sheet',1)

```

*[Published with MATLAB® R2020a](#)*

## A5.1

### Full FDS code for Stout Corner Geometry

- **Highlighted areas are modified for the Wide Corner Geometry**

October 2022

Genevieve Tan

Shelter 2 Approximate Shelter: Stout Corner Geometry

```
&HEAD CHID='BH150_StoutCorner', TITLE='Test burning shelter'/  
&TIME T_END=150./
```

```
&MESH ID='Mesh01', IJK=60,70,60, XB=-4.0,0.0,-3.5,0.0,0.0,3.0, MPI_PROCESS=0/  
&MESH ID='Mesh02', IJK=60,70,60, XB=-4.0,0.0,0.0,3.5,0.0,3.0, MPI_PROCESS=1/  
&MESH ID='Mesh03', IJK=60,70,60, XB=0.0,4.0,0.0,3.5,0.0,3.0, MPI_PROCESS=2/  
&MESH ID='Mesh04', IJK=60,70,60, XB=0.0,4.0,-3.5,0.0,0.0,3.0, MPI_PROCESS=3/  
&MESH ID='Mesh05', IJK=60,70,60, XB=-4.0,0.0,-3.5,0.0,3.0,6.0, MPI_PROCESS=4/  
&MESH ID='Mesh06', IJK=60,70,60, XB=-4.0,0.0,0.0,3.5,3.0,6.0, MPI_PROCESS=5/  
&MESH ID='Mesh07', IJK=60,70,60, XB=0.0,4.0,0.0,3.5,3.0,6.0, MPI_PROCESS=6/  
&MESH ID='Mesh08', IJK=60,70,60, XB=0.0,4.0,-3.5,0.0,3.0,6.0, MPI_PROCESS=7/
```

```
&REAC ID = 'Wood',  
  FYI='From Cicione and Xu and Robbins',  
  FUEL='REAC_FUEL',  
  C=3.4,  
  H=6.2,  
  O=2.5,  
  SOOT_YIELD=0.04,  
  CO_YIELD=0.0075,  
  HEAT_OF_COMBUSTION=11750/
```

```
&MATL ID= 'Polyethylene Matl',  
  FYI='Conductivity and specific heat for polyethylene, density for NIST tarp',  
  CONDUCTIVITY = 0.44,  
  SPECIFIC_HEAT = 1.8,  
  DENSITY = 72.5,  
  HEAT_OF_COMBUSTION= 43300/
```

```
&MATL ID= 'Bamboo Matl',  
  CONDUCTIVITY = 0.25,  
  SPECIFIC_HEAT = 2.26,  
  DENSITY = 687./
```

```
&MATL ID= 'Concrete Matl',  
  CONDUCTIVITY = 1.625,  
  SPECIFIC_HEAT = 0.6918,  
  DENSITY = 2400./
```

```
&SURF ID='Tarp',  
  COLOR='STEEL BLUE',  
  MATL_ID='Polyethylene Matl',  
  THICKNESS=0.00036,
```

```

IGNITION_TEMPERATURE=175,
BURN_AWAY=.TRUE.,
BACKING='EXPOSED',
RAMP_Q='Tarp_RAMP_Q',
HRRPUA=15./
&RAMP ID='Tarp_RAMP_Q', T=0.0, F=1.0/
&RAMP ID='Tarp_RAMP_Q', T=100.0, F=1.0/

&RAMP ID='Bamboo_RAMP_Q', T=0.0, F=1.0/
&RAMP ID='Bamboo_RAMP_Q', T=20.0, F=1.0/
&RAMP ID='Bamboo_RAMP_Q', T=1000.0, F=1.0/
&RAMP ID='Bamboo_RAMP_Q', T=2000.0, F=0.5/

&SURF ID='Bamboo Roof',
COLOR='KHAKI',
MATL_ID='Bamboo Matl',
THICKNESS=0.018,
IGNITION_TEMPERATURE=308,
HRRPUA=100.0,
RAMP_Q='Bamboo_RAMP_Q'/

&SURF ID='Bamboo',
FYI= 'HRRPUA value is 150 for Stout Corner and 125 for Wide Corner',
COLOR='KHAKI',
MATL_ID='Bamboo Matl',
THICKNESS=0.018,
IGNITION_TEMPERATURE=100,
HRRPUA=150.0,
RAMP_Q='BambooBurn_RAMP_Q'/

&SURF ID='Bamboo Burn',
COLOR='RED',
MATL_ID='Bamboo Matl',
THICKNESS=0.018,
HRRPUA=150.0,
RAMP_Q='BambooBurn_RAMP_Q'/
&RAMP ID='BambooBurn_RAMP_Q', T=0.0, F=1.0/
&RAMP ID='BambooBurn_RAMP_Q', T=1000.0, F=1.0/

&SURF ID='Concrete',
FYI='Thickness estimated 1ft',
COLOR='SILVER',
MATL_ID='Concrete Matl',
THICKNESS=0.3/

&MULT ID='Roof 1', DXB=0.15,0.15,0.0,0.0,0.05,0.05, N_LOWER=0, N_UPPER=11 /
&OBST XB=-1.85,-1.7,-2.35,2.35,1.9,1.95, MULT_ID='Roof 1', COLOR='WHITE',
SURF_ID='Tarp' /
&MULT ID='Roof 2', DXB=-0.15,-0.15,0.0,0.0,0.05,0.05, N_LOWER=0, N_UPPER=12 /

```

```

&OBST XB=1.7,1.85,-2.35,2.35,1.9,1.95, MULT_ID='Roof 2', COLOR='WHITE',
SURF_ID='Tarp' /
&MULT ID='Roof 3', DXB=0.3,-0.3,0.0,0.0,0.1,0.1, N_LOWER=0, N_UPPER=5 /
&OBST XB=-1.7,1.7,-2.35,-2.3,1.9,1.95, MULT_ID='Roof 3', SURF_ID='Bamboo Roof' /
&MULT ID='Roof 4', DXB=0.3,-0.3,0.0,0.0,0.1,0.1, N_LOWER=0, N_UPPER=5 /
&OBST XB=-1.7,1.7,2.35,2.3,1.9,1.95, MULT_ID='Roof 4', SURF_ID='Bamboo Roof' /
&OBST ID='Roof B', XB=-1.55,-1.5,-2.3,2.3,1.8,1.95, SURF_ID='Bamboo Roof'/
&OBST ID='Roof B', XB=-1.55,1.55,-2.35,-2.3,1.8,1.85, SURF_ID='Bamboo Roof'/
&OBST ID='Roof B', XB=-1.55,1.55,2.3,2.35,1.8,1.85, SURF_ID='Bamboo Roof'/
&OBST ID='Roof B', XB=1.5,1.55,-2.3,2.3,1.8,1.95, SURF_ID='Bamboo Roof' /

&OBST ID='Wall', XB=-1.55,-1.5,-2.3,2.3,0.0,1.8, SURF_ID='Tarp'/
&OBST ID='Wall', XB=-1.55,1.55,-2.35,-2.3,0.0,1.8, SURF_ID='Tarp'/
&OBST ID='Wall', XB=-1.55,1.55,2.3,2.35,0.0,1.8, SURF_ID='Tarp'/
&OBST ID='Wall', XB=1.5,1.55,-2.3,2.3,0.0,1.8, SURF_ID='Tarp'/
&HOLE ID='Door', XB=1.4,1.8,1.2,2.0,-0.01,1.5/

&MULT ID='Fuel Pile 1-F', DXB=0.0,0.0,0.0,-0.3,0.1,0.1, N_LOWER=0, N_UPPER=4 /
&MULT ID='Fuel Pile 1-F Burn', DXB=0.0,0.0,0.0,-0.3,0.1,0.1, N_LOWER=0, N_UPPER=4 /
&MULT ID='Fuel Pile 1-B', DXB=0.0,0.0,-0.05,0.0,0.1,0.1, N_LOWER=0, N_UPPER=5 /
&OBST XB=-1.3,-0.4,-1.45,0.05,0.0,0.1, MULT_ID='Fuel Pile 1-F Burn', SURF_ID='Bamboo
Burn'/
&OBST XB=-1.4,-1.3,-1.45,0.05,0.0,0.1, MULT_ID='Fuel Pile 1-F', SURF_ID='Bamboo'/
&OBST XB=-1.4,-0.4,-1.95,-1.45,0.0,0.1, MULT_ID='Fuel Pile 1-B', SURF_ID='Bamboo'/

&MULT ID='Fuel Pile 2', DXB=0.0,0.0,0.0,-0.1,0.1,0.1, N_LOWER=0, N_UPPER=4 /
&OBST XB=-1.4,-0.4,-2.25,-1.75,0.6,0.7, MULT_ID='Fuel Pile 2', SURF_ID='Bamboo'/
&OBST XB=-1.4,-0.4,-2.25,-2.2,1.1,1.6, SURF_ID='Bamboo'/
&HOLE ID='Porosity', XB=-0.75,-0.7,-2.3,0.1,0.0,1.65/
&HOLE ID='Porosity', XB=-1.1,-1.05,-2.3,0.1,0.0,1.65/

&SLCF PBX=1.5, QUANTITY='U-VELOCITY', CELL_CENTERED=T /
&SLCF PBX=-1.5, QUANTITY='U-VELOCITY', CELL_CENTERED=T /
&SLCF PBY=2.3, QUANTITY='V-VELOCITY', CELL_CENTERED=T /
&SLCF PBY=-2.3, QUANTITY='V-VELOCITY', CELL_CENTERED=T /

&VENT ID='Mesh Vent: Mesh01 [XMAX]', SURF_ID='OPEN', XB=4.0,4.0,-3.5,3.5,0.0,6.0/
&VENT ID='Mesh Vent: Mesh01 [XMIN]', SURF_ID='OPEN', XB=-4.0,-4.0,-3.5,3.5,0.0,6.0/
&VENT ID='Mesh Vent: Mesh01 [YMAX]', SURF_ID='OPEN', XB=-4.0,4.0,3.5,3.5,0.0,6.0/
&VENT ID='Mesh Vent: Mesh01 [YMIN]', SURF_ID='OPEN', XB=-4.0,4.0,-3.5,-3.5,0.0,6.0/
&VENT ID='Mesh Vent: Mesh01 [ZMAX]', SURF_ID='OPEN', XB=-4.0,4.0,-3.5,3.5,6.0,6.0/
&VENT ID='Floor', SURF_ID='Concrete', XB=-4.0,4.0,-3.5,3.5,0.0,0.0/

&TAIL /

```

## A5.2

### Equations relating radiative heat flux to integrated intensity

Radiative intensity, I:

$$I = P/\Omega$$

$P$ , incoming radiant power [W]

$\Omega$ , solid angle [sr]

Integrated intensity, U:

$$U = \int I d\Omega, \text{ integrated over } 4\pi$$

Radiative heat flux,  $\dot{q}_{ij,rad}$ :

$$\dot{q}_{ij,rad} = \varepsilon\sigma F_{ij}(T_i^4 - T_j^4) = \int I d\Omega, \text{ integrated over } 2\pi$$

$F_{ij}$  is the view factor for what the exposed area "sees."

$\varepsilon$ , emissivity

$\sigma$ , Stefan-Boltzman constant [kW/m<sup>2</sup>K<sup>4</sup>]

$T_i$ , temperature at location i [K]

$T_j$ , temperature at location j [K]

## A5.5

### Wide Corner Fuel Pile FDS Geometry lines

```
&MULT ID='Fuel Pile 1-F', DXB=0.0,0.0,0.0,-0.3,0.1,0.1, N_LOWER=0, N_UPPER=5 /  
&MULT ID='Fuel Pile 1-F Burn', DXB=0.0,0.0,0.0,-0.3,0.1,0.1, N_LOWER=0, N_UPPER=5 /  
&MULT ID='Fuel Pile 1-B', DXB=0.0,0.0,-0.05,0.0,0.1,0.1, N_LOWER=0, N_UPPER=5 /  
&OBST XB=-1.2,-0.4,-1.75,0.05,0.0,0.1, MULT_ID='Fuel Pile 1-F Burn', SURF_ID='Bamboo  
Burn'/  
&OBST XB=-1.4,-1.2,-1.75,0.05,0.0,0.1, MULT_ID='Fuel Pile 1-F', SURF_ID='Bamboo'/  
&OBST XB=-1.4,-0.4,-1.95,-1.75,0.0,0.1, MULT_ID='Fuel Pile 1-B', SURF_ID='Bamboo'/
```

### Stout Corner Fuel Pile FDS Geometry lines

```
&MULT ID='Fuel Pile 1-F', DXB=0.0,0.0,0.0,-0.3,0.1,0.1, N_LOWER=0, N_UPPER=4 /  
&MULT ID='Fuel Pile 1-F Burn', DXB=0.0,0.0,0.0,-0.3,0.1,0.1, N_LOWER=0, N_UPPER=4 /  
&MULT ID='Fuel Pile 1-B', DXB=0.0,0.0,-0.05,0.0,0.1,0.1, N_LOWER=0, N_UPPER=5 /  
&OBST XB=-1.3,-0.4,-1.45,0.05,0.0,0.1, MULT_ID='Fuel Pile 1-F Burn', SURF_ID='Bamboo  
Burn'/  
&OBST XB=-1.4,-1.3,-1.45,0.05,0.0,0.1, MULT_ID='Fuel Pile 1-F', SURF_ID='Bamboo'/  
&OBST XB=-1.4,-0.4,-1.95,-1.45,0.0,0.1, MULT_ID='Fuel Pile 1-B', SURF_ID='Bamboo'/
```

### A6.3

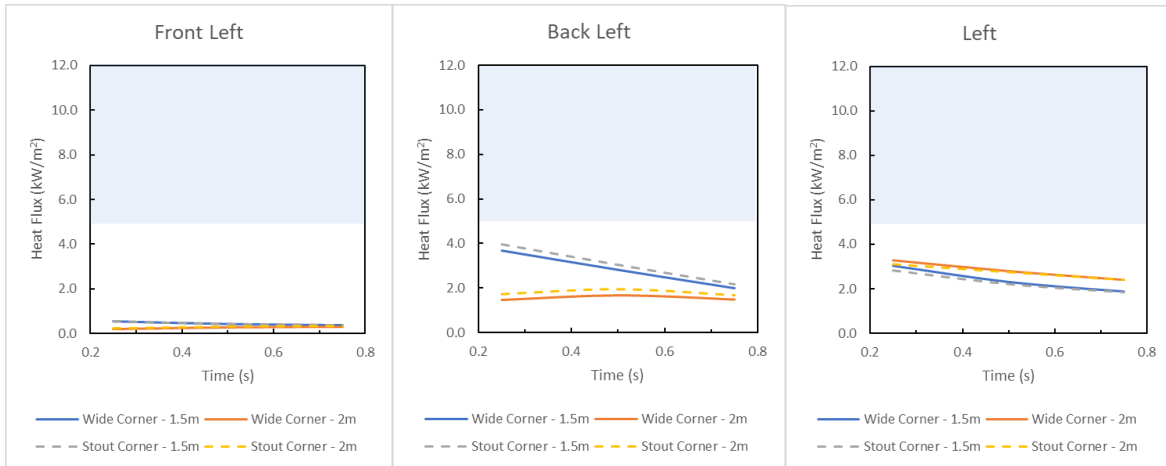


Figure A6-1. Radiative heat flux at varying distances from the shelter, averaged over 10-60 seconds.

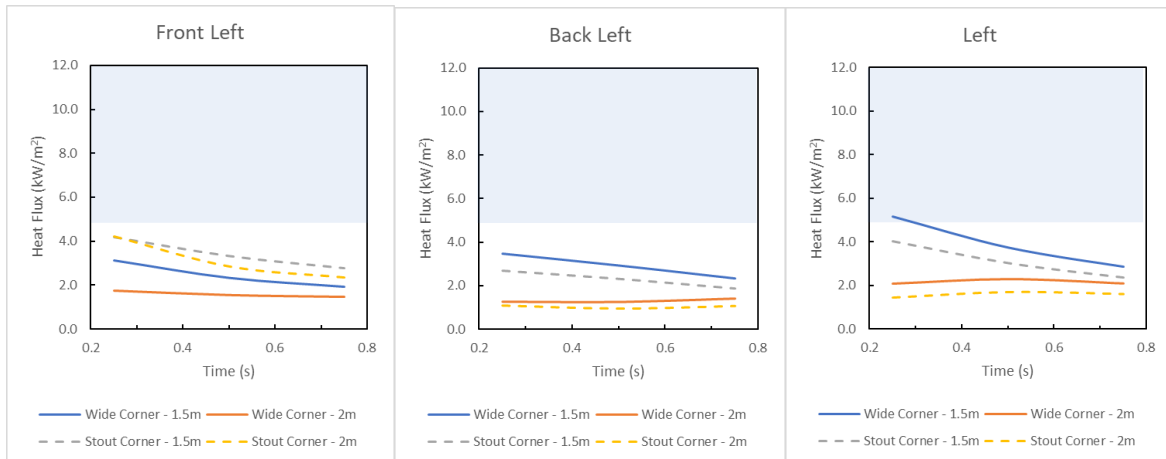


Figure A6-2. Radiative heat flux at varying distances from the shelter, averaged over 100-150 seconds.

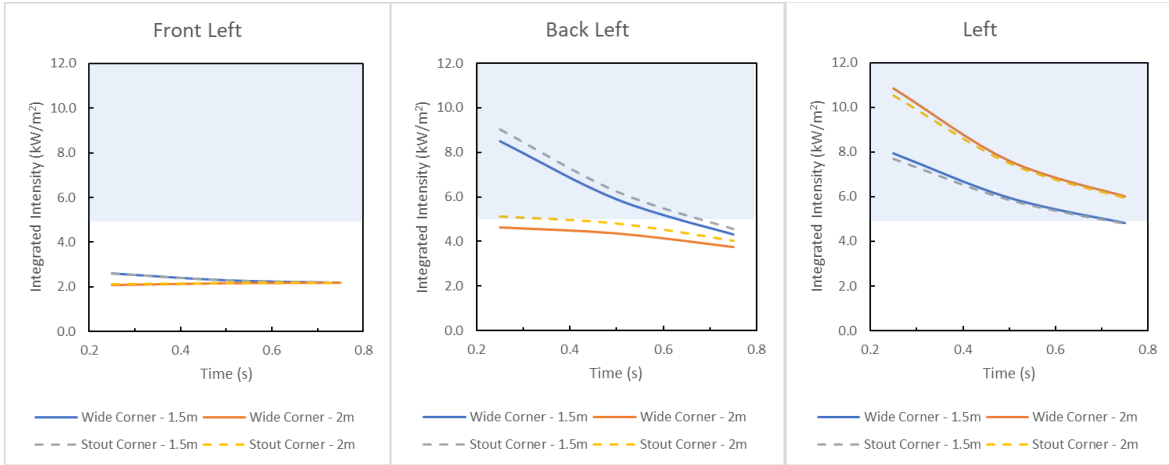


Figure A6-3. Integrated intensity at varying distances from the shelter, averaged over 10-60 seconds.

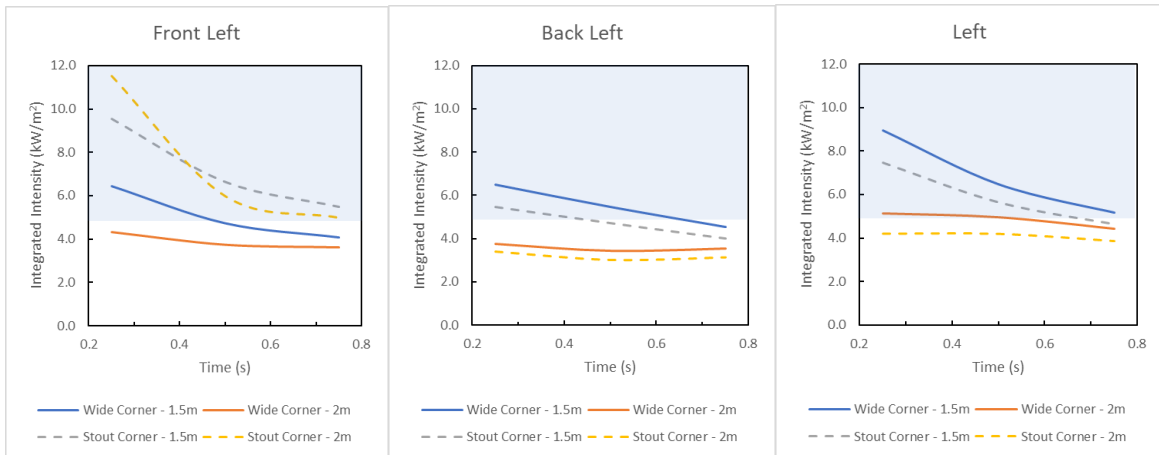


Figure A6-4. Integrated intensity at varying distances from the shelter, averaged over 100-150 seconds.

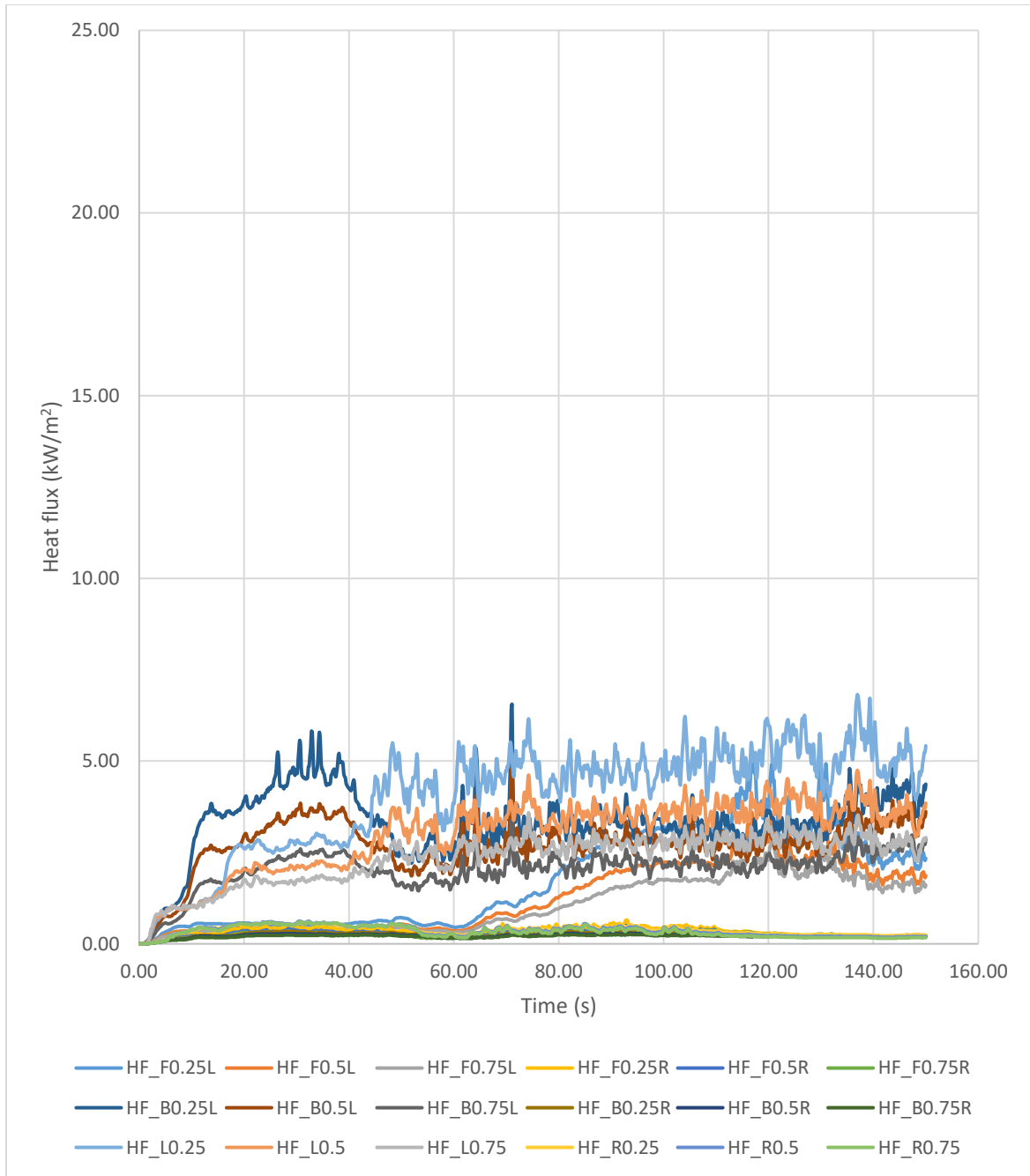


Figure A6-5. Raw heat flux over time for Wide Corner model devices at 1.5 m elevation.

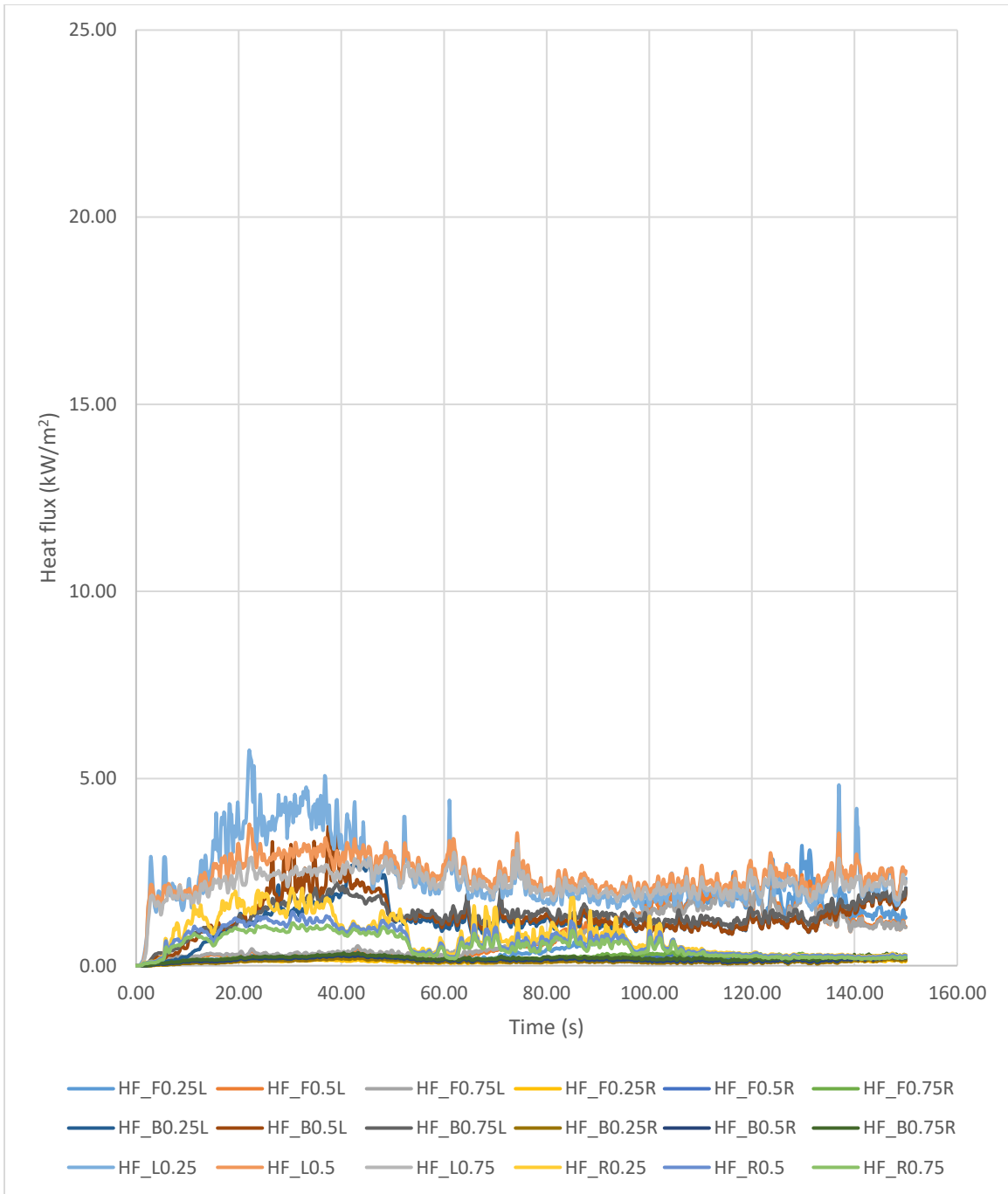


Figure A6-6. Raw heat flux over time for Wide Corner model devices at 2 m elevation.

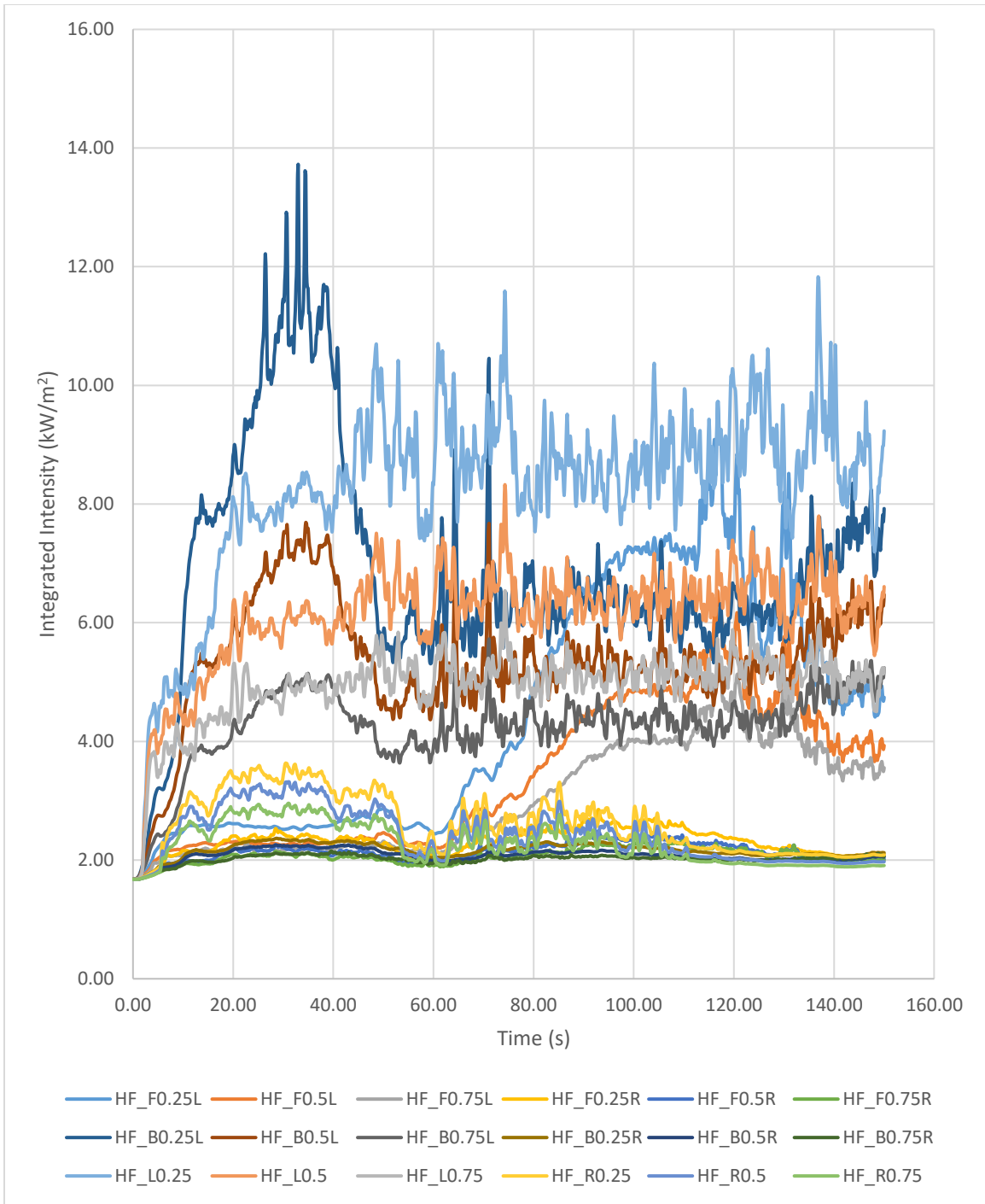


Figure A6-7. Raw integrated integrity over time for Wide Corner model devices at 1.5 m elevation.

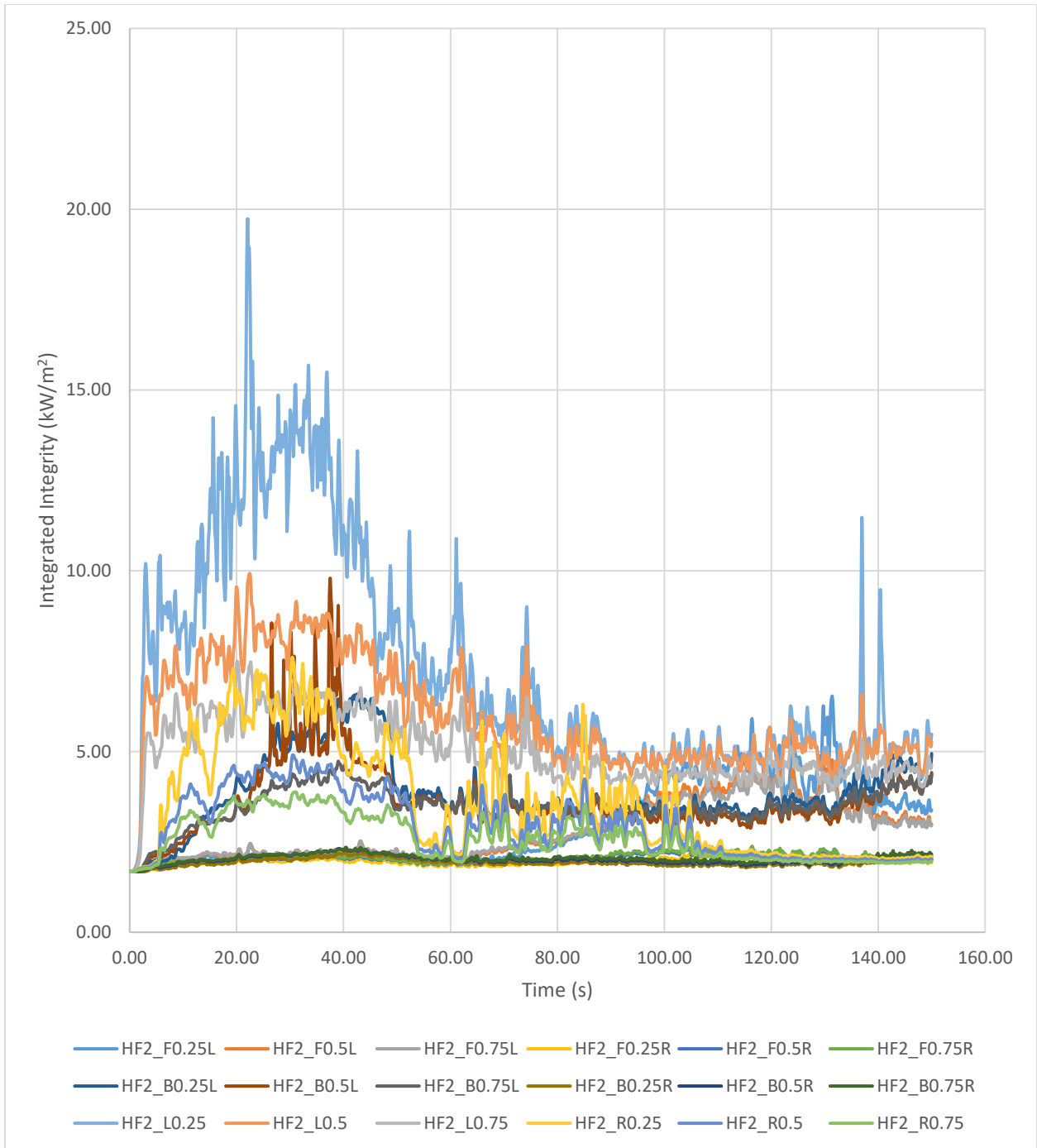


Figure A6-8. Raw integrated integrity over time for Wide Corner model devices at 2 m elevation.

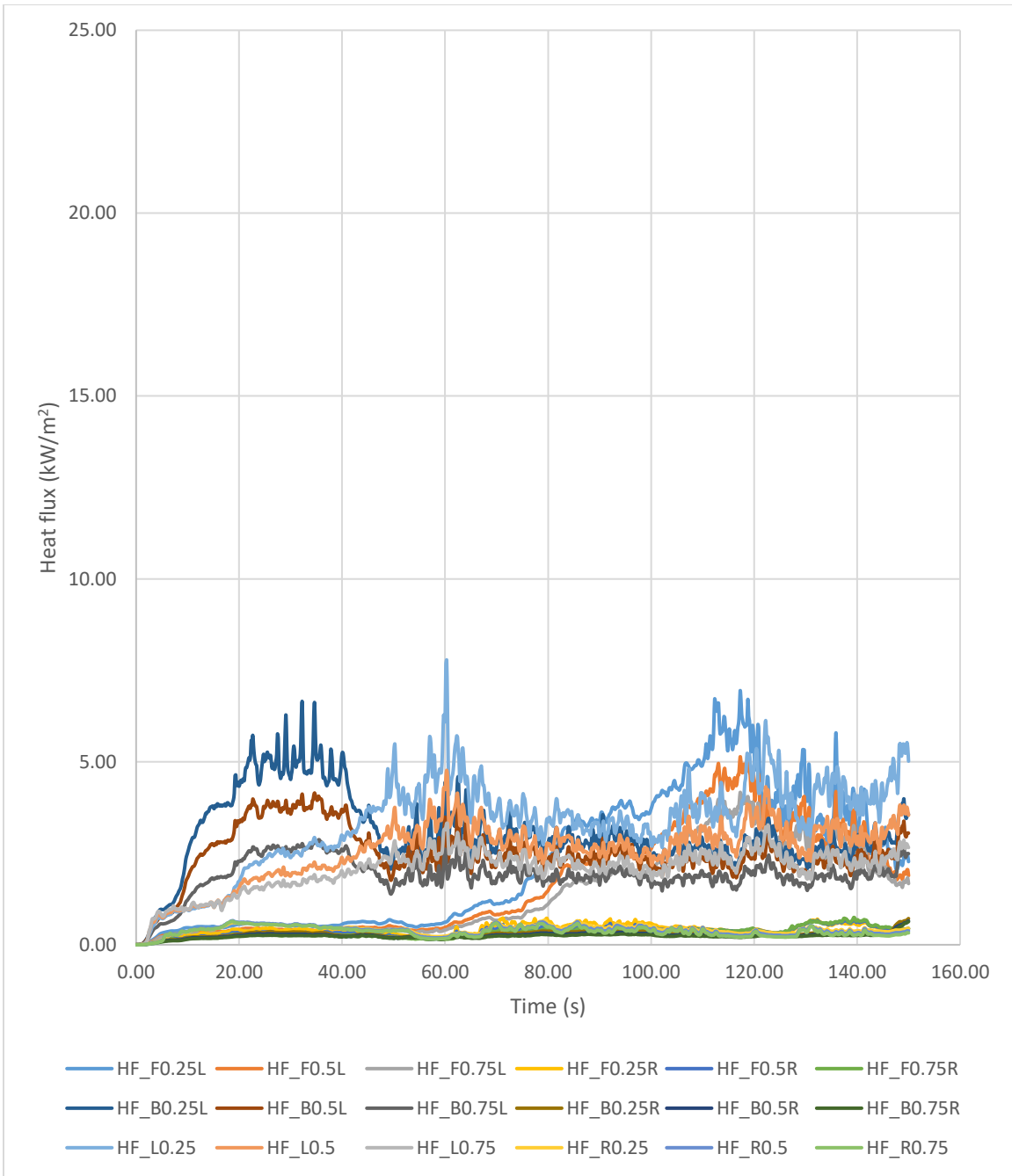


Figure A6-9. Raw heat flux over time for Stout Corner model devices at 1.5 m elevation.

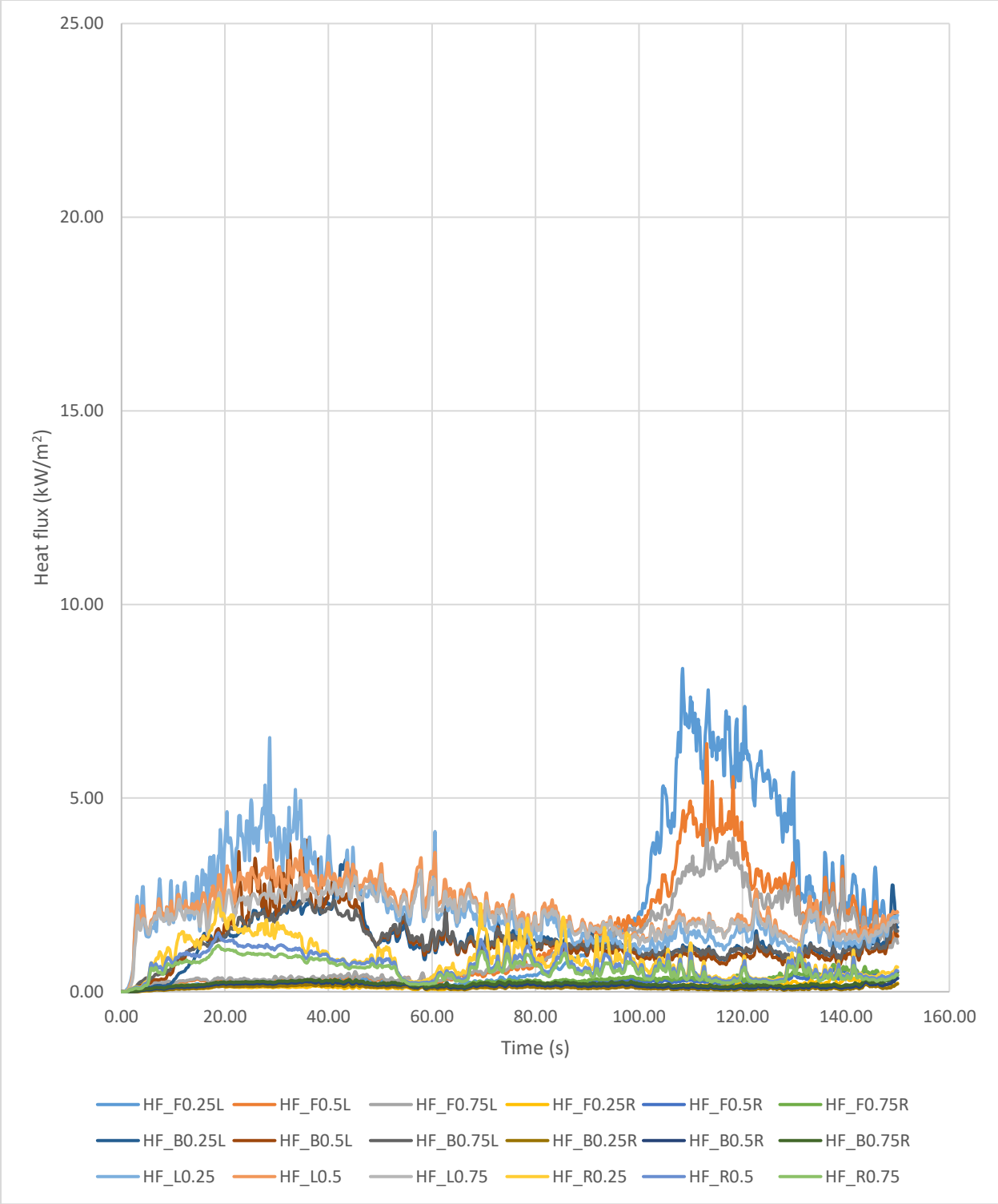


Figure A6-10. Raw heat flux over time for Stout Corner model devices at 2 m elevation.

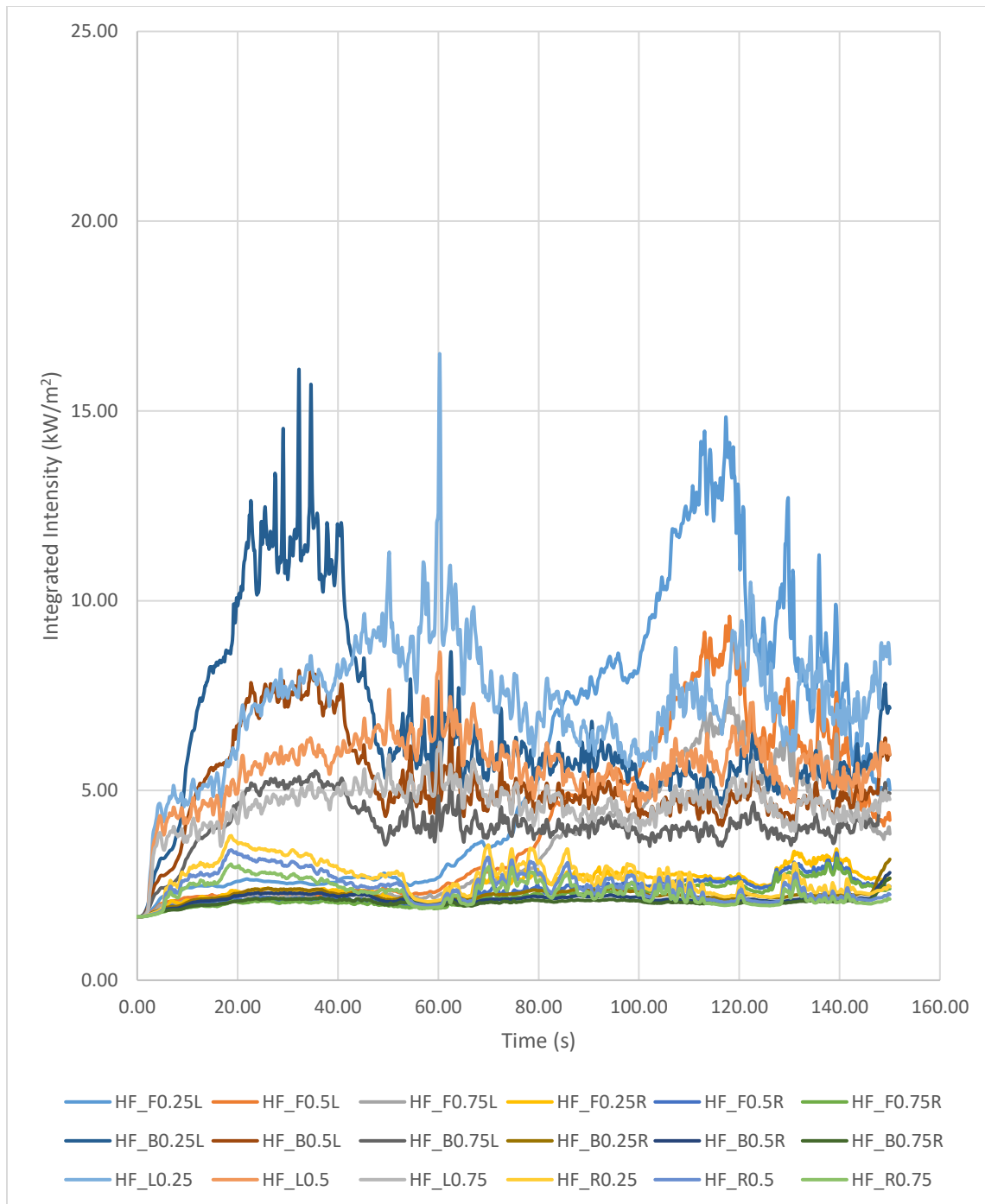


Figure A6-11. Raw integrated integrity over time for Stout Corner model devices at 1.5 m elevation.

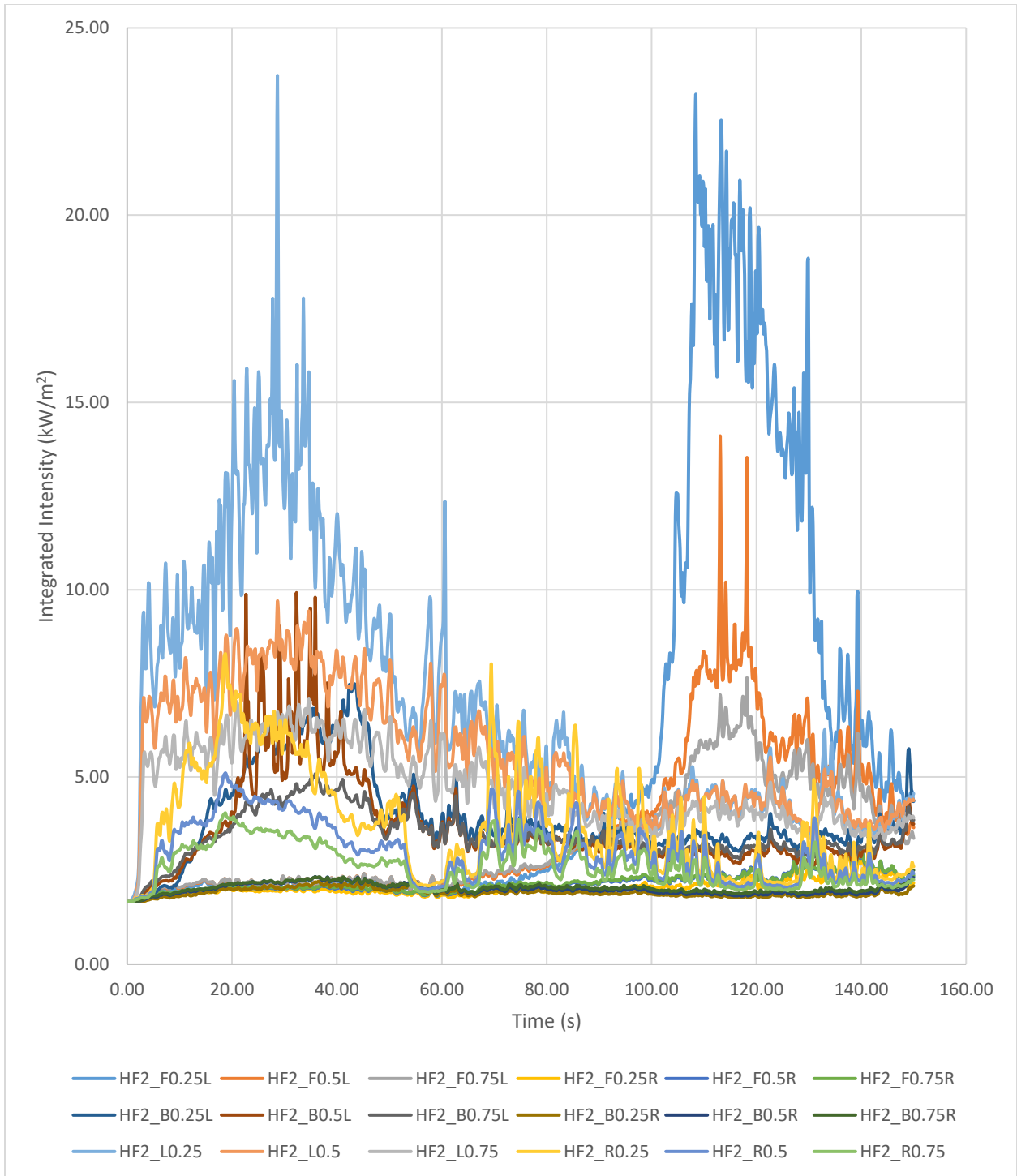


Figure A6-12. Raw integrated integrity over time for Stout Corner model devices at 2 m elevation.

# References

- [1] Human Rights Watch. (2021). Bangladesh: Refugee Camp Fencing Cost Lives in Blaze. Retrieved from [www.hrw.org/news/2021/03/25/bangladesh-refugee-camp-fencing-cost-lives-blaze#](http://www.hrw.org/news/2021/03/25/bangladesh-refugee-camp-fencing-cost-lives-blaze#)
- [2] IOM. (2022). Incident monitoring - Rohingya refugee camps, Bangladesh. Retrieved from [https://npm-iom.shinyapps.io/Incident\\_Dashboard/ w\\_c04b7eb8/#tab-8071-1](https://npm-iom.shinyapps.io/Incident_Dashboard/ w_c04b7eb8/#tab-8071-1)
- [3] Stokes, M. & Johnson, W. (2017). Burns in the Third World: an unmet need. *Annals Of Burns And Fire Disasters*, 30(4), 243. Retrieved from <https://www.ncbi.nlm.nih.gov/pmc/articles/PMC6033471/>
- [4] ARUP. (2018). A Framework for Fire Safety in Informal Settlements. Retrieved from <https://www.arup.com/perspectives/publications/research/section/a-framework-for-fire-safety-in-informal-settlements>
- [5] Shelter/NFI Partners. (2021). Standard 10'x15' Shelter for fire response in camps 8E, 8W, 9 Rohingya humanitarian crisis. Cox's Bazar, Bangladesh.
- [6] Carmignani, L. (2021). Flame Tracker: An image analysis program to measure flame characteristics, *SoftwareX*, 2021 (in Press), <https://www.sciencedirect.com/science/article/pii/S2352711021000984?via%3Dihub>
- [7] Zheng, L., Yu, M., Yu, S., and Lu, C. (2011). Measurement of flame height by image processing method. *Advanced Materials Research*. <https://doi.org/10.4028/www.scientific.net/AMR.301-303.983>
- [8] Tlemsani, M. (2022). Development and use of pixel-by-pixel pyrometry methods on smoldering wood embers and piles. University of Maryland.
- [9] McGrattan, K., Hostikka, S., Floyd, J., McDermott, R., & Vanella, M. (2021a). Fire dynamics simulator user's guide (tech. rep.). [https://github.com/firemodels/fds/releases/download/FDS6.7.6/FDS\\_User\\_Guide.pdf](https://github.com/firemodels/fds/releases/download/FDS6.7.6/FDS_User_Guide.pdf)
- [10] McGrattan, K., Hostikka, S., Floyd, J., McDermott, R., Vanella, M. (2019). Fire Dynamics Simulator: Technical Reference Guide. Retrieved from <https://nvlpubs.nist.gov/nistpubs/Legacy/SP/nistspecialpublication1018.pdf>
- [11] McGrattan, K., Hostikka, S., Floyd, J., McDermott, R., Vanella, M. (2020). Fire Dynamics Simulator Technical Reference Guide Volume 3: Validation. Baltimore, MD: NIST Special Publication 1018-3.
- [12] Sun, R. et al. (2005). An evaluation of FDS and Clark coupled wildfire model. Retrieved from <https://ams.confex.com/ams/pdfpapers/97572.pdf>
- [13] Mell, W. & Rehm, R. (2006). Numerical modeling of fire spread through trees and shrubs. Retrieved from <https://www.nist.gov/publications/numerical-modeling-fire-spread-through-individual-trees-and-shrubs>
- [14] Cicione, A., Beshir, M., Walls, R., Rush, D. (2020). Full-scale informal settlement dwelling fire experiments and development of numerical models. *Fire Technology*, 56: 639-672. <https://doi.org/10.1007/s10694-019-00894-w>
- [15] World Health Organization. (2011). Burn Prevention: Success Stories, Lessons Learned. Geneva.
- [16] World Bank Group. (2018). Population living in slums (% of urban population). Retrieved from <https://bit.ly/3yacyvJ>
- [17] UN-Habitat. (2020). Housing: The Challenge. Retrieved from <https://unhabitat.org/topic/housing>
- [18] Regional Economic and Social Analysis Unit. (2014). Global Wage Report 2014/15: Asia and the Pacific Supplement: Wages in Asia and the Pacific: Dynamic but uneven progress. International Labour Organization, Bangkok.
- [19] Cicione, A., Walls, R., Kahanji, C. (2019) Experimental study of fire spread between multiple full scale informal settlement dwellings. *Fire Saf J* 105:19–27. <https://doi.org/10.1016/j.firesaf.2019.02.001>

- [20] Beshir, M., Wang, Y., Gibson, L., Welch, S., Rush, D. (2019) A computational study on the effect of horizontal openings on fire dynamics within informal dwellings. In: Proceedings of the ninth international seminar on fire and explosion hazards (ISFEH9), pp 512–523. <https://doi.org/10.18720/spbpu/2/k19-122>
- [21] Beshir, M., Cicione, A., Wang, Y., Welch, S., Rush, D. (2019) Re-visiting NIST reduced/fullscale enclosures (R/FSE) experiments (2007–2008). In: Interflam proceedings, pp 2095–2107.
- [22] Wang, Y., Gibson, L., Beshir, M., and Rush, D. (2021) Determination of Critical Separation Distance Between Dwellings in Informal Settlements Fire, Fire Technology. <https://doi.org/10.1007/s10694-020-01075-w>
- [23] Stevens, S., Gibson, L., & Rush, D. (2020). Conceptualising a GIS-based risk quantification framework for fire spread in informal settlements: A Cape Town case study. International Journal of Disaster Risk Reduction, vol. 50, 101736. <https://doi.org/10.1016/j.ijdr.2020.101736>
- [24] UNHCR. (2022). Refugee Facts– What is a Refugee? Retrieved from <https://www.unrefugees.org/refugee-facts/what-is-a-refugee/>
- [25] UNHCR. (2022). Refugee Facts– Refugee Statistics. Retrieved from <https://www.unrefugees.org/refugee-facts/statistics/>
- [26] Sanderson, D. (2019). Good Practice Review: Urban humanitarian response. Overseas Development Institute, London.
- [27] Sova, C. (2017). "The "New Normal" of Protracted Humanitarian Crises," World Food Program USA. Retrieved from <https://www.wfpusa.org/articles/the-new-normal-of-protracted-humanitarian-crises/>
- [28] Burj el Barajneh Palestinian refugee camp in Lebanon - Anera. (2022). Retrieved from <https://www.anera.org/stories/burj-el-barajneh-palestinian-refugee-camp-lebanon/>
- [29] ACAPS. (2022). Pakistan Complex crisis. Retrieved from <https://www.acaps.org/country/pakistan/crisis/complex-crisis>
- [30] U.S. Agency for International Development. (2022). Humanitarian Assistance | Philippines. Retrieved from <https://www.usaid.gov/philippines/humanitarian-assistance>
- [31] ACTED. (2022). Colombia: Needs Assessment Report of La Guajira. Retrieved from <https://data.unhcr.org/en/documents/details/75659>
- [32] Brazil. (2022). Retrieved 12 October 2022, from <https://reporting.unhcr.org/brazil>
- [33] Lebrija, J. (2021). Conditions worsen at asylum seekers’ camps in north Mexico. Border Report. Retrieved from <https://www.borderreport.com/immigration/conditions-worsen-at-asylum-seekers-camps-in-north-mexico/>
- [34] Costa Rica Hosts More Refugees in Central America: UN. (2017). Retrieved from <https://qcostarica.com/costa-rica-hosts-more-refugees-in-central-america-un/>
- [35] Bolat, G. (2022). ANALYSIS - Fires in refugee camps: A coil of neglect. Retrieved from <https://www.aa.com.tr/en/analysis/analysis-fires-in-refugee-camps-a-coil-of-neglect/2477291>
- [36] Bryant, G., Jordan, S., Hirst, L., Musgrave, J., Salhani, N., Haj, R., and Shdeed, D. (2017). Fire risk reduction assessment of vulnerable displaced Syrian populations and host community in Lebanon. Save the Children International.
- [37] Shelter Projects. (2018). A.13 Bangladesh 2017-2018 / Rohingya crisis overview. Asia-Pacific.
- [38] UNHCR. (2019). Population Map : UNHCR, Bangladesh, Cox's Bazar- as of 15 July 2019. Retrieved from <https://data.unhcr.org/en/documents/details/70358>
- [39] UNHCR. (2018). Culture, context and mental health of Rohingya refugees, Retrieved from <https://www.unhcr.org/5bbc6f014.pdf>
- [40] “Life in the camps.” (2017). Reuters. Retrieved from <http://fingfx.thomsonreuters.com/gfx/rngs/MYANMAR-ROHINGYA/010051VB46G/index.html>
- [41] The UN Migration Agency. (2021). Fire Incident in Rohingya camps.
- [42] Shelter Sector. (2021). Cox’s Bazar Shelter Standard Assessment survey analysis. Shelter Sector.
- [43] Shelter Projects. (2020). A.12 Bangladesh 2019-2020 / Rohingya crisis. Asia-Pacific. 8th ed.

- [44] Puig-Diví, A., Escalona-Marfil, C., Padullés-Riu, J. M., Busquets, A., Padullés-Chando, X., & Marcos-Ruiz, D. (2019). Validity and reliability of the Kinovea program in obtaining angles and distances using coordinates in 4 perspectives. *PloS one*, 14(6), e0216448. <https://doi.org/10.1371/journal.pone.0216448>
- [45] Kawagoe, K. (1958). "Fire Behaviour in Rooms", Report No. 27, Building Research Institute, Tokyo.
- [46] Zheng, L. (2011). Measurement of flame height by image processing. *Advanced Materials Research*. DOI: 10.4028/www.scientific.net/AMR.301-303.983
- [47] Quintiere, J. (2006). *Fundamentals of Fire Phenomena*. John Wiley & Sons, Inc.
- [48] Krishnan, M. (2020). Otsu's method for image thresholding explained and implemented. Retrieved from <https://muthu.co/otsus-method-for-image-thresholding-explained-and-implemented/>
- [49] Robbins, A., & Wade, C. (2008). Soot Yield Values for Modelling Purposes – Residential Occupancies. Study Report No. 185. Branz.
- [50] Xu, Q., Chen, L., Harries, K., Li, X. (2016). Combustion performance of engineered bamboo from cone calorimeter tests. Springer. <https://par.nsf.gov/servlets/purl/10063494>
- [51] Cafe, T. (2007, June 17). Physical Constants for Investigators. T.C. Forensic: Article 10 - Physical Constants for investigators. Retrieved April 20, 2022, from <https://www.tcforensic.com.au/docs/article10.html>
- [52] Which Materials Make the Best Tarpaulin? | Brumleve Industries. (2022). Retrieved 11 November 2022, from <https://brumleveind.com/pages/which-materials-make-the-best-tarpaulin#:~:text=Traditional%20tarps%20are%20often%20made,type%20of%20material%20like%20canvas.>
- [53] Pope, I., Hidalgo, J. P., Osorio, A., Maluk, C., & Torero, J. L. (2019). Thermal behaviour of laminated bamboo structures under fire conditions. *Fire and Materials*, 45(3), 321–330. <https://doi.org/10.1002/fam.2791>
- [54] IOM. (2015). Plastic Sheet / Tarpaulin. IOM Global NFI catalogue. Retrieved from <http://www.iom.int/shelter>
- [55] Tarps Now. (2022). High Temperature Tarps - Heat Resistant Covers. Retrieved from <https://www.tarpsnow.com/high-temperature-fabric-tarps-covers.html>
- [56] Andersson, P. & Bäckström, G. (1973). Pressure dependence of the thermal conductivity, thermal diffusivity, and specific heat of polyethylene. *Journal of Applied Physics* 44, 2601; <https://doi.org/10.1063/1.1662620>
- [57] Chang, S. & Bestul, A. (1973). Heat Capacities of Polyethylene from 2 to 360 K. *Journal of Research of the National Bureau of Standards - A. Physics and Chemistry* Vol. 77A, No.4.
- [58] Professional Plastics. Thermal Properties of Plastic Materials. <http://www.professionalplastics.com/>
- [59] Snell, C., Tempest, B., Gentry, T. (2017). Comparison of the Thermal Characteristics of Portland Cement and Geopolymer Cement Concrete Mixes. *American Society of Civil Engineers*. DOI:10.1061/(ASCE)AE.1943-5568.0000240.
- [60] McGrattan, K. (2020). Heat Release Rates of Multiple Transient Combustibles. NIST Technical Note 2102. DOI:10.6028/NIST.TN.2102
- [61] Federal Emergency Management Agency, U.S. Department of Transportation, and U.S. Environmental Protection Agency. 1988. *Handbook of Chemical Hazard Analysis Procedures*. Washington, D.C.: Federal Emergency Management Agency Publications Office.
- [62] Drysdale, D. (2011). *An Introduction to Fire Dynamics* (3rd ed.). Singapore: John Wiley & Sons Limited.

